University of Nottingham
UK | CHINA | MALAYSIA

Towards development of a liposome-based vaccine to combat *Clostridium difficile* infection

Panayiota Palazi

Thesis submitted to the University of Nottingham for the degree of Master in Research

21 January 2021

I hereby certify that this project report is my own work. Contributions from other authors have been specifically indicated where relevant:

Student’s signature:

Acknowledgements

I would like to take this opportunity to thank Dr. Nicholas Mitchell for all the guidance and supervision throughout this year. I am truly grateful for being able to conduct my Masters degree as part of your research group. A huge thanks to our collaborators, Dr. Patrick Tighe for his assistance on ELISA robotics and especially; Dr. Ruth Griffin, Cansu Karyal and Dr. Jaime Hughes for their extraordinary protein work and for allowing me to be involved in all aspects of this project. The experience I have gained is invaluable. I would also like to thank Dr. Nigel Neate for helping me image the formulation samples with TEM and with the use of the Oxford INCA system for EDX. Lastly, big thanks to the students in B11 and C17 for our good communication and cooperation regarding lab organisation.

Funding for all consumables was provided by the MRC, grant ID CiC2018041, 'Validation of a novel mucosal vaccine platform against test pathogen, *Clostridium difficile*' awarded to Dr Ruth Griffin (PI), Dr Nicholas Mitchell and Dr Paddy Tighe.

ABSTRACT

Antimicrobial resistant infections are now one of the most serious global threats due to the misuse of commonly prescribed antimicrobial agents. This crisis has led researchers towards the development of alternative methods of action. Treatment of *Clostridium difficile*, a bacterium with growing hyper-virulent strains causing thousands of deaths annually, is attracting widespread interest. The purpose of this study is to design and develop a vaccine against this enteropathogen using liposomal formulations as both the delivery system and as an adjuvant. A synthetic lipid linker bearing a maleimide group is used to mimic the natural presentation of several antigenic lipoproteins successfully expressed aiming at blocking all disease stages. Attention is focused on characterisation and optimisation of liposomal structures and formulation reactions using a number of analytical techniques including DLS and FACS.

List of Abbreviations

Ab Antibody

Ag Antigen

APC Antigen presenting cells

AMR Antimicrobial resistance

Aq. Aqueous

CC Column Chromatography

CDC Centers for Disease Control and Prevention

CDI *Clostridium difficile* infection

CDT Binary toxin

CLRs C-type lectin receptors

CLSI Clinical and Laboratory Standards Institute

DCM Dichloromethane

DIC N,N′-Diisopropylcarbodiimide

DMAP 4-(Dimethylamino)pyridine

DMF Dimethylformamide

DPPC 1,2-dipalmitoyl-sn-glycero-3-phosphocholine

DPPS 1,2-dipalmitoyl-sn-glycero-3-phospho-L-serine

DLS Dynamic Light Scattering

MeOH Methanol

Edx Energy-dispersive X-ray

ELISA Enzyme-linked immunosorbent assay

Eq Equivalent

FACS Fluorescence-Activated Cell Sorting

GFP Green fluorescent protein

HCl Hydrochloric Acid

iPr_2NEt N,N-Diisopropylethylamine

Mal Maleimide linker

MHC Major histocompatibility complex

mL Millilitre(s)

mmol Millimole(s)

mM Millimolar

MS Mass spectrometry

m/z Mass to charge ratio

Na_2SO_4 Sodium Sulfate Anhydrous

NMR Nuclear Magnetic Resonance

Nm Nanometer

Non-Mal No Maleimide linker

PAMPs Pathogen associated molecular patterns

PBS potassium buffer solution

PDI Polydispersity Index

PMC Pseudomembranous colitis

PRR Patter recognition receptors

RPM Rounds per minute

RT Room temperature

SPPS Solid Phase Peptide Synthesis

TCEP Tris(2-carboxyethyl)phosphine

TEM Transmission electron microscopy

TFA Trifluoroacetic acid

THF Tetrahydrofuran

TLRs Toll-like receptors

VADS Vaccine Adjuvant Delivery System

Table of Contents

1. INTRODUCTION

1.1 The problem of Antimicrobial Resistance and the need for alternative methods of treatment

While powerful, our body fails to tackle all pathogens (disease causing microorganisms) on its own and therefore antimicrobials are used to treat a disease related to microorganisms. Antibiotics are substances that can inhibit the growth and replication of bacteria or can kill bacteria, namely bacteriostatic and bactericidal respectively. There are broad-spectrum antibiotics that attack a wide range of bacteria and others that are highly specialised. The discovery of antibiotics was one of the greatest achievements of the 20th century as it revolutionised the way infectious diseases were treated, including the way surgeries were performed.

Many antibiotics, including penicillins, work by attacking the cell wall of bacteria and prevent them from synthesising peptidoglycan, which provides the wall with the strength it needs to survive in the human body.[1] Other antibiotics, like the fluoroquinolones, prevent successful DNA replication in bacteria.[1] A class called the tetracyclines are protein synthesis inhibitors and therefore prevent bacteria from reproducing. Others fight bacteria by inhibiting mycolic acid (isoniazid) and others folic acid synthesis (sulfonamides and trimethoprim).[1]

Bacteria employ defense strategies to protect themselves against antibiotics. The ability to do so comes through antibiotic resistance genes that encode for certain changes allowing the bacteria to acquire resistance. Bacteria can transfer these genes, found on plasmids (circular genetic structure that replicates independently from chromosomes) through a process called conjugation. Bacterial defense strategies include:

- Restricted access to the antibiotic: by gram negative bacteria that have an outer membrane limiting the number of pores in their cell wall.[2]
- Expulsion: e.g. *Pseudomonas aeruginosa* use pumps in their cell walls to remove the drug.[2]
- Degradation: *Klebsiella pneumoniae* use enzymes that break down beta-lactams.[2]

- Altering the chemical structure: *Staphylococcus aureus* bacteria add compounds to drugs to change their function.[2]
- Bypassing its effects: *Staphylococcus aureus* bacteria have developed new processes to make nutrients that trimethoprim cannot have an effect on.[2]
- Changing the targets: *E. coli* bacteria can add a compound to the outside of the cell wall so that drugs cannot latch onto it.[2]

Bacterial resistance to a drug, antimicrobial resistance (AMR), is a natural biological process, however with the on-going abuse of antibiotics this process has been accelerated leading to the number of resistant bacteria growing immensely during recent years. According to a World Health Organisation (WHO) survey taking place in 12 countries in 2015 almost 2 in every 3 people (64%) believe that antibiotics can treat colds and flus, caused by viruses, whilst 32% of the 10,000 people questioned believe they should stop taking antibiotics when they start to feel better rather than completing the prescribed course of treatment. With no new classes of antibiotics being developed since the 1980s[3], the misuse of commonly prescribed treatments and the rapid development of resistant bacteria antimicrobial resistance (AMR) infections are now one of the most serious global threats.[4] AMR occurs when microbes (microorganisms that can exist as single cells such as bacterial, viruses, fungi and parasites) no longer respond to the drugs designed to treat the infections they cause. AMR infections result in 700,000 deaths annually, a number predicted to rise to 10 million by 2050 according to the National Institute for Health Research (NIH).

Certain bacterial strains of *Mycobacterium tuberculosis*, *Staphylococcous aureus* and *Clostridium difficile* no longer respond to antibiotics usually employed in the clinic[5], whilst there is also worrying emergence of multidrug resistance of bacterial strains resistance relevant to all available antibiotics[6]. Specifically, *Clostridium difficile* - a gram-positive[7] (displaying a thick peptidoglycan layer) anaerobic bacterium able to infect either humans or animals and commonly found in the environment - that causes opportunistic gut infections, has been declared an urgent public health threat. The limited antibiotics

for *Clostridium difficile* infection (CDI) and increasing antibiotic resistance has made treating recurrent episodes impossible. After the initial episode, up to 33% of patients experience recurrent CDI and recurrences can reach 45% after a second episode.[8] There are about 435,000 CDI cases and 29,000 deaths annually in the United States as reported by the Centers for Disease Control and Prevention (CDC) in 2015 whereas in 2017 there were 13,286 documented cases in England, resulting in 1,977 deaths within 30 days of onset of *Clostridium difficile* infection.[9] Understanding how microbes – and in particular bacteria in this instance – can be fought could lead to alternative methods of treatment.

1.2 Immune responses to infections

Innate immune response

The immune system is a network of lymphoid organs that defends the body against attack by foreign invaders, primarily microbes. First line of defense includes the skin and mucus membranes of the respiratory, intestinal and genital tract and an innate immune response.

The innate system is made up of white blood cells including *Natural killer* cells that attack cells and *phagocytes* which are vital to the immune responses as they can engulf and digest microbes, a process called *phagocytosis*.[10] Phagocytes include *neutrophils* which attack bacteria, *monocytes* which circulate in the blood and migrate into tissues where they develop into *macrophages* that remove dead and dying cells and *dendritic* cells. These cells are known as Antigen Presenting Cells (APC). This happens through pathogen associated molecular patters (PAMPs)[11] as they differ from host markers. PAMPs can be either whole microbes or parts of microbes i.e. specific surface structures (such as proteins, peptides or carbohydrates) called antigens (Ags). APCs that specialise in the uptake and processing of pathogens (microbe that causes disease) into fragments, will recognise these non-self markers through pattern recognition receptors (PRR) which are mainly transmembrane receptors (C-type lectin and Toll-like receptors; CLRs and TLRs respectively). Bacteria are usually recognised by TLR_1, TLR_2 and TLR_5.[12,13] As the APCs

process pathogens they present Ags on their surfaces as epitopes which are therefore able to interact with T cells and B cells which leads to an adaptive immune response.

Adaptive immune response

T cells and B cells, begin as stem cells in the bone marrow and differentiate into immunocompetent cells in the thymus and bone marrow respectively.[10] These cells then colonise the secondary lymphoid tissues; lymph nodes, spleen and mucosa-associated lymphoid tissue (MALT).[14] From there, two different types of adaptive immune response are created; cell-mediated and humoural (antibody-mediated). Most bacterial pathogens are extracellular (do not live or replicate within host cells but outside of host cells in the body and extracellular bacteria are typically cleared by antibodies.[15] This thesis will focus on antibody mediated immunity.

Humoural immune response

Macrophages are transformed into white blood cells after responding to different cytokines (chemical messages), they are then stimulated by the interactions of antigens into cytotoxic T lymphocytes and plasma cells (B lymphocytes) respectively (*figure 1*). Once in the bloodstream these cells are transported to tissues around the body to recognise the foreign antigens.[10] Plasma cells cannot enter other cells, however, each one is specialised to generate and secrete specific antibodies into the body's fluids. Antibodies (Abs) are protective proteins that will attack a specific antigen by binding to it. This makes up the humoural immunity (ability to resist a particular infection). The binding of an antibody called antitoxin, for example, to a specific toxin will neutralise the poison produced by that toxin by changing its chemical composition. Different Abs, otherwise known as immunoglobulins, have different roles in tackling the foreign species, as follows:

- Immunoglobulin G (IgG): coats microbes speeding up their uptake.
- Immunoglobulin A (IgA): abundant in mucosal fluid such as intestinal fluid and saliva guarding the body's entrances and is usually the first antibody to encounter a pathogen which typically enters via an orifice.

- Immunoglobulin M (IgM): kills bacteria but it is not very antigen-specific.
- Immunoglobulin E (IgE): is responsible for symptoms of allergy
- Immunoglobulin D (IgD): remains attached to B cells and initiates B cell response.[10]

T cells do not recognise free floating antigens like B lymphocytes, but rather antigens on surfaces of infected cells through major histocompatibility complex class I and class II molecules (MHC-I, MHC-II)[16]; i.e. proteins providing recognisable scaffolding to present a foreign antigen to the T cell. The T lymphocytes mediate the cell-mediated immunity and there are two types being developed when the APCs come in contact with an antigen, one being the Helper T cells (Th cells) that coordinate the immune responses, i.e. by stimulating other cells through cytokine release. The other, is Killer T or cytotoxic T lymphocytes that directly attack cells[10] carrying the foreign markers on their surfaces using potent chemicals (*figure 1*).

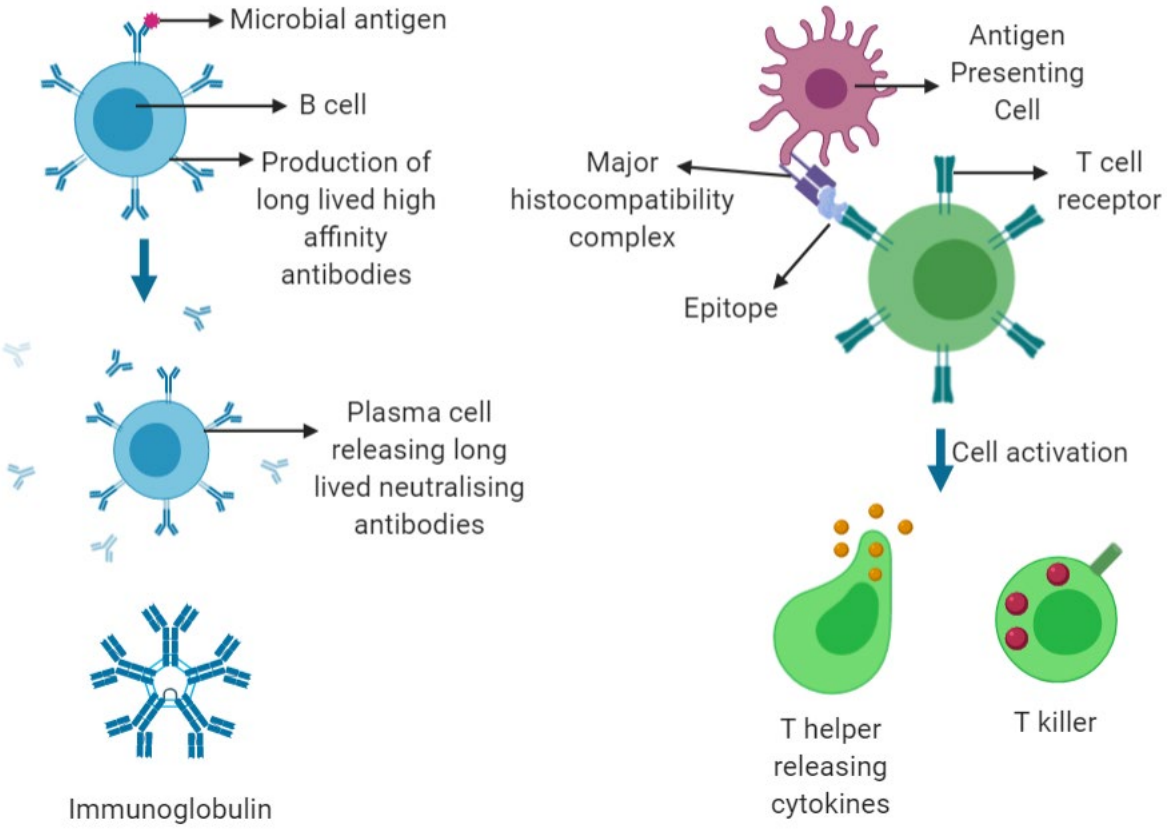

Figure 1. B cell and T cell differentiation in response to cytokines, the humoural immune response.

The complement system also aids the destruction of pathogens. It consists of 25 proteins that once activated by the first Ab interlocking with an Ag, causes blood vessels to dilate, redness in affected areas, warmth, swelling and pain, i.e. the *inflammatory response* and then a series of steps (*complement cascade*) to get rid of antibody coated antigens and burst invading cells (*apoptosis*).[10]

After the primary immune response (first encounter of the immune system with a particular pathogen), activated T and B cells become *memory* cells and have the ability to confer long lasting immunity as they recognize the previously tackled antigens on microbes and trigger faster, more effective secondary immune responses. Immunity against a pathogen as described, can be *innate* i.e. born with, *passive*; borrowed from another source like our mother and doesn't last or *adaptive* therefore acquired through life, as we get exposed to disease and a library of antigens develops in the body.[17]

1.3 *Clostridium difficile*

Clostridium difficile, is an example of a bacterium that has developed AMR for certain strains.[6] It was isolated for the first time in 1935[18] from the intestinal flora of neonates and was initially considered a normal non-pathogenic resident of the gut, today found in the digestive system of about 1 in every 30 healthy adults.[19] Only in 1970s was *C. difficile* identified as one of the microbes responsible for antibiotic-related diarrhea and pseudomembranous colitis[8] (90% of the cases).[20] It is a spore-forming (metabolically inactive particles able to survive in soil, water, and on surfaces in clinical settings) bacterium and if ingested, spores can survive in the stomach of infected individuals and subsequently reach the intestine.[8] Aerobic conditions of the host likely inhibit germination of spores[21] (switching from their dormant state to become active vegetative cells) and growth of the bacterium during its passage through the small intestine. In the large intestine of healthy individuals, spores can persist asymptomatically and their germination is generally prevented through the action of bile acids. However, in the absence of the normal intestinal microbiota (flora), *Clostridium difficile* spores can germinate.[22] Once vegetative cells have been released from the germinant spores, they

can penetrate the mucus layer with the help of flagella.[23,34] The contact with host epithelial cells triggers the upregulation of genes that will help bacteria adapt to the new environment.[8] The bacterium remodels its surface, for example by exposing proteolytic enzymes such as Cwp84 – an extracellular protein which degrades elements of the host epithelium – in order to survive.[24] This lytic action induces the release of nutrients from the damaged epithelium and also promotes toxin diffusion. *Clostridium difficile* cells cause disease by secreting two very large enterotoxins, TcdA and TcdB.[25,30] These toxins have similar structures and have the ability to alter the cytoskeleton, activate apoptosis and impair the intestinal barrier resulting in sever intestinal damage.[26] In addition to TcdA and TcdB, up to 35% of *C. difficile* strains also express binary toxin (CDT) which enhances virulence of *C. difficile*.[27]

Symptoms of CDI include, diarrhea, fever, and inflammation of the bowel causing severe abdominal pain.[28] It can rapidly progress to pseudomembranous colitis (PMC) and intestinal perforation often resulting in colectomies and death to a good 10%.[29,30] Current treatment of CDI includes oral antibiotics such as metronidazole, vancomycin and fidaxomicin[31] however as mentioned, reports all over the world show *C. difficile* becoming resistant. In 2013, Gouarzi *et al*. tested the antimicrobial susceptibility of 75 *C. difficile* isolates from 390 CDI patients. They found 5.3% of the isolates were resistant to metronidazole based on the Clinical and Laboratory Standards Institute (CLSI) breakpoint ($<$8 μg/ml)[52]. The bacterium also proves to be resistant to multiple other antibiotics which are commonly used in the treatment of infections in clinical settings, such as tetracyclines, fluoroquinolones, erythromycin, clindamycin, cephalosporins, and penicillins.[31] More specifically, *C. difficile* 630 (CD630) genome harbors resistance genes encoding β-lactamase-like proteins and penicillin-binding proteins, modification of target sites and antibiotic degrading enzymes, all of which mediate the resistance to the β-lactam antibiotics such as penicillin and cephalosporins.[6] These sequences are also found in other strains with a minimum 75% identity.[6] Transposons mediate the transfer of erythromycin ribosomal methylases genes of class B (*ermB)* which induce the resistance to the MLS_B family of antibiotics (macrolide, lincosamide and streptogramin), including

clindamycin and erythromycin.[6] Biofilm formation, a multilayered thick multicomponent matrix is said to be responsible for resistance in both metronidazole and vancomycin.[32] Resistance to the second-generation cephalosporins (cefotetan and cefoxitin) was found to be at 79% of the strains tested and to second generation fluoroquinolones (ciprofloxacin) at 99%. Furthermore, 38% of the strains tested also show resistance to third-generation cephalosporins (ceftriaxone and cefotaxime).[31] Due to this increasing resistance *C. difficile* epidemiology is rapidly evolving and new hyper-virulent strains of *C. difficile* like the RT027 are emerging and spreading globally.[33] This strain is characterized by a high rate of recurrences and mortality due to the increased production of TcdB and TcdA, presence of CDT, absence of gene TcdC which regulates toxin production.[25]

Antibiotic treatment not only fails in most cases to protect against *C. difficile* but also disrupts microbiota-host homeostasis and creates an environment within the gut that promotes *C. difficile* spore germination.[22] The absence of natural competitors for nutrients due to the broad-spectrum of antibiotic use and antibiotic resistance of the strains permits *C. difficile* to colonise empty niches in the colonic tract.[22] This is especially common in elderly or immuno-compromised individuals.[35] The use of drugs to suppress gastric acid production has also been associated with an increased risk of *C. difficile* infection. In 2017 monoclonal antibody treatment (antibodies made by identical immune cells for better response to antigen) was licensed in the UK, to be administered alongside antibiotics.[36] An example is Bezlotoxumab, a monoclonal antibody against TcdB, however, the protective effect of this passive immunisation strategy is short-lived and the process costly.[37] Faecal transplants are also an option which is however very unpopular as individuals are reluctant to receive it.[7]

1.4 Vaccines: mimicking natural protective immune responses

Bacteria rapidly reproducing and individuals spreading resistant bacteria through the population further amplifies AMR. A viable solution would be immunisation through vaccination to prevent an infection, since prevention of recurrence is the most challenging aspect of treatment, especially with CDI. It has been shown that antibodies against TcdA

and TcdB (serum IgG antitoxins) are associated with protection against CDI[34] highlighting that acquired immunity with high levels of serum antitoxin protects against recurrence.[38]

Vaccines are biological preparations containing agents resembling disease causing microbes able to stimulate the immune system into developing active, acquired, long lasting immunity against a specific pathogen without enduring the illness it causes. This can be achieved by installing the same antigen(s) found on the pathogen causing the infection and controlling the exposure to that antigen. Types of vaccines include *live attenuated* vaccines created by reducing the virulence of the pathogen while keeping it viable, *inactivated*; containing killed (inactive) antigen i.e. with no disease producing ability, *subunit* vaccines containing fragments of pathogens usually surface proteins and therefore purified antigens and *toxoid*; containing inactivated toxins.[39]

Formulation of a vaccine against *C. difficile* bacteria has attracted recent widespread interest. Several studies were driven by the assumption that local anti-toxin immunity was necessary to confer protection, since CDI in humans is clearly confined to the intestinal tract.[8] However, passive immunisation studies demonstrated that circulating anti-toxin antibodies are effective in the treatment of severe CDI. Formalin-inactivated TcdA and TcdB were the first antigen mixture proposed for vaccine use, as was the Sanofi Pasteur toxoid vaccine that was terminated during phase III clinical trials as the results were far from optimal and it has failed to protect against CDI.[40] Pfizer is currently evaluating a genetically modified recombinant full-length TcdA and TcdB vaccine in healthy adults older than 50, while Valneva is developing VLA84; a genetic fusion of the truncated cell-binding domains of the two toxins that is purported to be less complex to formulate compared to the toxoid vaccines.[40,41] Pharma has focused on solely targeting secreted antigens which is an impractical option due to the inability to target the bacterial cells. In this way colonisation and transmission cannot be prevented. A viable approach would be targeting the bacterium through development of an immunotherapeutic specific for surface components.[41]

Subunit vaccines (fragment of a pathogen) are usually unstable and often induce insufficient immune responses. To overcome this, nanoparticles with compositions

mimicking the components of the pathogenic organism, in this case *C. difficile*, can be developed as a vaccine carrier in order to form vaccine adjuvant delivery systems (VADSs) which can potentially not only protect antigens and deliver substances to the lymphocytes but also enhance the initiation of antigen specific immune responses (adjuvant).[42] Several studies indicate that colonisation with non-toxigenic strains is associated with a decreased number of disease incidences, suggesting that a vaccination with non-toxin components could aid in the prevention of the disease manifestations.[8]

1.5 Delivery system

Liposomes are spherical structures made up of several different lipids and often cholesterol. Phospholipids are most commonly the main constituent of a liposome formulation.[44] These molecules are amphiphilic in character, owing to their hydrophobic tail consisting of two fatty acids linked by a glycerol backbone to a hydrophilic head group made up of phosphate (and potentially another organic moiety), and therefore form bilayers when in contact with an aqueous phase[45] (*figure 2*). The lipids' hydrophobic tails are repelled by water molecules resulting in liposome self-assembly, forming hollow spheres with an internal hydrophilic compartment.[44] They can form either single (unilamellar) or multiple bilayers (multilamellar vesicles). Liposomes were first described in the early 1960s, observed under an electron microscope by Bangham and co-workers, they were defined as vesicles with small size and spherical shapes that can be generated from phospholipids, cholesterols, non-toxic surfactants and even membrane protein[77]. These vesicle structures can encapsulate and deliver both hydrophilic and hydrophobic substances. Antigen incorporation can be achieved by covalent lipid conjugation[46] either pre- or post-vesicle formation, encapsulation, electrostatic interactions or surface adsorption according to Henriksen-Lacey et al. depending on the antigen's hydrophilic and hydrophobic properties (*figure 2*).

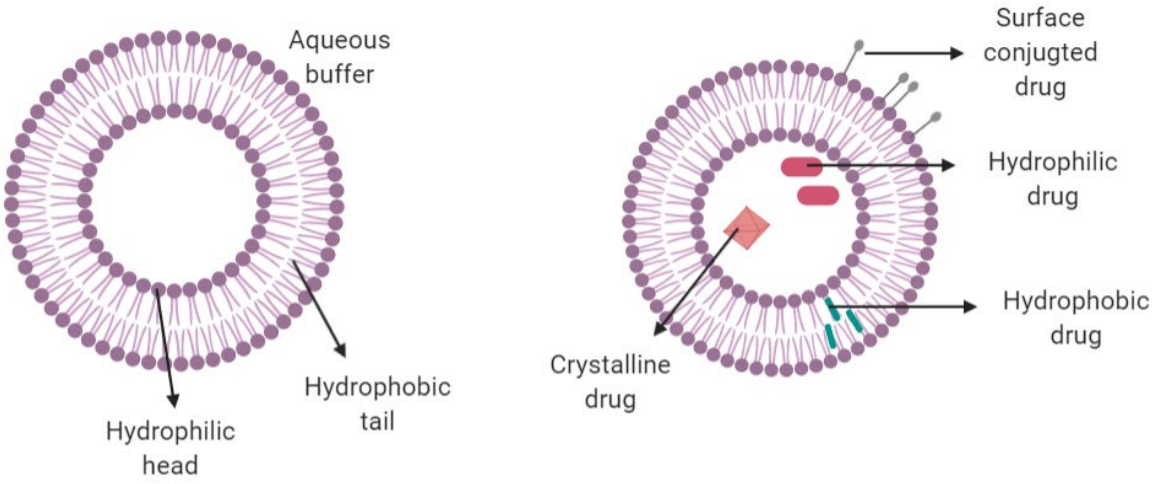

Figure 2. Representation of the phospholipid bilayer of a liposome vesicle and incorporation of different drugs into the vesicle depending on their properties, respectively.

In liposome preparation, types and ratio of phospholipids (i.e. lipid tail and charge) are important factors that determine the final liposomal structure and properties. The final structure affects the cellular immune responses produced, the physical properties play a major role in the function of the formulation. More specifically, intestinal absorbance is affected by particle size and electrical charge. The smaller the diameter and the higher the positive charge the more effective the delivery system and liposomes applied to medical use are typically 50-450 nm.[47] Cationic liposomes are the most extensively studied liposome types due to their enhanced interaction with the negatively charged bilayer of immune cells, however, negatively charged liposomes have been shown to contribute to increased permeation of drugs e.g. through the skin.[48] The ability to deliver antigens also depends on the formulation's fluidity.[46] Phospholipids with phase transition temperatures (temperature required to induce change in the physical state of lipid from ordered gel phase to disordered liquid crystalline phase) below 37 °C are completely disrupted by bile salts, however phospholipids with higher than 37 °C are better preserved and therefore elicit higher immune response.[46] Cholesterol is often used in formulations as it is a membrane constituent widely found in biological systems which serves a unique purpose of modulating membrane fluidity, elasticity and permeability and

it serves the same purpose in liposomes. It increases the separation between head groups and reduces electrostatic interactions which stabilises the formulation.[48] Addition of 30-40% cholesterol has been shown to increase the integrity of vesicles enabling a condensed packing of the lipid bilayer.[49] Higher levels of cholesterol have been associated with reduced immune responses, for example in a study by Kaur et al.,[53] where less IgG was detected as cholesterol increased in the system. Formulation of a multilayer phospholipid bilayer usually involves the combination of lipids in a specific ratio in an organic solvent and removal of the solvent under reduced pressure to afford a thin-film. Addition of an appropriate buffer and sonication produces multilamellar liposomes of 50 – 500 nm depending the method of sonication (probe or bath).[50] Extrusion can further refine the formulation to afford the desired size of particles at low polydispersity.[50]

1.6 Administration of vaccine

Liposomes would typically be administered orally[56,69], which is ideal to treat enteropathogens. The gastrointestinal mucosal site delivery is essential to stimulate production of mucosal antigen specific secretory lgA in the gastrointestinal tract and systemic lgG.[70] However macrophages prevent the bulk of the liposomes to reach their targets. The introduction of enteric coated capsules has been proposed to reduce the recognition of liposomes by macrophages thereby improving absorption as more liposomes survive and are exposed in small intestine.[67,71] The packed capsules must also survive the acidic environment of the stomach (pH 2-3), successfully releasing their contents in the small intestine (pH 6.5-7). Formulations coated with Eudragit L100 have shown to enhance the oral bioavailability of alendronate sodium by 12-fold in rats when compared with the commercial tablets.[71]

1.7 Aims and objectives

In this study we will examine the formulation of a novel vaccine based on a liposomal delivery system. Our target would be to develop a prophylactic vaccine whose

formulation will contain immunogenic receptor binding domain of *Clostridium difficile* toxins[43] and individual lipoprotein antigens, using a liposomal delivery system, structure baring a maleimide lipid linker for protein attachment to enhance mucosal immunogenicity and protective efficacy. This approach is different to the approaches of other commercial vaccines for *Clostridium difficile* where only secreted proteins have been targeted. In addition the vaccine will display a bespoke lipid linker projecting outwards from the surface of the liposome and proteins that are known to be antigenic and will be directly conjugated to this linker. The aim is to optimise liposomal formulations with a lipid linker for conjugation to protein antigens provided by the Griffin lab. The ratio of the protein to lipid link will be optimised using GFP and the formulations will be purified using size exclusion chromatography (SEC). The particles will be characterised for size and polydispersity**.**

Formulation

Antigens identified as vaccine candidates are chosen based on surface exposure, potential immunogenicity and role in pathogenesis: CD630_08730; a colonisation lipoprotein, known to be immunogenic and to provide partial protection[43,51] and receptor binding domains TcdB[51] and cell wall protein Cwp84 known to be immunogenic with 40% protection in hamster models.[54] Using all of the above we aim to block colonisation and neutralise TcdB. These antigens are codon optimised, chemically synthesised and cloned into the pTWIN1.His vector.

The liposomal vehicle will be formulated using 1,2-dipalmitoyl-sn-glycero-3-phosphocholine (DPPC), the sodium salt of 1,2-dipalmitoyl-sn-glycero-3-phospho-L-serine (DPPS), cholesterol and a bespoke lipid carrying protein-conjugation linker (maleimide) synthesised under the remit of this project. The ratio of lipids in this formulation will dictate the half-life of the particles in the gut and efficiency of uptake.[55] The outer liposomal lipid layer resembles outer membrane of phospholipid bilayer of bacteria which serves to anchor the lipid of the lipoprotein facilitating the presentation of immune epitopes yet also permits dissociation of the incorporated lipoproteins to engage with the host.[56] The percentage of mal-lipid in the formulation will control the amount of antigen

that can be conjugated to the outer envelope of the liposomes. Several different formulations will initially be investigated (keeping the percentage of mal-lipid constant); the particles will be formulated as large multilamellar bilayers, their size and polydispersity confirmed using dynamic light scattering (DLS) and transmission electron microscopy (TEM) and the protein-conjugation reaction optimised to ensure maximal loading. The lipid structures making up the liposomal formulations are as follows:

DPPC

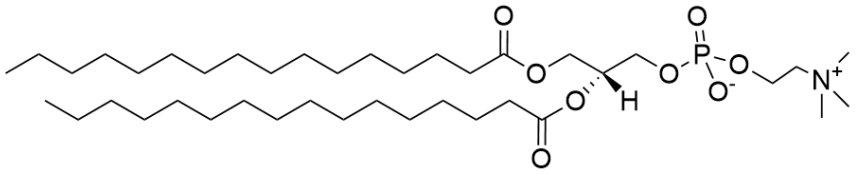

DPPS as the sodium salt

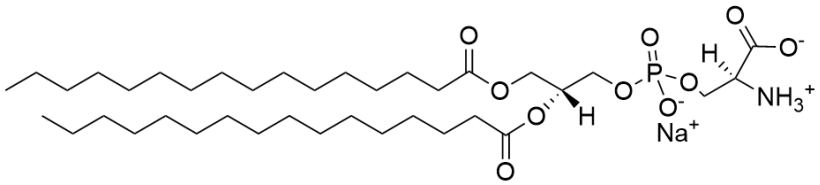

Cholesterol

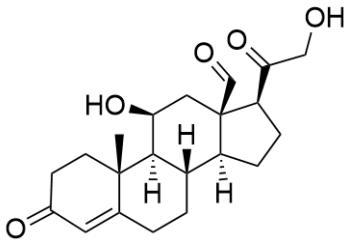

***(S)*-N-(2,3-bis(hexadecyloxy)propyl)-3-(2,5-dioxo-2,5-dihydro-1H-pyrrol-1-yl)propanamide (Maleimide diether)**

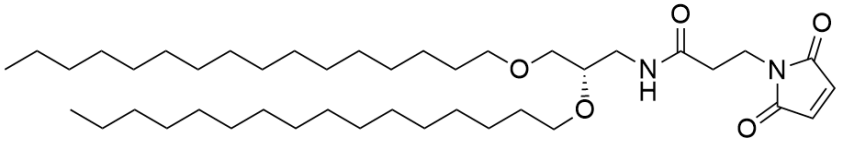

***(S)*-3-(3-(2,5-dioxo-2,5-dihydro-1H-pyrrol-1-yl)propanamido)propane-1,2-diyl dipalmitate (Maleimide diester)**

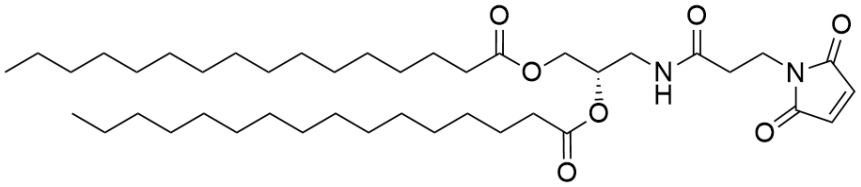

The DPPS and DPPC lipids are commercially available, the two mal-lipids will be chemically synthesised for this project. Both of them will be synthesised to identify the most suitable maleimide linker for the vaccine vehicle. The ether is a more stable moiety, however the maleimide digester has the native presentation of lipoproteins. This bespoke lipid contains dipalmitoyl (two palmitic acid) chains and a maleimide head group linked through a glyceryl moiety. Conjugation of the protein to the maleimide groups protruding from the surface of the particles occurs via Michael addition of the thick side chain from the N-terminal cysteine (Cys) residues mutated into the recombinant protein antigens. This linker system is designed to mimic the native bacterial lipoproteins (an *S*-glycerol palmitoyl linker)[57] to ensure maximal immune response whilst enabling the utilisation of robust protein conjugation chemistry (*figure 3*). For the *S*-glyceryl Pam (i.e. the thio of a Cys directly attached to the glyceryl unit), the (R)-stereochemistry is very important as it has been shown to be more biologically active.[58] Due to attachment of a nitrogen attached to the glyceryl unit, the stereochemistry employed is (S), however the orientation of the groups is the same, thus high biological activity is expected.

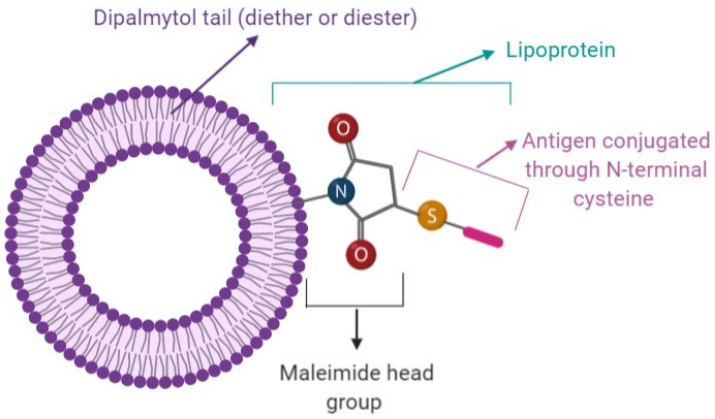

Figure 3. The final vaccine formulation of the antigen conjugated onto the maleimide linker on the liposome, mimicking the native presentation of lipoproteins for optimal exposure of immunologically important epitopes and maximum stimulation of host immunity by exploiting the natural adjuvant properties of the lipid.

To optimise production of the vaccine, different amounts of the synthetic lipids will be used as well as a range of sonication methods for the formation of vesicles. It is believed that the formulated liposomes will help to increase the structural stability of the lipoproteins, preserving antigen integrity.[66] Lyophilisation of our formulation with trehalose will be studied in an attempt to make the formulation more stable and easier to handle.[72] Moreover, the use of Green Fluorescent Protein (GFP) will be employed to investigate protein conjugation protocol. GFP is a protein expressed by the jellyfish *Aequorea victoria* that exhibits green fluorescence, which has proved very stable and versatile imaging agent[73] and thus used in this study to mimic the antigenic proteins for optimisation of reactions. Conjugation of GFP in place of the *C. difficile* antigens will enable us to quantify and optimise the protein conjugation to ensure the required loading is reached. Conjugation to liposomes is examined using Florescence-Activated Cell Sorting (FACS), a specialised form of flow cytometry that counts, sorts, and profiles cells in a heterogeneous fluid mixture providing quantitative recording of fluorescent signals.

1.8 Rationale

Bacterial lipoproteins (as also formed through the conjugation of the phospholipid to the protein (*figure 3*)), are surface exposed antigens that elicit protective antibody responses[60], highly potent agonists of the TLR_2[57] and have proven safe in humans[61], are therefore ideal vaccine candidates. Gram-positive bacterial lipoproteins contain two fatty acid chains that are frequently palmitic acids (16 carbon chains linked to a glycerol head group via an ester bond).[57,62] Structure–activity relationship (SAR) investigations of related lipoproteins showed that the thioether bridge and palmityl esters are essential for activity i.e. the generation of an immune response.[63] Hopp and co-workers in the 1980s found a significant improvement in antigen-specific antibody response when a hepatitis virus peptide epitopes was conjugated to a dipalmitoyl-lysine moiety. The lipid itself forms a potent adjuvant[57] and is therefore a substance that potentiates or modulates (prolongs) the immune responses to an antigen and improves them providing both adaptive but also strong immune responses. This is due to its high structural similarity with lipoteichoic acid; a major constituent of the cell wall of gram positive bacteria, and is therefore a TLR_2 agonist.[64] The two *O*-linked fatty acid chains are in parallel in the lipid binding channel of TLR_2 bringing the C-terminal domains of these receptors in closer contact[57] (illustration of idea in *figure 4*). As recognition by the TLR_2 depends on carbon chain, the importance of the two ester-bound acyl chains is highlighted.[57,65] We have chosen to deviate slightly from the native linkage to enable us to develop a versatile vaccine platform. Though maleimide linkers have been reported before, we're using them as a non-native linker (or a mimic for the native version) to attach the antigen. Conjugation of the antigen to the external surface of the particles allows us to use the liposomes as a delivery vehicle, an antigen display scaffold (to present the protein) and an adjuvant to enhance immune response.

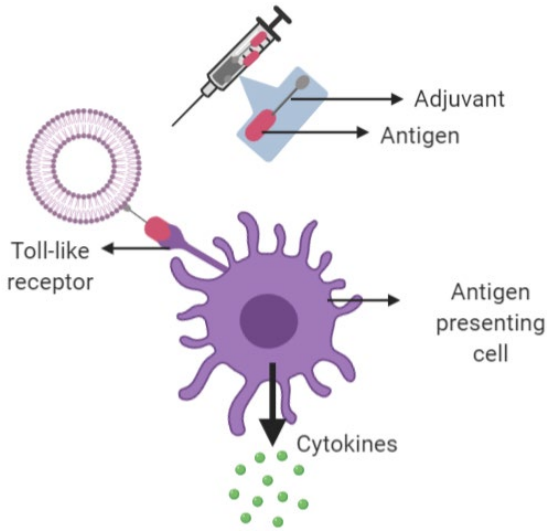

Figure 4. Showing the protein exposed by the adjuvant (vaccine formulation) when in contact with Toll-like Receptor$_2$.

The phosphatidylserine head group (PS) is naturally exposed on the surface of cells undergoing apoptosis, and in this way liposomes containing PS may effectively trigger phagocytosis by macrophages.[67] DPPC has a transition temperature of 41°C and DPPS of 54°C[68] allowing for hydrocarbon chains to be fully extended and closely packed up to high temperatures. Liposomal formulations would be solidified, with good reconstituting capacities to avoid cold chain and generate a vaccine that is stable at room temperature. They would have the ability to withstand the harsh conditions of the gastrointestinal tract (DPPC/cardiolipin liposomes incubated at room temperature for 7 days at RT were shown to dramatically improve the thermal stability of the protein[78].

Formulations composed of DPPC, DPPS and cholesterol in the molar ratio 1:1:2 were reported stable in acidic, bile and pancreatic solution[75]. Therefore our initial formulation is based upon the Han and co-workers study of liposomal stability in the gut. The maleimide involved in addition, is a stable and easy-to-handle moiety that rapidly and covalently conjugates to thiol groups via Michael addition.[59] Since any protein bearing an N-terminal Cys can be conjugated to the particles, our vaccine platform can be applied to a range of infectious pathogens. As described, the lipid moiety attached to the N-terminal

Cys residue of the protein integrates into bacterial cell membrane and holds protein in place, thus presenting the immunogenic epitope on the surface of cells.

As the formulation contains both antigen and adjuvant, the vaccine will be self-adjuvanting, both adjuvant and antigen are taken up by the same APC therefore maximal histocompatibility class II presentation of antigens with potent stimulation of Th and B cell antibody responses should occur.[60] This would mean less antigen is needed to achieve the required protective immunity response resulting in fewer vaccination doses therefore reducing adverse effects. Low doses make liposomal vaccines safe limiting off-target reactogenicity[46] and therefore reduced symptoms like allergies, fever or pain at the injection site. Other advantages include their biocompatibility and biodegradability due to the properties of the lipids used.

2. EXPERIMENTAL

2.1 Materials and methods

MATERIALS

Commercially available reagents were purchased from Sigma, Merck, Fluorochem or Fisher and used without further purification. Anhydrous solvents were purchased from Sigma Aldrich, with the exception of THF and DCM which were freshly distilled. Reagent grade solvents were purchased from Sigma, Merck or Fisher and used as they were received. All aqueous solutions were prepared using deionised water. Dry solvents were used when indicated in the procedure. Glassware was dried at 100 ^{o}C in a vacuum oven for 24 hours.

Thin Layer Chromatography (TLC)

Thin-layer chromatography was recorded using aluminium backed plates coated with Merck Kieselgel 60 GF_{254}. Visualisation was under UV light (254 or 365 nm) and/ or using chemical staining with the appropriate staining solution. The staining solutions used were aqueous potassium permanganate and ninhydrin.

Reduced pressure refers to the use of a Vaccubrand CVC 3000 vacuum pump to remove solvent under reduced pressure on a Büchi Rotavapor R-3000 or Heidolph Vei-Vap Value G3 apparatus, with a water bath at 35 ^{o}C.

Column chromatography was carried out using Davisil grade silica 60 A, with eluent as indicated.

Mass spectrometry (MS)

High resolution mass spectrometry: samples were dissolved to make up 0.01mg/mL solutions in methanol and analysed using a Bruker micrOTOF focus II MS operating in positive or negative ionisation mode.

Nuclear Magnetic Resonance (NMR)

Analysis performed by dissolving 20.0 mg of product in a suitable deuterated solvent. The sample was then analysed on a Bruker AVIII 400 NMR system. The frequency used for ^{1}H NMR was 400 MHz and data is reported as chemical shift (δ), relative integral, multiplicity (s = singlet, d = doublet, dd = doublet of doublets, t = triplet, q = quartet, m = multiplet, or combinations of the listed patterns), coupling constant, J in hertz (Hz). For ^{13}C NMR, spectra were recorded at a frequency of 75 MHz.

Lyophilisation

Samples were frozen using liquid Nitrogen and freeze dried using a FreeZone 4.50 L, -84°C Benchtop Freeze Dryer operating at -78°C with vacuum 0.125 mbar.

Zetasizer for particle analysis (DLS: Dynamic Light Scattering)

The instrument used was a Malvern Zetasizer Nano-ZS. 1.00 mL of sample (formulation in PBS) was used for the analysis in a plastic disposable cuvette at 25°C. A standard operating procedure (SOP) was generated for the analysis that included a set value for the material refractive index at 1.45 and the viscosity of PBS solution at 0.8872 cP and absorbance set to 0.100. 5 measurements were taken per sample each one involving 14 scans at 173° scattering angle. Another SOP was also generated to analyse conjugated samples with large amounts of protein, for which the material refractive index again 1.45 but absorbance was set to 0.001.

Size exclusion Chromatography (SEC)

AKTA Pure Chromatography System was used with a Superdex^{TM} 200 10/300 GL column (1 x 30 cm, packed column volume: approx. 24 mL). Column equilibration was performed for at least 2 column volumes in equilibration solvent (filtered distilled water) and elution solvent (PBS). 0.5 mL of sample was used per injection which was filtered through a 0.22 filter. Elution solvent was PBS at a flow rate of 0.75 mL/min. The wavelength detector was

set to 280 nm and fractions were collected manually. Unicorn7.0 software was used to record chromatograms.

Transmission electron microscopy (TEM)

All samples were imaged in 1X PBS (as prepared) by being retrieved on copper grids and allowed to dry for 1h. A JEOL 2000FX TEM was operated at approximately 160 pA/cm^2 and 80.0 KV acceleration voltage and nanoparticles were imaged using an Orius^{TM} CCD camera controller (Oxford instruments X-max^N).

Energy-dispersive X-ray (EDX)

Elemental analysis (using an Oxford XMax 80 INCA system) was carried out as a service. Sample was imaged as suspension in PBS.

Fluorescence-Activated Cell Sorting (FACS)

FACS analysis: 400 µL of sample was used and analysed using the Astrios machine within the Flow Cytometry Facility.

NANODROP

Protein quantification with a NanoDrop Lite UV-Vis Spectrophotometer recording concentration by measuring absorption at 280 nm using 1 µL of sample.

2.2 Expression of proteins

The following *C.difficile* antigens were expressed and purified from larger scale preps, provided by the Griffin group for this project:

Protein expressed	Function
08730	Colonisation lipoprotein
TcdB	Toxin B receptor binding domain
GFP	Used as surrogate to the antigens

Table 1. Showing the proteins expressed to be used as possible vaccine candidates with their role in pathogenesis stated briefly.

A small scale expression, extraction and purification of antigen 08730 was conducted in this project as follows.

Expression of CD630_08730

Protein sequence:

CSQGGDSGNSKQESNSKDKEVKKIGITQLVEHPALDATRTGFVKALEKNGFKDGENIDIDFQNAQN
DMPTTQSIASKFASDKKDLIFAISTPSAQAAFNATKDIPILITAVSDPVAAGLVKTLEKPGTNVSGTSDF
VSVDKGLELLKIFAPKAKTIGVMYNTSEVNSKVQVDALKEYASKNGFKVVEKGITTSNEVNQGISSLV
GKIDVLYVPTDNLVASSMPIVSKIATENKIPVIAAESGPVEKGALAAQGINYEKLGYKTGEMAVKILNG
ESVSDMPVATSDDTDIIVNEDILKALGMEKPSNENISYVKTKQELQEGDPLVPRGSSAHHHHHHHH
HH

Cloning

Construction of plasmids harbouring recombinant *C. difficile* genes used for all expression steps (produced by Cansu Karyal) were cloned in *E.coli* DH5α and transferred in T7 express *E. coli* cells (patent in development). All *E.coli* strains were grown overnight at 37°C on LB agar or in LB broth with 200 rpm shaking.

Protein expression

Double intein-His tagged protein was expressed in T7 express *E. coli* cells. A freshly grown single colony was used to inoculate 10 mL LB broth containing ampicillin and incubated overnight at 37°C with 200 rpm shaking. 10 mL of overnight culture was used to inoculate 250 mL LB broth containing ampicillin. Cells were incubated with 200 rpm shaking at 37°C until an OD600 0.7 was reached and induced for protein expression using 0.3 mM Isopropyl β-D-1-thiogalactopyranoside (IPTG) and further incubated at room temperature with 200 rpm shaking overnight. The cell cultures were centrifuged at 4°C for 10 minutes at 5,000 x g.

Protein extraction

Protein extraction was performed using a binding buffer made up of 20 mM Tris-HCl, 1 M NaCl and 40 mM imidazole at pH 8. All stages to lyse bacterial cells were performed on ice. The pelleted cells were re-suspended in 20 mL ice-cold binding buffer and sonicated for 20 minutes using a 10 seconds on pulse and 30 seconds off pulse method. This was followed by centrifugation at 19,000 x g for 30 minutes at 4℃. The supernatant soluble fraction was harvested and run on an SDS PAGE gel. Lysates were prepared by mixing 15 µL 2 X SDS sample buffer (100 mM Tris-HCl, 4% SDS, 0.2% bromophenol blue, 20% glycerol (v/v) and 200 mM DTT) with 15 µL cell lysate and heated for 5 minutes at 100°C. Each sample was loaded in 10.0 µL volumes. 7.50 µL of SeeBlue® Pre-stainaned standard was run on each gel. The gels were run using 1X Tris-glycine buffer containing 25 mM Tris, 192 mM glycine, 0.1% SDS at pH 8.3 in the X-Cell SureLock (Bio-Rad) tank at 120 volts for 1 hour and 30 minutes. Protein gels were then stained with Coomassie blue (1% Coomassie brilliant blue, 49% water and 50% methanol (v/v/v)) for 20 minutes with gently shaking at room temperature. This was followed by destaining using a destain solution (50% methanol, 10% glacial acetic acid and 40% water (v/v/v)) for 1 hour and then further destained in distilled water overnight.

Protein purification

Crude cell extracts were passed through a pre-charged Ni^{2+} column using Blue Sephrose 6 Fast Flow resin. Wash steps were performed using binding buffer. The elution buffers were performed using 0.1 M TrisHCl and 2.5 M NaCl and increasing concentrations of imidazole (50 mM, 100 mM, 250 mM and 500 mM). In a Poly-Prep® Chromatography Column, 3.00 mL of slurry was loaded for a 1.50 mL bed volume of beads. The beads were washed with distilled water (7.50 mL) followed by binding buffer (7.50 mL). The lysate was loaded in 5.00 mL volumes and the flow through collected. The beads were then washed with binding buffer (12.0 mL) for the removal of unbound proteins and the flow through collected. The protein was then eluted stepwise using increasing concentrations of imidazole, all eluates collected and run on SDS-PAGE gels as described in section **2.1** with electrophoresis conducted at 125 volts for 95 minutes. All gels were imaged using the Gel Doc™ XR + Gel Documentation system and software. All pure elutions were then combined and dialysed in PBS.

Purification of large scale preparations of GFP, 08730 and TcdB was conducted in the Griffin lab and provided for this project. Further purification of these three recombinant proteins was performed by SEC.

2.3 Linker synthesis

Dipalmitoyl diester lipid

(S,E)-3-(benzylideneamino)propane-1,2-diol (1a)

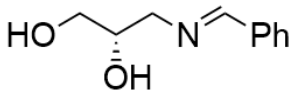

(S)-3-amino-1,2-propanediol (0.43 g, 2.50 mmol) was dissolved in a DCM/MeOH mixture (50.0 mL, 8:2). Sodium sulfate anhydrous was added to the flask and the mixture stirred for 30 mins at RT. Benzaldehyde (1.01 g, 5.00 mmol) was added to the flask and the reaction mixture left stirring over night at RT. Mass spectrometry showed complete consumption of the starting material. The RM was filtered to remove the drying agent

and the solvent was removed under reduced pressure and dried under high vacuum for 6h to give an oil (0.77 g, 4.32 mmol, 95%). HRMS Calc: 180.1002 ($M+H^+$) Act: 180.1020 ($M+H^+$). R_f = 0.45 eluent: DCM/ MeOH (9:1). Crude was used in the next step without purification.

(S,E)-3-(benzylideneamino)propane-1,2-diyl dipalmitate (1b)

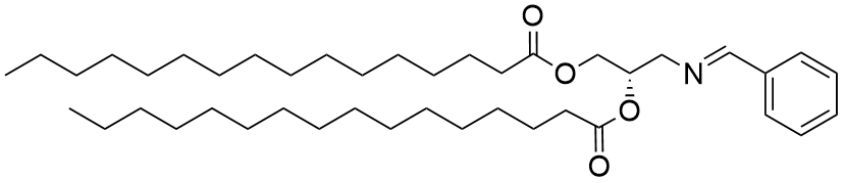

1a (0.77 g, 4.32 mmol) was dissolved in DMF (5.00 mL). The solution was diluted with DCM (20.0 mL). Palmitic acid (3.95 g, 15.3 mmol) was dissolved in DCM (5.00 mL). DMAP (0.53 g, 4.32 mmol) was dissolved in DFM (0.50 mL). DIC (6.76 mL, 43.2 mmol) was added to the reaction flask, followed by the addition of all dissolved reagents. The flask was sealed and left stirring overnight. TLC was carried out to monitor the progress of the reaction. Once complete, the reaction was quenched by addition of water (100 mL) and the aqueous layer extracted with DCM (4x 50.0 mL). The organic layer was washed with water (50.0 mL) and brine solution (3 x 50.0 mL), and dried over magnesium surface, filtered and the solvent removed under reduced pressure to give a light brown solid. Mass spectrometry showed the reaction had gone to completion and indicated presence of **1b** (1.97 g, 3.01 mmol, yield 70%). HRMS Calc: 656.5619 ($M+H^+$) Act: 656.5621 ($M+H^+$). R_f = 0.39 eluent: DCM/ MeOH (9:1). Crude was used in the next step without purification.

(S)-3-aminopropane-1,2-diyl dipalmitate (1c)

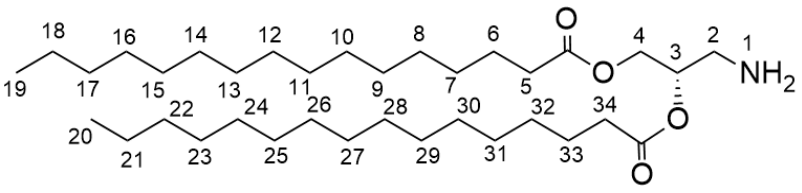

1b (1.97 g, 3.01 mmol) was treated with a TFA/DCM mixture (24.0 mL, 1:1). White fumes were observed and heat was given off. Mass spectrometry showed complete consumption of the SM after 1h. The RM was concentrated in vacuo and TFA co-evaporated with toluene. The product was purified using column chromatography (DCM to DCM/MeOH (8:1)) to give a yellow solid (0.50 g, 0.89 mmol, 51% yield). R_f = 0.22 eluent: DCM/ MeOH 8.5:1.5. HRMS Calc: 568.5321 ($M+H^+$) Act: 568.5331 ($M+H^+$). ^1H NMR (crude) (400 MHz; $CDCl_3$): δ_H 5.19 (2H, m, H-1), 3.61-3.90 (6H, m, H-2, H-4, H-34, H-5), 1.26 (s, 52H, H-5-18, H-21-33), 0.86 (t, *J*= 8.1 Hz, 6H, H-19, H-20).

(S)-3-(3-(2,5-dioxo-2,5-dihydro-1H-pyrrol-1-yl)propanamido)propane-1,2-diyl dipalmitate (1d)

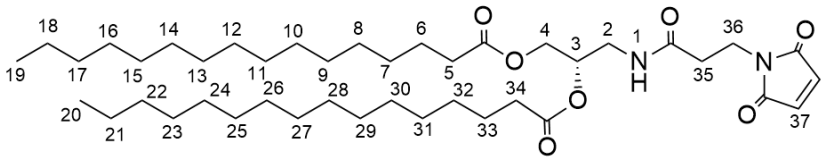

1c (0.15 g, 0.27 mmol) was dissolved in toluene/acetonitrile (5:1, 10.0 mL). 3-maleimidopropionic acid (0.05 g, 0.32 mmol) was dissolved in toluene/acetonitrile (4:1, 5.00 mL), along with DIC (2.41 mL, 0.02 mol) and HOBt (0.32 g, 2.65 mmol). The mixture was left stirring for 10min. The lipid solution was added to the reaction mixture and it was left stirring over-night. The progress of the reaction was monitored with TLC. Mass spectrometry confirmed the presence of **1d**. The crude was purified by column chromatography (DCM to DCM:MeOH (10:1)) to give a yellow solid (0.08 g, 0.11 mmol, 40%) R_f = 0.31 eluent: DCM/ MeOH 10:0.25. HRMS 718.6174 ($M+H^+$), 741.5390 (M+Na). ^1H NMR (crude) (400 MHz; $CDCl_3$): δ_H 6.76 (2H, s, H-37), 5.80-5.95 (1H, m, H-1), 3.70-3.82 (5H, m, H-2, H-4, H-35), 2.69 (2H, t, *J*=7.1 Hz, H-36), 1.59-1.63 (4H, m, H-5,H-34), 1.27 (s, 54H, H-5-18, H-21-33), 0.87 (t, *J*= 7.5 Hz, 6H, H-19, H-20).

Dipalmytol diether lipid

(S,E)-3-(benzylideneamino)propane-1,2-diol

Repetition of synthesis of **1a** formation.

Hexadecyl methanesulfonate (2a)

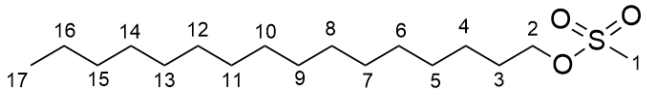

To a solution of cetyl alcohol (2.50 g, 10.3 mmol) and DIPEA (2.08 g, 20.6 mmol) in DCM, MSCl (1.42 g, 12.4 mmol) was added dropwise a 0°C for 30min. The resulting light brown mixture was stirred at RT overnight. A saturated solution of ammonium chloride was added to separate the aqueous layer which was extracted with DCM. The organic layer was washed with water (50.0 mL) and brine solution (3 x 50.0 mL), dried over anhydrous magnesium surface, filtered and the solvent removed under reduced pressure. The light brown solvent (2.80 g, 8.76 mmol, 85% yield) was dried under high vacuum for 5h. HRMS Calc: 343.2283 (M+Na) Act: 343.2279 (M+Na). ^{1}H NMR (400 MHz; $CDCl_3$): δ_H 4.17-4.20 (2H, m t, H-2), 3.13-3.18 (3H, m, H-1), 1.28 (28H, s, H-3-16), 0.87 (3H, m, H-17).

(S,E)-N-(2,3-bis(hexadecyloxy)propyl)-1-phenylmethanimine (3a)

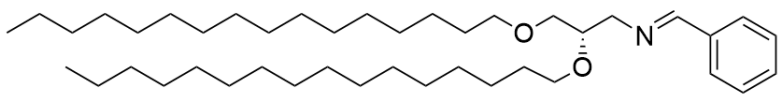

To an oven dried and argon flushed RBF containing NaH (60% dispersion in mineral oil, 0.60 g, 2.50 mmol) and **1a** (0.45 g, 2.50 mmol) in anhydrous THF (40.0 mL), a solution of **2a** (2.01 g, 6.30 mmol) was added drop wise. The RM was heated under reflux for 72h at 70°C. Reaction was quenched by addition of water (100 mL) and the aqueous layer extracted with DCM (3x50 mL). The organic layer was washed with water (50.0 mL) and

brine solution (3 x 50.0 mL), and dried over magnesium surface, filtered and the solvent removed under reduced pressure to give a light yellow solid (0.89 g, 1.43 mmol, yield 57%). R_f = 0.30 eluent: DCM/ MeOH 8.5:1.5. Crude was used in the next step without purification. HRMS Calc: 628.6023 ($M+H^+$) Act: 628.6019 ($M+H^+$).

(S)-2,3-bis(hexadecyloxy)propan-1-amine (3b)

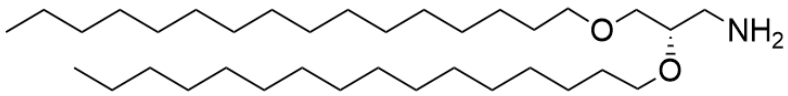

3a (7.72 mg, 0.01 mmol) was treated with a TFA/DCM mixture (50.0 mL, 1:1) and the solution was left to stir overnight. TLC was carried out to monitor the progress of the reaction. The RM was concentrated in vacuo and the TFA co-evaporated with toluene. The resultant oil was dried under high vacuo and then purified by column chromatography (DCM TO DCM:MeOH (8:2)) to give a light yellow solid (5.01 mg, 0.00930 mmol, 65% yield) R_f = 0.27 eluent: DCM/ MeOH 8.5:1.5, HRMS Calc: 540.5720 ($M+H^+$) Act: 540.5708 ($M+H^+$).

(S)-N-(2,3-bis(hexadecyloxy)propyl)-3-(2,5-dioxo-2,5-dihydro-1H-pyrrol-1-yl)propanamide (3c)

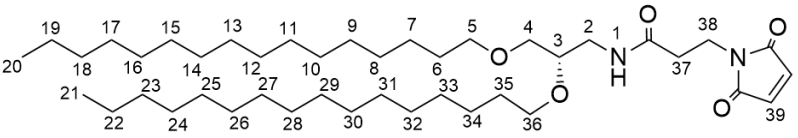

To a solution of 3-maleimidopropionic acid (0.05 g, 0.25 mmol) in DMF (10.0 mL), HATU (0.11 g, 2.5 mmol) and DIPEA (0.07 g, 0.50 mmol,) was added. The mixture was stirred for 5min before **3b** (4.32 mg, 0.00801 mmol) was added. RM was left stirring overnight. It was then acidified with 1M HCl, the aqueous layer extracted with EtOAc (3 x 50.0 mL) and the organic layer washed with water (2 x 50.0 mL) and brine (50.0 mL), dried over

anhydrous $MgSO_4$ and the solvent removed under reduced pressure. The crude was purified by column chromatography (DCM to DCM:MeOH (9:1)) to give a light yellow solid (3.10 mg, 0.00449 mmol, 56%) HRMS Calc: 691.6036 (M+H) Act: 691.6136 ($M+H^+$). ^1H NMR (crude) (400 MHz; $CDCl_3$): δ_H 6.74 (2H, s, H-39), 5.97-6.05 (1H, m, H-1), 3.57-3.88 (5H, m, H-2, H-4, H-37), 2.53 (2H, t, *J*= Hz, H-38), 1.55-1.63 (4H, m, H-5,H-36), 1.28 (s, 56H, H-6-19, H-22-35), 0.88 (t, *J*= 7.1 Hz, 6H, H-20, H-21).

2.4 Liposome formulation

General procedure

A 1mM stock solution of each of the lipids was prepared in $CHCl_3$ for maleimide diether (mal-lipid (**3c**)), DPPC and cholesterol and in $CHCl_3$/MeOH (1:1) for DPPS. Once prepared, the solutions of lipids were combined at a certain ratio (specific for each formulation), based on volume (as stated in experiment 1 – section **2.4**). The solvent from the combined solutions was removed under reduced pressure and the resultant film dried under high vacuum overnight. 1X PBS (volume equal to the final volume of the organic solvent used each time) was added and the suspension formed was sonicated on ice upon addition of the aqueous phase (*figure 5*). Particle size and polydispersity was determined using dynamic light scattering (DLS) for all samples prepared as outlined in section **2.1**. The melting point of a lyophilised sample was determined (> 310°C), using the capillary method.

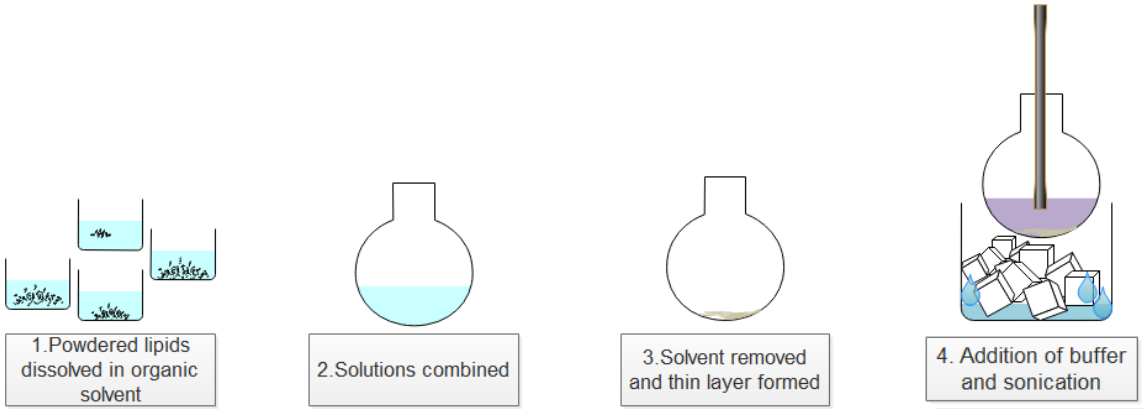

Figure 5. General procedure employed for the formulation of liposomes.

Optimisation of liposomal formulations

Experiment 1:

Formulations were prepared containing different ratios of the commercial lipids, the mal-linker and cholesterol to assess which formulation gave the better size and size distribution for this study. This was done by preparing 4 different formulations containing:

A: 30% DPPS, 30% DPPC and 40% cholesterol (v/v/v)

B: 15% DPPS, 15% DPPC and 70% cholesterol (v/v/v)

C: 45% DPPS, 45% DPPC and 10% cholesterol (v/v/v)

D: 10% mal-lipid, 25% DPPS, 25% DPPC and 40% cholesterol (v/v/v)

Using the 1 mM solutions of each lipid prepared, the lipids were combined in the correct ratio by volume, depending on the total volume of the formulation prepared. All % regarding ratios of lipids in formulations are essentially mol%.

Samples were prepared as stated in the **general procedure**. Sample formulations A,B and C were then analysed by DLS to assess size and size distribution. Sample preparation for DLS: Following the sonication step, 1 mL samples of each formulation were placed in disposable plastic cuvettes. DLS was performed using the Zetasizer as stated in the methods section (**2.1**), following preparation of SOP.

TEM was also performed (as outlined in section **2.1**) on all of the formulations prepared (A-D) to assess the shape and morphology. TEM was also performed on a small amount of lyophilised D type formulation to confirm liposomes retain their spherical structure after being freeze dried. All liposomal formulations passed this point of the study were prepared containing either:

A: Maleimide linker (10%), cholesterol (40%), DPPS (25%) and DPPC (25%) (v/v/v/v) or

B: Cholesterol (40%), DPPS (30%) and DPPC (30%) (v/v/v).

Experiment 2:

Samples were prepared as stated in the general procedure as type **B** formulations. Each formulation had a final volume of 6.50 mL and was sonicated for different periods of time at different amplitudes using three different sonicators (*table 2*). Repetitions of each of the formulation production and therefore the sonication procedure indicated in brackets were carried out to improve reliability and reproducibility of results.

Liposomal formulation	**Sonicator**	**Amplitude**	**Time**
1	Bath FB15051	N/A	10 min continuous pulsing
2	QSONICA	50%	10min continuous pulsing
3 (x2)	Sonic Dismembrator-Ultra Liquid Processor	50%	10min continuous pulsing
4 (x2)	QSONICA	90%	10min continuous pulsing
5 (x2)	Sonic Dismembrator-Ultra Liquid Processor	90%	10min continuous pulsing
6	QSONICA	50%	3 x 2min pulse on, 30 sec pulse off
7	Sonic Dismembrator-Ultra Liquid Processor	50%	3 x 2min pulse on, 30 sec pulse off
8	QSONICA	100%	10min continuous pulsing

Table 2. Showing the different sonication methods used for the optimisation of liposome formulations, altering power and time of sonication with the use of a bath and two probe sonicators.

2.5 Conjugation reactions

General reaction protocol

The liposomal formulations were conjugated to the specified protein overnight. Each reaction contained TCEP solution of pH 7, given number of equivalents with respect to the protein. The conjugated samples were then purified through size exclusion chromatography (SEC). The liposomal peaks were collected manually. These were combined and concentrated using 10K molecular weight cut off (MWCO) spin columns.

Protein concentration

Protein concentration was determined by nanodrop (outlined briefly in section **2.1**). Bradford assays were also run on the conjugated samples used for the *in vivo* study to confirm the amount of protein present. 96 well plate assay standard procedure was used for protein concentration of 0.1-1.4 mg/mL with BSA (bovine serum albumin) as the standard protein. The Bradford reagent was added to the plate and then the protein samples (standards at concentrations: 12.5, 25, 50, 100, 200, 400, 800 and 1600 µg/mL and the unknown 08730/ TcdB conjugate formulations) were added. PBS and naked liposomal formulation were used as blanks. The absorbance at 600 nm was recorded.

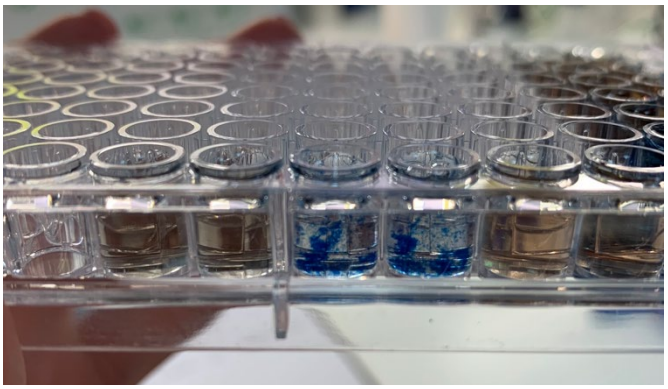

Figure 6. Showing plate with standards and protein formulations (TcdB and 08730) with Bradford reagent used for the determination of protein concentrations in the conjugated formulations.

GFP conjugations

Experiment 3:

Liposomal samples were prepared as stated in the **general procedure** with final total volumes of 5.00 mL. Conjugations were then performed as stated in section **general reaction protocol** using amounts stated in *table 3*. All GFP conjugated samples were then analysed using FACS as stated in section **2.1**.

Formulation	Volume of formulation conjugated (μL)	Mass of GFP (mg)	Equivalent to mal-lipid
A	150	0.27	0.2
A	500	2.69	2
B	500	2.69	N/A (Amount that would equal to 2 eq)
A	500	6.73	5
A	500	13.5	10

Table 3. Showing amounts of liposomal formulation and GFP used in the first GFP conjugation to liposomes.

Experiment 4:

Experiment 3 was repeated with the addition of TCEP (2 eq with respect to GFP) to each reaction. 150μL from each formulation were used per conjugation. Concentration of GFP solution was determined using Nanodrop and amounts shown in *table 4* were used.

Formulation	Amount of GFP (nmol)	GFP equivalent to mal lipid	Amount of TCEP (mg)
A	30	2	0.0517
B	30	N/A (Amount that would equal to 2 eq)	0.129
A	75	5	0.0517

Table 4. Showing amounts used in the second round of conjugations of GFP to liposomes with excess lipid.

Experiment 5:

Experiment 2 was repeated with total volume of the formulations generated 14.51 mL. This was then separated into 2 fractions of 3.71 mL and 10.8 mL. The latter was then concentrated to make 5.70 mL solutions with a 1.9 mM concentration. TCEP (12.8 μg) was added. Each batch was conjugated to GFP using the amounts that follow:

Formulation	Volume of liposomal formulation (mL)	Amount of GFP
A	3.71	1.00 mg
A	5.70	10.0 mg
B	3.71	1.00 mg
B	5.70	10.0 mg

Table 5. Showing amounts for GFP conjugations to liposomes with and without maleimide lipid used in the third round of GFP conjugations to liposomes.

2.6 Lyophilisation with trehalose

Part of conjugated sample B to 10.0 mg of GFP was then split into 6 Eppendorfs each containing 1.50 mL of solution each (1.045 mg of total lipid using the average lipid mass and assuming complete retention of the formulation). Each of the samples was freeze dried with a different percentage of trehalose sugar with respect to the amount of lipid. 10.0 mL Stock solutions of trehalose in PBS were produced, from which 10.0 µL of the different solutions were added to the different sample preparations depending on the desired percentage (*table 6*). For 1000% by mass, 10.0 mg of sugar were added to the sample. Once lyophilised the samples were reconstituted through addition of 1.50 mL of water to each and analysed.

Sample No.	Amount of trehalose (percentage by mass)	Amount on trehalose sugar in 10.0 mL of stock (g)
1	0%	0
2	15%	0.1567
3	30%	0.3135
4	50%	0.5225
5	100%	1.045
6	1000%	10.023

Table 6. Showing amounts of sugar used to determine the formulation with the best consistency, size and size distribution using different percentages (by mass) of trehalose sugar.

2.7 *In vivo* sample formulation

Liposomal formulation samples were prepared as stated in the general procedure. Type **A** formulations (Maleimide linker (10%), cholesterol (40%), DPPS (25%) and DPPC (25%) (v/v/v/v)) were prepared 4 times, with a final total volume of 10.8 mL each. They were then combined to make two liposomal mixtures, one for each antigen. The final solution

was concentrated and then conjugated to 20.0 mg of the specified antigen, as stated in *table 7*. Type **B** formulations (Cholesterol (40%), DPPS (30%) and DPPC (30%) (v/v/v)) were also prepared (x2) with a final total volume of 10.8 mL were used as the naked non conjugated control groups. All conjugation reactions were carried out as stated in the **general reaction protocol** (section **2.5**). Bradford assay was carried out as stated (**protein concentration** section **2.5**) to determine loading of conjugated samples.

Formulations type A	**Final volume after concentrating**	**Final concentration of liposomal formulation**	**Antigen conjugated**	**Amount of TCEP**
1	1.55 mL	13.9 mM	08730	0.315 mg (=2 equivalents)
2	1.25 mL	17.3 mM	TcdB	0.188 mg (=2 equivalents)

Table 7. Showing amounts of liposome, TCEP and protein used in the conjugation reactions for the in vivo samples.

2.8 Final stage of *in vivo* sample preparation

Samples were then freeze dried so that each one contained 1.00 mg of protein. The respective 1000% by mass of sugar was added as shown in *table 8.* 12 samples were prepared for each group. Antigen names not quoted in full for simplicity.

Sample group	Volume of conjugated formulation in each Eppendorf	Amount of total lipid present in each sample	Amount of trehalose sugar added
08730 loaded samples	1.33 mL	0.846 mg	8.46 mg
TcdB loaded samples	0.928 mL	1.00 mg	10.0 mg
Naked liposomes	1.13 mL	0.728 mg	7.28 mg

Table 8. Amounts of conjugated samples and sugar used in the final in vivo sample formulations.

Samples were then packed into capsules (Clear porcine hard gelatin capsules (capsule volume 0.025 mL)) manually. Capsules were also packed with 08730 and TcdB free antigens freeze dried with trehalose and trehalose sugar only. Six different types of capsules were generated for the immunisation study as stated below:

A: 1.00 mg 08730 loaded liposomal formulation lyophilised with trehalose sugar x12

B: 1.00 mg TcdB loaded liposomal formulation lyophilised with trehalose sugar x12

C: 1.00 mg 08730 antigen alone lyophilised with 10.0 mg trehalose sugar x12

D: 1.00 mg TcdB antigen alone lyophilised with 10.0 mg trehalose sugar x12

E: naked liposomal formulations lyophilised with trehalose x12

F: 10.0 mg trehalose only x6

Coating determination of the capsules was performed by Cansu Karyal. The packed and coated capsules were then used for an *in vivo* immunisation study conducted with Syrian hamsters.

2.9 Further studies

In vitro pathogenicity assays will also be performed with anti-CD630_08730 (antibody) to test ability to block colonisation using Caco-2 cell. Anti-CD630_TcdB-RBD sera and blood will be used to test the ability to neutralise toxins in toxin-neutralisation assays while binding to IgGE using the same sera from the hamsters will also be determined by ELISA microarrays. Should the formulation prove immunogenic *in vivo*, the immunisation study will be repeated to find the minimum dose for the vaccine formulation: i.e. dose that promotes the highest, safe level of antigen specific secretory IgA and serum IgG.

Preparation of the liposomes using the bespoke lipids could also be performed using a heating method were lipids are hydrated for 1 hour and then heated for 1 hour above the transition temperature in the presence of a hydrating agent, avoiding the use of any organic solvents. As cholesterol is part of the formulation the reaction medium could be heated to 100^{o}C thus the resultant liposomes could be used without any sterilisation treatment.[74]

Surface charge determination of liposomal formulations would be another aspect of analysis (using the Zetasizer) as it also has an effect on intestinal absorption.

3. RESULTS AND DISCUSSION

3.1 Expression and purification of CD630_08730 protein

Protein expression was achieved through exploitation of the pTWIN1 vector system to express recombinant *Clostridium difficile* proteins.[76] In our case, capturing the target protein was proven challenging therefore an adaptation of the system was performed (developed by the Griffin group- patent under development) to prevent loss of the target proteins, which allowed for purification through by immobilised metal affinity chromatography (IMAC) and *in vivo* cleaved proteins to be trapped by the Ni^{2+} column.

Briefly, after induction of expression, the supernatant containing proteins in the cytosol (soluble fraction) was harvested. In order to check if the protein of interest had formed inclusion bodies or aggregated, the pellet (insoluble fraction) was further re-suspended in binding buffer. Cell lysates of induced and non-induced T7 express cells expressing recombinant proteins were fractionated by 10% (w/v) SDS-PAGE and visualised by coomassie blue staining. The expected molecular weight of CD630_08730 after intein cleavage was 36 kDa. Expected molecular weights of the rest of the antigens successfully expressed by the Griffin group were as follows; CD630_TcdB-RBD (61 kDa), GFP (26 kDa).

Protein purification of doubled affinity proteins was performed by affinity chromatography performed with Nickel beads. 08730 was purified bypassing induced cell lysates through a column containing Ni^{2+}. The intein tag was cleaved during a shift of pH. Release of target protein with N-terminal cysteine occurred due to the natural cleavage of the intein tag. Increasing concentrations of imidazole were used to elute the target protein from the Ni^{2+} beads. Elutions were visualised by 10% (w/v) SDS-PAGE (*figure 7).*

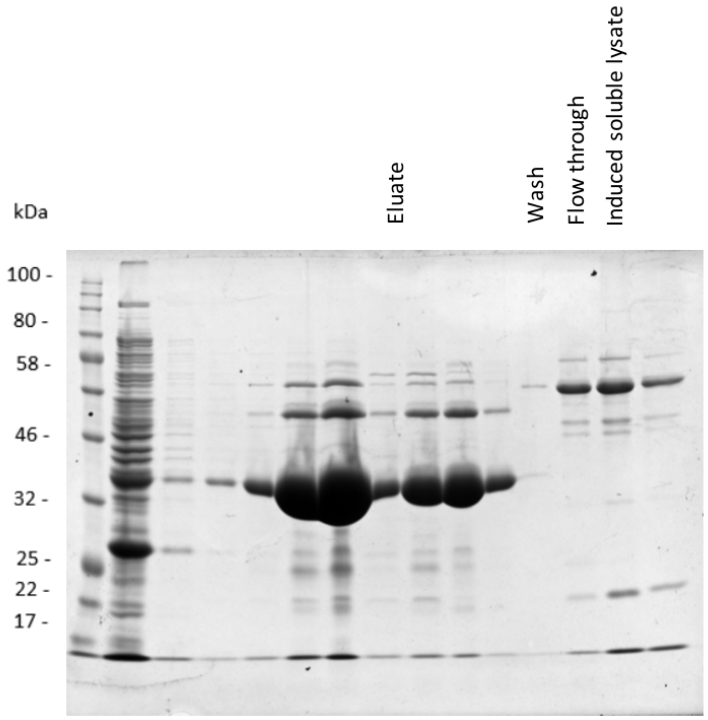

Figure 7. Showing purification of recombinant protein CD630_08730. The protein is present at a high concentration in the eluate.

The intein tag was successfully cleaved following purification however the eluates obtained gave insufficient yield. More large scale preps were made that were also of low purity for downstream conjugation to liposomes. The protein was therefore dialysed in PBS and further purified by size exclusion chromatography as described in section and shown in section **3.2**. This expression system was previously used by the Griffin lab to produce a number of batches of the different proteins. In this project they were all further purified with SEC and the results obtained for some are described below.

3.2 Purification of proteins with Size Exclusion Chromatography

Size exclusion chromatography (SEC) separates molecules in a solution by their size and shape as they pass through a resin packed column (section **2.1**). The resin consists of a porous matrix of spherical particles. As a sample is applied, molecules larger than those

pores are unable to diffuse into the beads and therefore elute first. Molecules that vary in size penetrate the pores to different degrees based on that size (and shape). The very small molecules will elute last as they enter the pores and travel the length of the column. SEC was used to purify 08730, TcdB and GFP used for conjugations to liposomes. The wavelength detector was set to 280 nm and all proteins were eluted in PBS in an attempt to preserve their confirmation which indeed proved better in PBS rather than in deionised water, and also prevent any changes in concentrations of liposomes that were formulated in PBS during conjugations to antigens purified. It should be noted that for some of the chromatography elution profiles, elution points were specified in elution time. Elution volume was also calculated in these cases, using Column Volume (CV) and flow rate, and is given in brackets.

08730 purification

08730 purification trace using SEC is shown in *figure 8*. Three peaks were detected, after the injection peak, (elution points 1, 2 and 3) that corresponded to the three higher molecular weight band proteins viewed on the gel of the crude protein, at about 59kDa, 56kDa and 50kDa respectively. 08730 eluted at peak 4, having the highest absorbance due to its considerably higher concentration in the sample injected. Identification of peak 4 was confirmed by running only peak 4 elutions on a gel. This also confirmed the idea of having the ability to further purify our antigens with SEC as high purity samples were needed for the *in vivo* study and for a potential vaccine formulation at a later stage. 08730 protein eluted at about 19 minutes passed the injection point (assigning minute 0 to the injection point each time), therefore at around 14 mL (=0.75 CV). High molecular weight proteins started eluting 11 minutes from injection (elution volume: 8 mL). Peak 5 was the lower molecular weight impurity (27 kDa), also viewed on the gel of the crude protein. It took about 23 minutes (approximately one column volume) for the whole of the sample to pass through the column assuming conductivity change (brown line in *figure 8*) indicates last amount of sample has eluted.

Collecting the peaks manually and with high degree of precision, for example changing vials when the protein is eluted and not when it's being detected, or collecting the peak (=narrowest part) of the peak in a separate vial presuming it will be cleanest fraction containing the targeted protein, increased purity of desired proteins significantly. These methods employed were, however, time consuming and caused tremendous loss of material. Lyophilising batches of proteins produced and reconstituting in the minimum amount of solvent in order to minimise number of injections performed for each batch of antigen prepared helped with this issue. Nevertheless, multiple injections were performed for the purification of each batch of each antigen, as a maximum volume of 0.5 mL of the prepared sample was used per injection. All chromatography elution profiles shown are limited to one injection only i.e. only showing 0.5 mL of the sample purified, for simplicity.

Following collection of elution point 4 from each injection, gels were run to confirm the purify of the protein in question (*figure 8*) and removal of lower and higher weight bands.

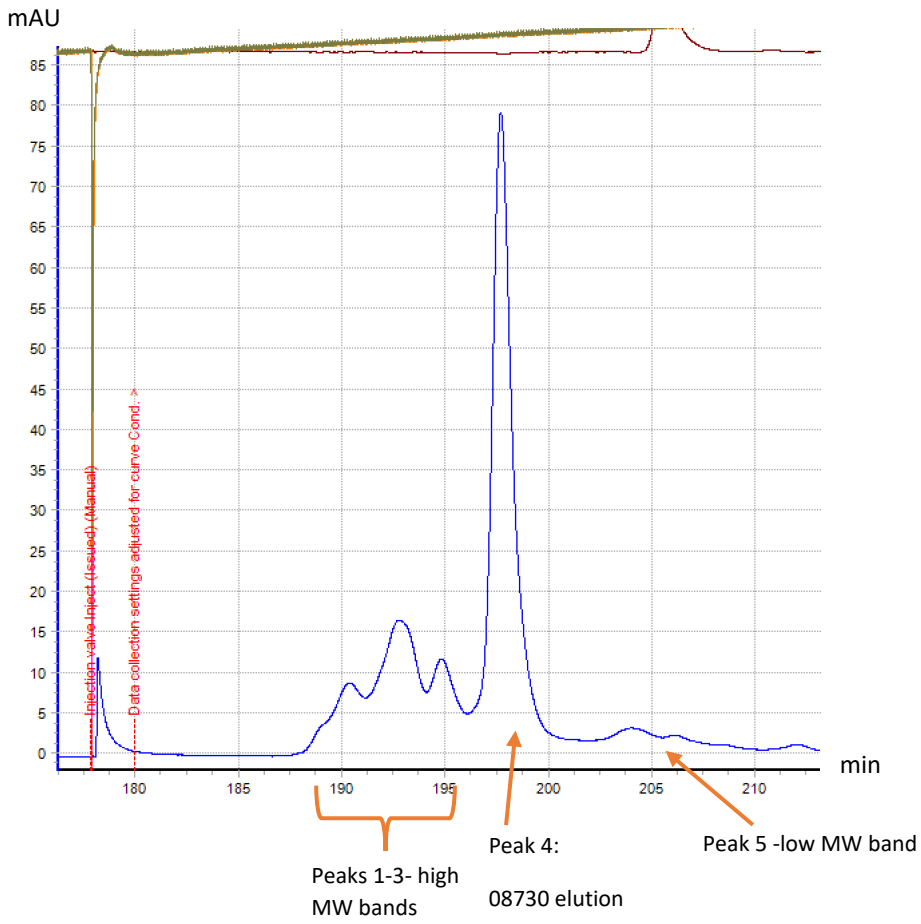

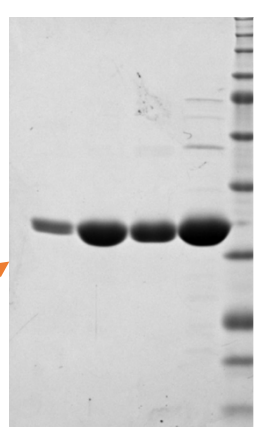

Elution No. 4 from 4 injections performed to purify that batch of 08730 confirming protein at 36 kDa

Figure 8. SEC trace of the 08730 protein purification showing 0.5 mL of sample purification, where peaks 1-3 are higher MW bands, peak 5 is a lower MW impurity, peak 4 is 08730 protein eluting 14 mL passed the injection point. Key: brown line: conductivity, red line: injection inlet, blue line: UV absorption at 280 nm. SDS PAGE run of peak number 4 elutions obtained from four different injections (purification runs) of the sample of crude 08730 protein in the AKTA.

TcdB purification

Purification of TcdB crude protein provided by the Griffin group was performed in a similar manner. As shown in *figure 9* TcdB eluted at about 15 minutes passed the injection point (elution volume: 11 mL) as peak 2 and therefore the second highest MW protein detected (band 3 at 61 kDa in *figure 9*). The whole crude sample had passed through the column after 29 minutes from the time of injection (22 mL). The higher molecular weight protein (elution point 1 on the chromatography and band 4 at 79 kDa on the SDS-PAGE gel (*figure 9*)) started eluting just 10 minutes in the run (elution volume: 7.5 mL). Lower molecular weight bands 1 (48 kDa) and 2 (50 kDa) lightly showing on the SDS PAGE corresponded to peaks 4 and 3 on the chromatogram, respectively.

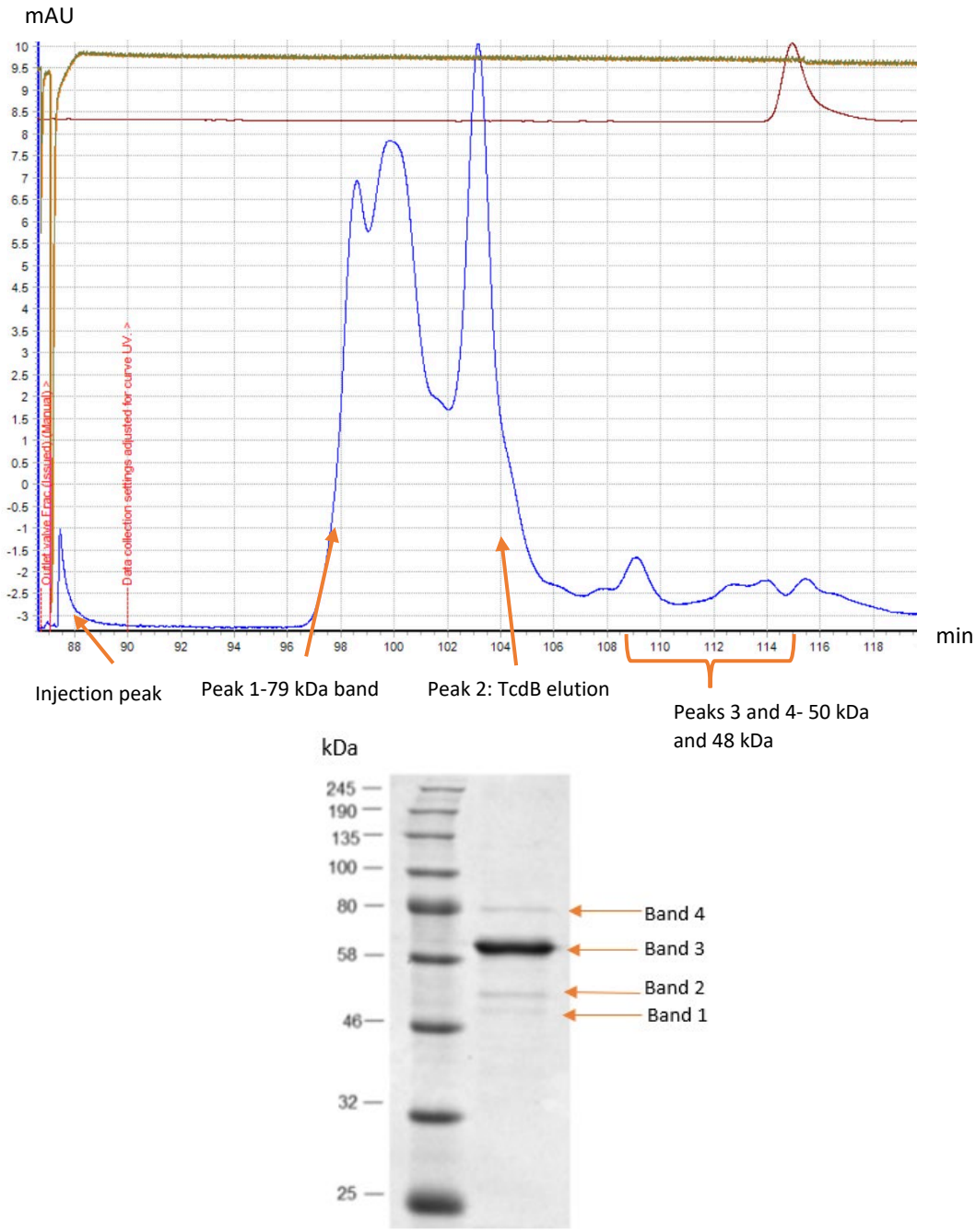

Figure 9. Showing SEC trace from a single injection (0.5 mL) of the crude TcdB in the AKTA, where peak 1 is a high molecular weight impurity (band 4 at 79 kDa), peak 2 is TcdB protein eluting 11 mL passed the injection point (band 3 at 61 kDa) and the two low molecular weight impurities are the smaller peaks 3 (band 2) and 4 (band 1) on the chromatogram. Key: brown line: conductivity, red line: injection inlet, blue line: UV absorption at 280 nm. SDS PAGE run (provided by the Griffin group) of the crude protein.

GFP purification

SEC traces (chromatogram) are shown in *figure 10.* Visualisation of the GFP SDS PAGE before and after AKTA purification is shown in *figure 11*. GFP was used as a surrogate to the antigens in order to confirm conjugations were feasible, ensure conjugations could occur at any scale (with lipid and therefore liposomes in excess or with protein in excess) and determine loading on protein on to the liposomes in order to be able to create a vaccine formulation with the desired amount of antigens. It did, however, prove to be the most difficult of the proteins to purify. Injecting a crude sample into the AKTA gave four elution peaks (*figure 10*), with the last being identified as GFP. The desired protein eluted 20 minutes passed the injection time (15 mL, 0.75 CV) whereas the higher molecular weight proteins started eluting after minute 10 (7.5 mL).

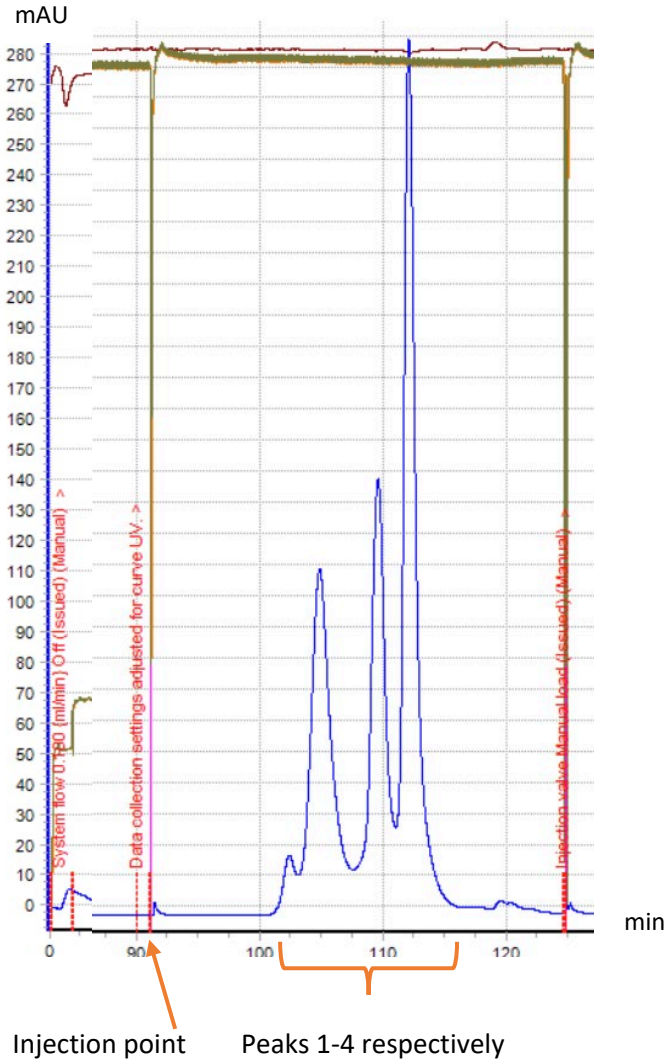

Figure 10. Showing the chromatogram of crude GFP, where the target molecule elutes at 15 mL (20 minutes passed injection) giving peak 4. Key: brown line: conductivity, pink line: injection point, blue line: UV absorption at 280 nm. Figure has been edited to omit the column equilibration section for better visualisation.

Running peak 4 elutions on a gel gave a double band as shown (*figure 11*) indicating the presence of a higher molecular weight protein, no matter how precisely that peak was collected. This impurity could not be identified. Purifications of GFP using AKTA were repeated several times until the cleanest possible GFP band could be obtained. SEC purification was also attempted with elution solvent however peak 4 was no longer

fluorescent therefore the assumption that GFP's conformation was better preserved in PBS was drawn and the purifications were then conducted in PBS.

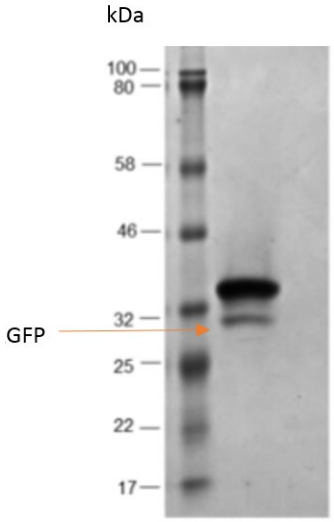

Figure 11. Showing SDS PAGE of AKTA purified GFP. Marked GFP is the targeted protein band at 27 kDa.

Running several different batches of GFP down the AKTA and running peak 4 elution on a gel always gave that higher molecular weight band. When however, that same elution was put down the SEC again, a single peak was obtained and therefore a fairly pure sample identified (*figure 12*). Absorption of the two other small peaks observed is probably minor (< 0 mAU). Conjugations to liposomes were performed with those re-purified samples as any other protein that might have still been present should not have a cysteine residue and therefore could not conjugate to the lipid linker. The higher molecular weight bands i.e. all peaks appearing before the GFP one were not fluorescent under UV and therefore would not have interfered with interpretation of FACS analysis and data. They shouldn't have interfered with the liposomes either as these were formulated prior to conjugations, since the method employed was not an encapsulation technique and as stated it shouldn't be able to bind to the maleimide linker.

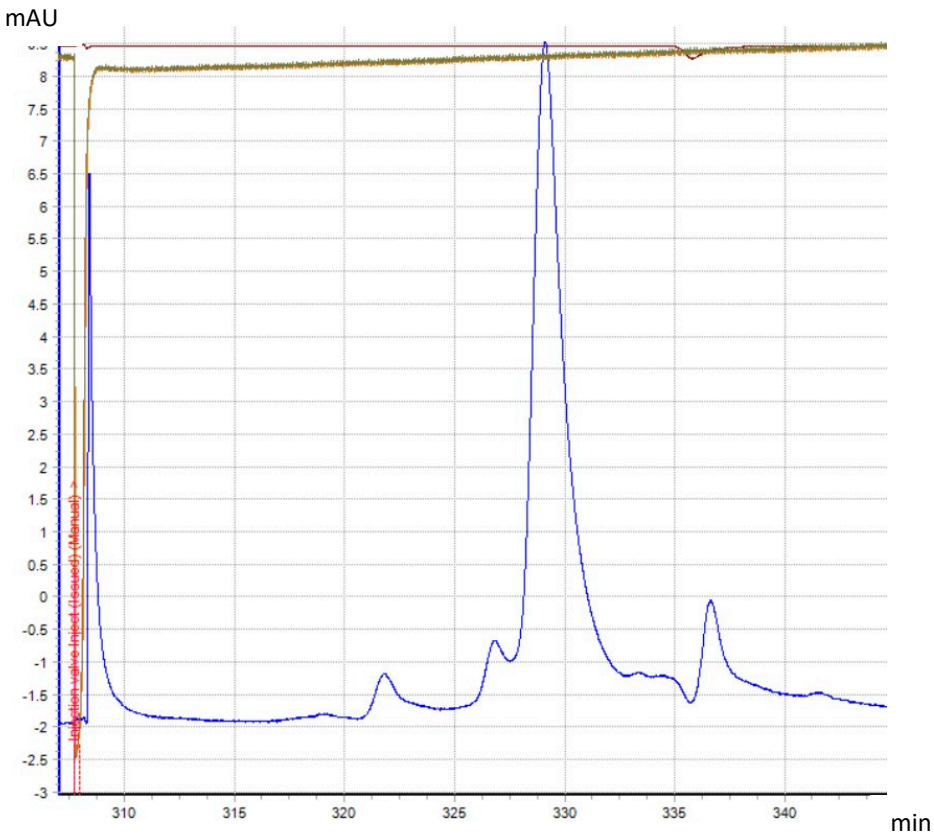

Figure 12. SEC trace of the purified fraction of GFP alone (peak 4 from the first purification of the crude -figure 10). The protein eluded 15 mL passed injection (20 minutes from injection time).

Immunogenicity of antigens CD630_08730 and CD630_TcdB-RBD, successfully expressed and purified was tested using using *C. difficile* patient serum form 20 infected individuals. Serum from non patients and serum from cystic fibrosis patients were used as the negative and positive control respectively. Ability to retain immunogenicity after lyophilisation was also tested for 08730 by using both a freshly prepared sample antigen stored in PBS stored at -20℃ and a lyophilised sample stored at RT and reconstituted in PBS. GFP provided the baseline to determine immunogenicity. Based on the confirmed immunogenicity of CD630_08730 and CD630_TcdB-RBD *in vitro*, these two antigens were taken forward to be used in the *in vivo* studies conjugated to liposomal formulations via a maleimide linker.

3.3 Synthesis of mal-lipid

Maleimide diester

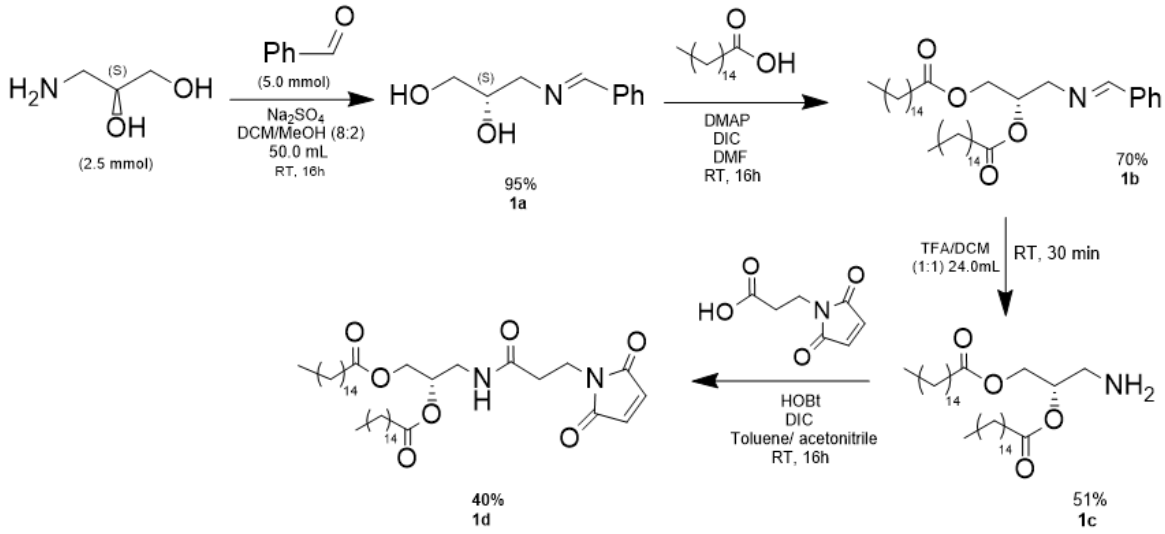

Scheme 1. Maleimide diester synthetic route.

As shown in scheme *(S)*-1, 3-amino-1,2-propanediol was reacted with benzaldehyde in a dichloromethane and methanol mixture in the presence of sodium sulfate anhydrous at RT for 16h (overnight). TLC was inconclusive so mass spectrometry was used to confirm completion of the reaction and formation of the *(S)*-diol product (product **1a**). *(R)*-stereochemistry is the most biologically active one for a glyceryl Pam lipid (i.e. thiol of a cysteine directly attached to glyrecyl unit). Attaching a nitrogen creates a product with *(S)*-stereochemistry as the nitrogen on the glyceryl molecule has a lower priority relative to the oxygen. The orientation of the groups however is still the same as the more biologically active *(R)*-glyceryl pam lipid. Product **1a** was then directly used in the following step where palmitoyl groups were introduced on the structure via esterification reactions between the alcohols of **1a** and palmitic acid using DMAP catalytically. **1a** was dissolved in DMF and the RM diluted in DCM. This reaction run overnight at RT to give the dipalmitoylated product **1b** in a good yield of 70% after work-up. This product was treated with a mixture of TFA/DCM monitoring the reaction progress with TLC dipped in ninhydrin until a new spot appeared that stained purple. After MS confirmed the presence the free amine; product 1**c**, this was isolated with 51% yield after purification. The acid, 3-

maleimidopropionic acid, was reacted with HOBt and DIC for 30min before **1c** was added to the reaction mixture in a toluene/acetonitrile solvent mixture. After 16h the maleimide lipid, **1d**, was identified by mass spectrometry. Repetition of this last time quite a few times allowed for a purification step yielding product **1d** (40% yield), however, impurities were still present after multiple purifications. ^{1}H NMR indicated presence of HOBt. The challenges associated with isolating this lipid in a suitable level of purity caused us to move away from this diester lipid for the formulations.

Maleimide diether

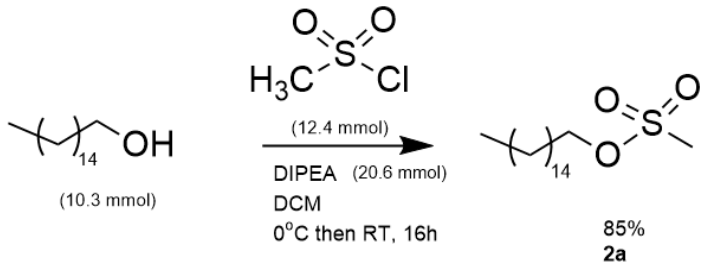

Scheme 2. First step of maleimide diether synthesis.

Scheme 2 shows synthesis of hexadecyl methanesulfonate, **2a**, via the reaction of cetyl alcohol in DCM in the presence of DIPEA and methanesulfonyl chloride. Addition of MsCl was carried out dropwise and on ice over 30 min. After 16h, the organic product was extracted in DCM to give a good yield (85%). Product **2a** was dried under very high vacuum to ensure complete removal of water for the next step (as shown in scheme 3) in order to prevent any contact with NaH that could lead to the release of flammable gases that ignite spontaneously.

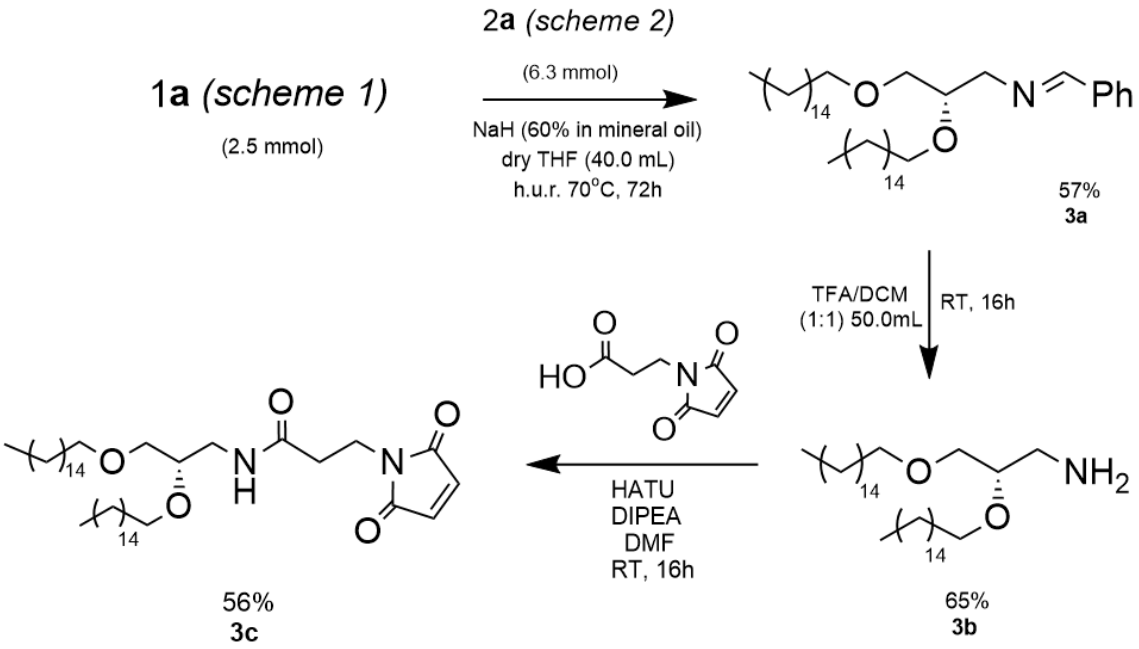

Scheme 3. Synthetic route for maleimide diether. Preparation of the first product (3a) involves the use of structures of 1a and 2a from schemes 1 and 2 respectively.

Products **1a** from scheme 1 (after being dried for several hours) and **2a** from scheme 2 were used as shown in the first step of the synthetic route shown in scheme 3. The reaction mixture was heated under reflux at 70℃ and took 72 h to reach completion. This formed the dipalmitoylated product **3a** which was used directly without purification to form product **3b** (65% yield after purification) through treatment with TFA overnight. The compound **3c** was formed via an esterification reaction in DMF, with HATU as the coupling agent and DIPEA as the catalyst. 3-maleimidopropionic acid was added to the reaction mixture first and allowed to react for 5 min before the dipalmitoyl was added. The reaction was completed over 16h and gave a pale yellow solid (**3c**), with 56% yield after purification. The amount of this synthetic linker needed in the liposomal formulations to conjugate proteins is minimal and therefore synthesis of a few milligrams was adequate, however, again challenges were faced purifying this batch as identified through NMR. Formulation of liposomes was therefore carried out using the batch previously made in the group (Rhys Griffiths).

3.4 Liposomal formulations

Liposomal formulations were prepared as indicated in section **2.4**. 1X PBS was chosen to be the aqueous phase over dionised water as all antigenic lipoproteins had better solubility in PBS and some also seemed to keep a preferred conformation in PBS in contrast to water, where for example GFP was not always fluorescent. To optimise size and shape of liposomes, that play a major role in their biologically function, the formulation procedure was optimised. To achieve this, the ratio of lipids used and the method of sonication were extensively studied as follows.

Lipid ratio optimisation – TEM/EDX

To determine the best ratio of lipids in the formulation and more specifically the ideal amount of cholesterol (mol%) present in the liposomes, samples were formulated as described in section **2.4.** Both DLS and TEM analysis was carried out on all formulations.

As shown in *figure 13* where **A** images were taken from a **Maleimide diether (mal) containing liposomes (10%) and 25% DPPS, 25% DPPC, 40% cholesterol** (v/v/v/v), liposomal formulations have spherical structures and a size of about 200 nm in this case. **B** images were taken from liposomes containing **30% DPPS and 30% DPPC lipids and 40% cholesterol** (v/v/v). This shows that the spherical structure of the vesicles is also true for 'no maleimide linker' (non-mal) formulations. From images **B** we can also conclude that the percentage of cholesterol has a major effect on the shape and size of the formulations as expected due to its well-known structural role in biological systems. In a study for the application of liposomes as oral vaccines it is reported that liposomes composed of DPPC, DPPS and Cholesterol in the molar ratio of 1:1:2 have relatively high stability and results also indicate that stability is improved by the increase of cholesterol content.[75] Stability in that study is determined by the leakage of carboxyfluorescein and therefore it can be argued that stability is a measure of preservation of shape and structure although not necessarily directly related. Interestingly here, by comparing images **B** to images **C (15% DPPS and 15% DPPC lipids and 70% cholesterol** (v/v/v)**)** and **D (45% DPPS and 45% DPPC lipids and 10% cholesterol** (v/v/v)**)** we can see that 'too much' or 'too little' cholesterol

does not allow for the spherical shape desired to be formed. The spherical structure of the nanoparticles is very important for their *in vivo* applications as antigens are required to anchor round the surface of the sphere to mimic native presentation of lipoproteins and have maximum immunogenicity effects. Liposomal formulations with both 70% (by volume) and 10% (by volume) cholesterol look distorted and uneven. Therefore the formulation containing 40% (by volume) cholesterol was the one used in further optimisation experiments and therefore conjugation reactions. Images **E** show **Maleimide linker containing liposome (10% by volume)** that has been **lyophilised and reconstituted in water to make 1X PBS**, the solution in which the liposomes were originally formulated in. The liposomal vesicles are clearly identified as black spheres. Viewing these images showed the formulations retain their structures after being freeze dried which is ideal for storing the formulations at room temperature. A high melting point (> 310 ^{o}C) has also been determined in that formulation which can be considered as high stability (along with phase transition temperatures) as the conditions at which the liposomes change state are an important consideration when assessing stability. The aim was to formulate stable liposomes that could be solidified and used as powders *in vivo* and have good reconstituting abilities, which has been met.

A: 10%Mal, 25%DPPS, 25%DPPC, 40%Chol (v/v/v)

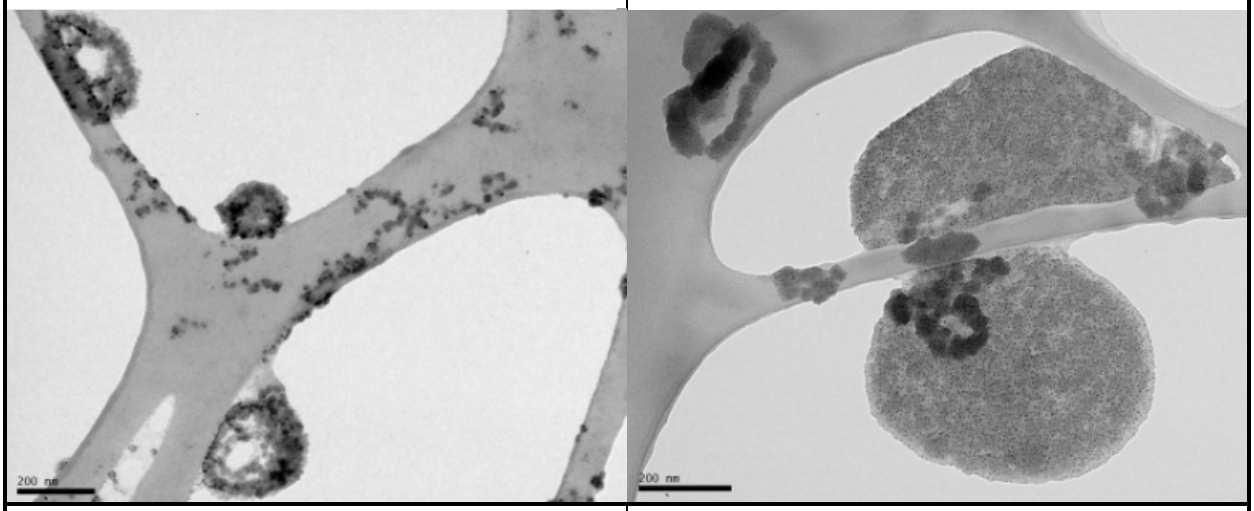

B: 30%DPPS, 30%DPPC, 40%Chol (v/v/v)

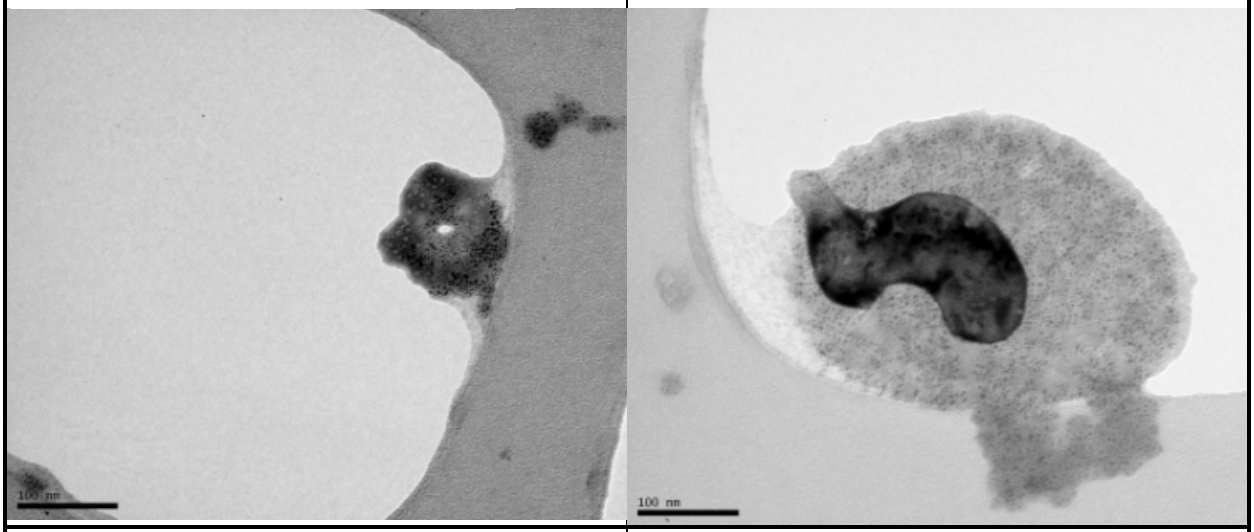

C: 15%DPPS, 15%DPPC, 70%Chol (v/v/v)

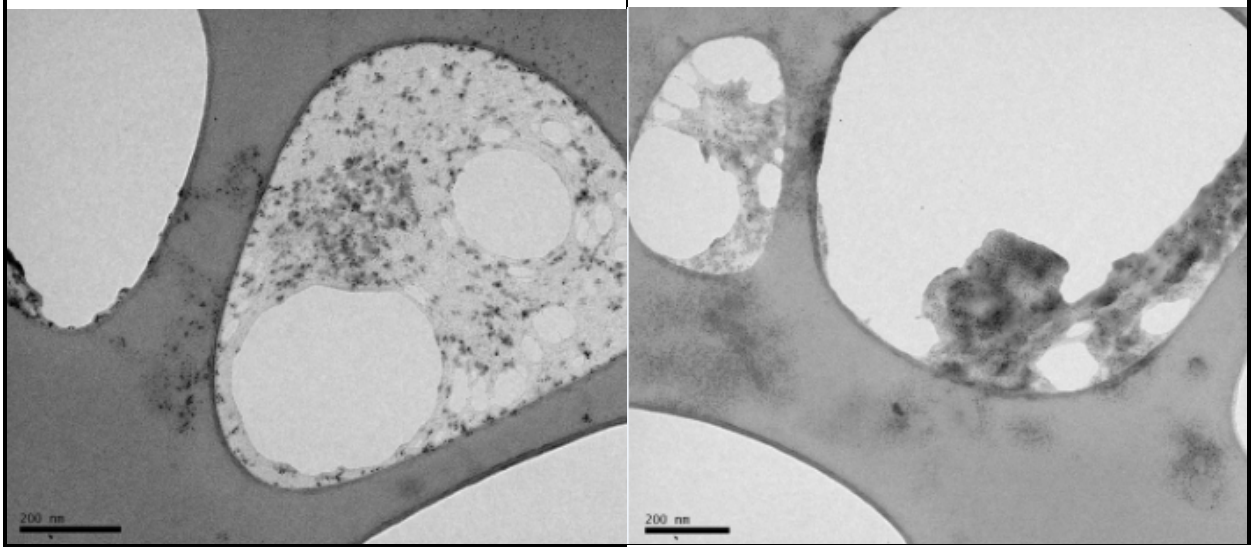

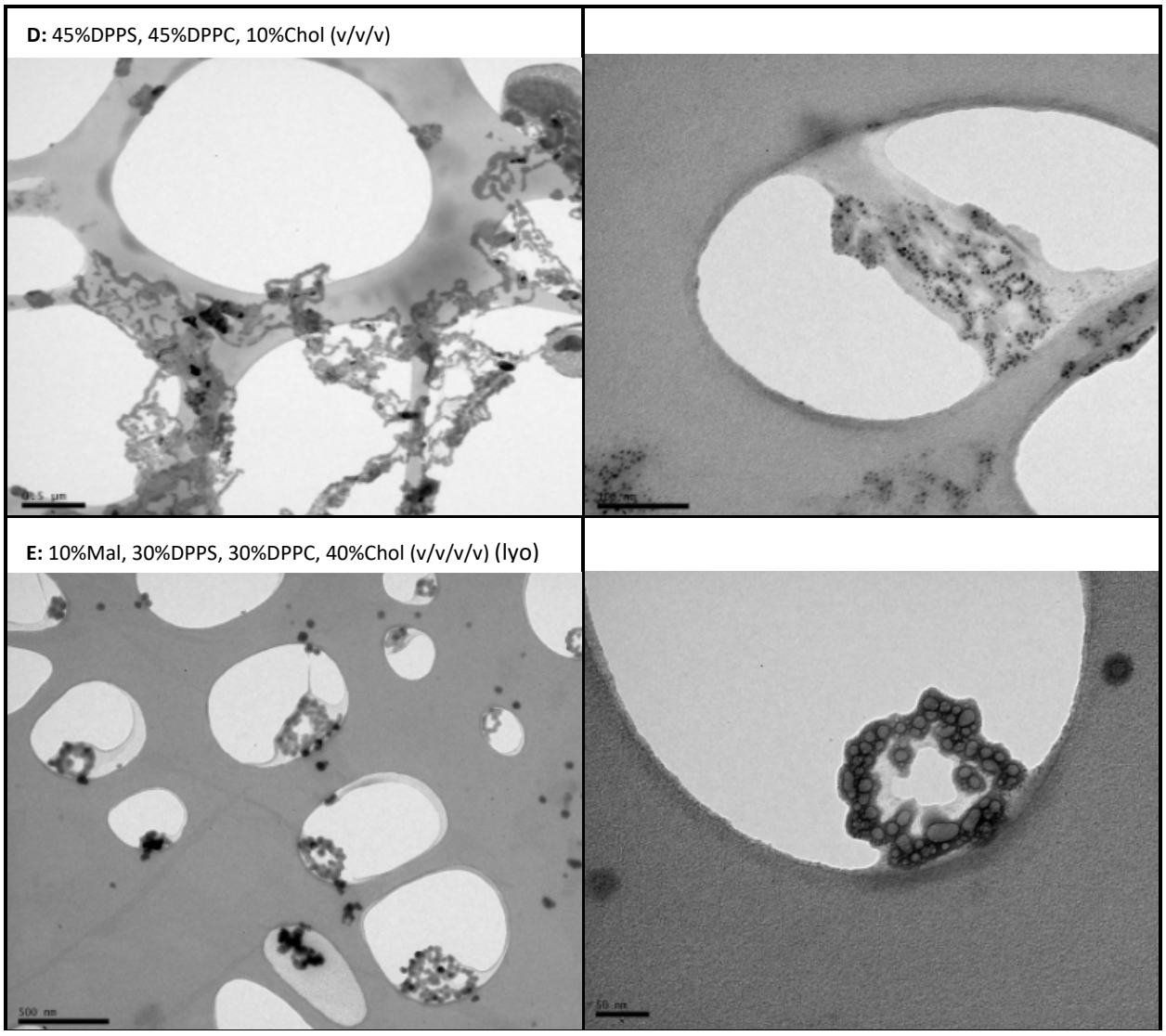

Figure 13. Transmission electron microscopy images of liposomes, consisting of different percentages of the maleimide diether (Mal), the commercial lipids (DPPS, DPPC) and cholesterol (chol), suspended in 1X PBS solution. Image E shows the liposomes with the ratio stated following lyophilisation (lyo) and reconstitution in 1XPBS.

Energy-dispersive X-ray elemental analysis was also carried out to confirm the elements present in the nanoparticles observed. As shown in *figure 14* the main elements present are Cu coming from the rings holding the material, K, Na, P and Cl from PBS solution hydrating the lipids, C, O, P and Na making up the lipids forming the liposomes. As

observed in most images in *figure 14* above, dark spots appear that are presumed to be the phosphate head groups on lipids which are electron dense regions.

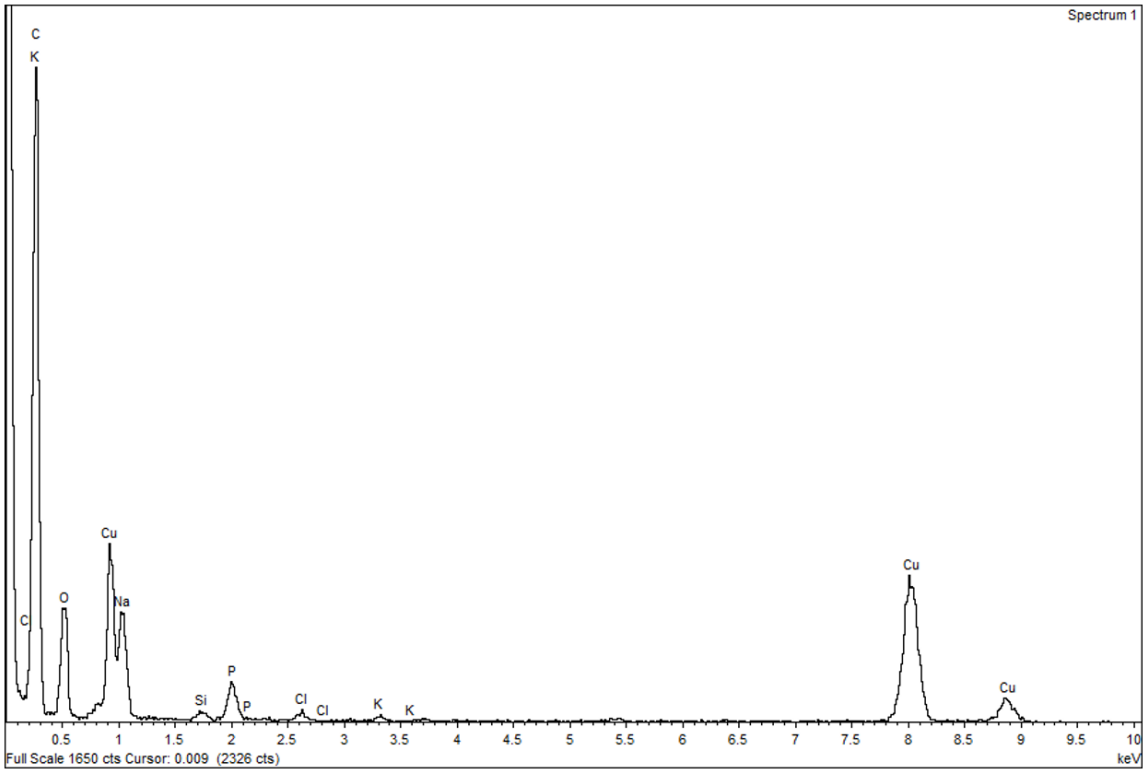

Figure 14. EDX elemental analysis of Maleimide linker containing liposomal formulation (10% mal-linker, 25% DPPS, 25% DPPC, 40% Cholesterol (v/v/v/v)).

Lipid ratio optimisation – Dynamic Light Scattering

Similar conclusions were also drawn by analysing formulations with Dynamic Light Scattering. The operational principle of DLS is based on Brownian motion, continuous movement of particles due to them being bombarded by solvent molecules, causing therefore the scattering of light applied. The size is then deducted by the amount of light scattered which depends on the diffusion rate which is in turn related to particle diameter. For each of the samples analysed 70 scans were recorded (14 scans per measurement). The software then produced an average size and distribution of that size population using data from all scans. Specifically, it provides the z-average which is the

intensity weighed mean hydrodynamic size of the collection of particles and the PDI (polydispersity index) which is the square of the light scattering polydispersity (standard deviation/mean) , therefore PDI= (stddev/mean)^2. Graphs (*appendix figure 6.13*) were plotted from data obtained by analysing formulations with **A**: 40% cholesterol, 30% DPPS and 30% DPPC (v/v/v), **B**: 70% cholesterol, 15% DPPS and 15% DPPC (v/v/v) and **C:** 10% cholesterol, 45% DPPS and 45% DPPC (v/v/v). For ease of comparison of results obtained for average size and distribution of that size are stated in *table 9*. It is observed that liposomes formed with 40% cholesterol by volume, gave the smallest nanoparticles with an ideal size (100-200 nm) for *in vivo* studies for efficient uptake by host cells as the smaller the diameter in that range the higher the efficiency of intestinal absorbance. Type **A** liposomes also produced the most monodisperse solution, indicated by the very low polydispersity index (PDI) of 0.195 (*figure 15*). PDI is an estimate of the width of the distribution, with values between 0-1 inclusive where 0 indicates a highly monodisperse population of nanoparticles and 1 a high degree of polydispersity. In this study the cut off point was set to be a PDI of 0.3, assuming that this value would change after freeze drying and rehydration, aiming at the lowest possible value for the liposomal formulations before any further treatments. As also derived from *figure 13*, liposomal formulations with 70% and 10% cholesterol by volume did not form even spherical vesicles of good size and therefore were not considered further in this study.

Liposome formulation	Z-average (d.nm)	PDI
Type **A**	135.7	0.195
Type **B**	370.5	0.574
Type **C**	245.0	0.381

*Table 9. Showing DLS data (Z-average: mean hydrodynamic size and PDI: size distribution index) obtained by analysis of liposomes formulated with varying percentages of cholesterol to optimise ratio of lipids to be used in in vivo studies based on size and distribution of size, where types **A**: 40% cholesterol, 30% DPPS and 30% DPPC (v/v/v), **B**: 70% cholesterol, 15% DPPS and 15% DPPC (v/v/v) and **C:** 10% cholesterol, 45% DPPS and 45% DPPC (v/v/v).*

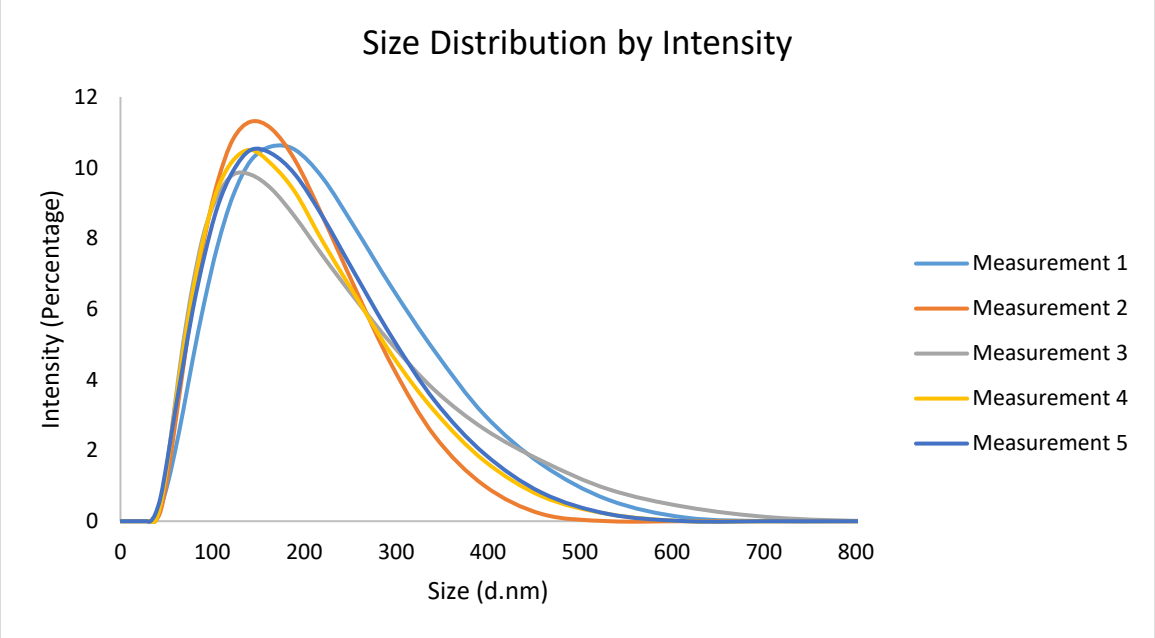

Figure 15. DLS plot of analysis of type A liposomes (40% cholesterol, 30% DPPS and 30% DPPC (v/v/v)) with average size 135.7 nm and PDI 0.195.

All liposomes passed this point in the study were formulated as either 10% mal-linker, 25% DPPC, 25% DPPS, 40% cholesterol (v/v/v/v) referred to as *mal-liposome* (**A**) or 30% DPPC, 30% DPPS, 40% cholesterol (v/v/v) referred to as the *non-mal liposome* (**B**).

Sonication method optimisation

To determine liposomal population size and distribution using different sonication methods, i.e. variable sonication times, amplitudes and sonicator types involved and thus optimise the formulation of the liposomes, DLS and FACS analysis was carried out on a range of liposomes sonicated under different conditions. All formulations were made up with 30% DPPC, 30% DPPS and 40% cholesterol (v/v/v) (type **B**: non-mal liposomes) and were prepared as described in section **2.4**. Analysing the derived plots (*appendix figure 6.14-figure 6.17*) we can conclude that using Qsonica sonicator at an amplitude of 90% for 10 minutes with continuous pulsing gave the best formulation of liposomes with regards to average size and polydispersity and therefore the most uniform population.

From this point onwards all liposomal formulations were sonicated using this preferred method, in an attempt to optimise the formulations produced for the in vivo study and to also work with uniform populations throughout all experiment to allow for more reliable comparison of results. For ease of comparison results are quoted in *table 10*.

Sonicator	Amplitude	Pulsing	Z-average (d.nm)	PDI
Bath	N/A	10 min continuous	564.0	1.00
Q	100%	10 min continuous	124.4	0.204
S	50%	10 min continuous	201.8	1.00
Q	50%	10 min continuous	132.8	0.412
S	50%	2 min (x3) 30 sec off	301.7	0.732
Q	50%	2 min (x3) 30 sec off	156.5	0.668
S	90%	10 min continuous	276.0	0.527
Q	90%	10 min continuous	119.1	0.210

Table 10. DLS data (Z-average and PDI) obtained by examining different sonication methods while altering power and time of sonication on non-mal liposomes (type B: 30% DPPC and DPPS and 40% cholesterol (v/v/v)), where Q is Qsonica sonicator, S is Sonic Dismembrator-Ultra Liquid Processor.

Findings from DLS were also confirmed with FACS analysis, were the number of fluorescent signals are recorded occurring from the way light is scattered, which depends on the size, shape and uniformity of the population being analysed. Scatter plots were drawn after approximately 22, 000 events of population occurring. Graphs seen in *figure 16* have forward scatter plotted on their x-axes and side scatter on their y-axes. As seen from DLS data in *table 10* and confirmed from the plots below, using Qsonica at 90% amplitude with 10 minutes of continuous pulsing (image **F**) produced the most homogeneous formulation, as determined by surface area. Forward and side scattering are plotted forming the graphs below as light is scattered from the nanoparticles allowed for the determination of the most uniform liposomal population which is required in order to ensure similar loading with antigenic proteins and optimal uptake by host cells.

From this point onwards, all liposomal formulations was prepared using the proposed procedure.

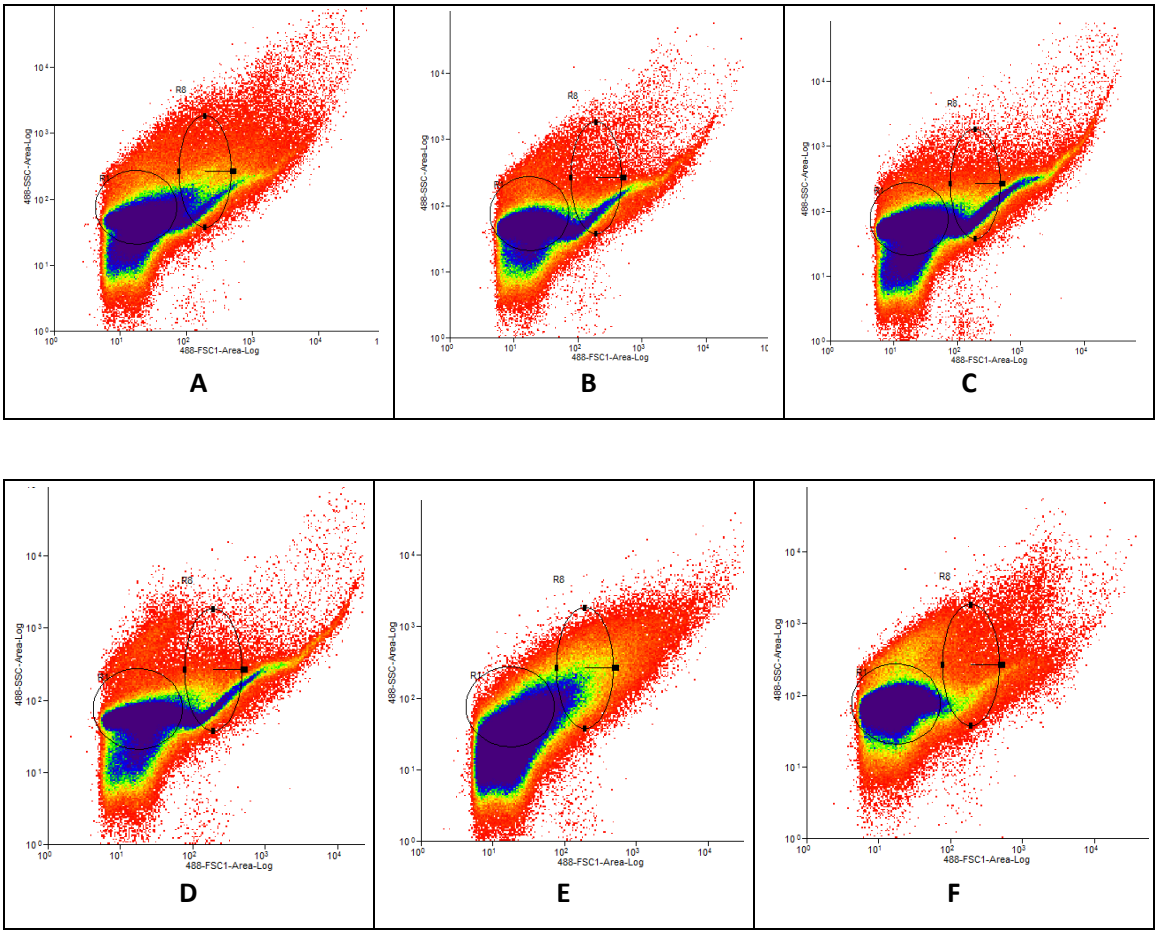

*Figure 16. FACS data for the determination of the best sonication method, where scatter plot **A** is analysis of a sample that was formulated using the Sonic Dismembrator-Ultra Liquid Processor (SDULP) at 50% amplitude for 10 min continuous pulsing, **B** using Qsonica at 50% for 10 min continuous pulsing, **C** SDULP at 50% for 3X 2min pulsing on, 30sec pulsing off method, likewise **D** however using the Qsonica sonicator, **E** prepared with SDULP at 90% on 10min continuous pulsing and **F** following the same method as **E** but using Qsonica instead.Data obtained on analysis of n on non-mal liposomes (30% DPPC, 30% DPPS and 40% cholesterol (v/v/v)).*

3.5 GFP conjugations

Purification of conjugates

GFP was employed in a number of experiments to optimise the potential vaccine formulations generated. This involved the optimisation of the conjugation of antigens to the liposomes. Having the N-terminal cysteine, GFP can conjugate onto the maleimide head of the synthetic lipid mimicking the final vaccine formulation. TCEP was used as a reducing agent to ensure all disulfide bonds were broken and increase efficiency of conjugation. GFP was conjugated to liposomes in a number of different ratios of protein with respect to lipid (lipid or protein in excess). All conjugated samples were purified using SEC and 50K molecular weight cut off (MWCO) spin columns before being analysed with FACS or used further along in the project. In this case the elutions were recorded as elution volumes (in mL). As shown in *figure 17*, the conjugated maleimide containing liposomes to GFP (150 μL of a 1 mM liposome formulation i.e. 15 mmol of mal lipid, to 30 mmol of GFP i.e. 2eq with 51.7 μg of TCEP) targeted product eluted 7.5 mL after injection of the sample for 2.5 mL volume. Conjugates gave the first peak in each trace as they were the largest molecules in all samples being purified. As free GFP eluted at 20 minutes after injection (15 mL= 0.75 CV) seen in *figure 10* and *17* we can conclude that the liposomal peaks have successfully been separated from any free protein present in the sample.

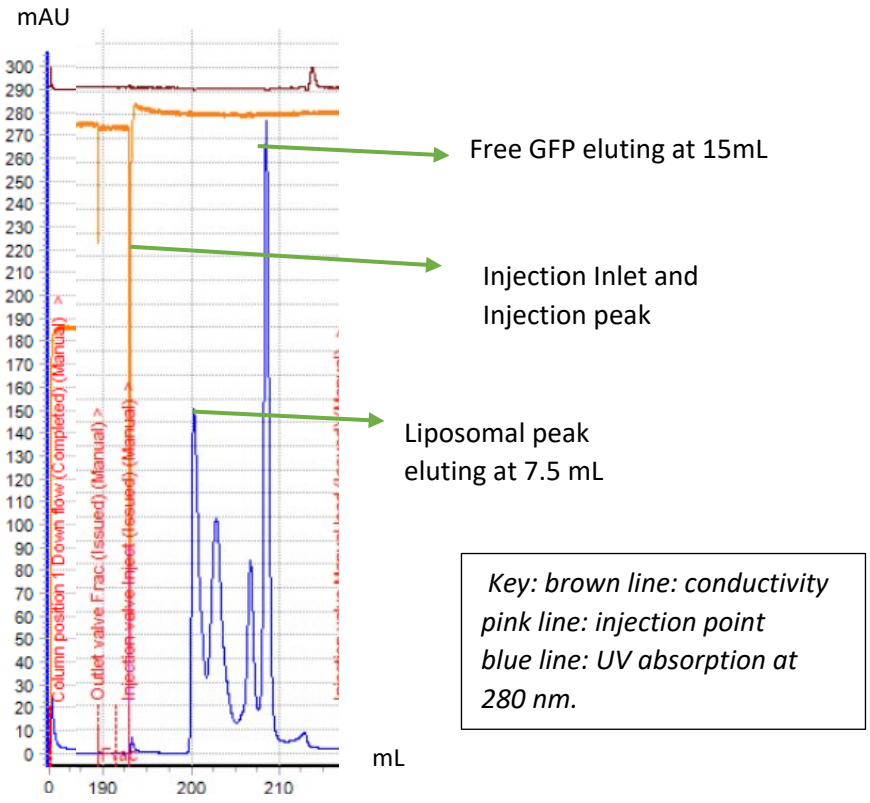

Figure 17. Showing SEC trace from a single injection (0.5 mL) of the conjugation product of a 10% mal-lipid, 30% DPPC, 30% DPPS, 40% cholesterol (v/v/v/v)- liposome and 2eq of GFP. Figure has been edited to remove the column equilibration section for better visualisation of the results.

Similar results were obtained through purification of a non-mal (30% DPPC, 30%DPPS, 40% cholesterol (v/v/v)) liposomal formulation conjugated to what would have been equal to 2eq with respect to mal-lipid, i.e. 30 mmol, of GFP. The liposomal peak eluted 6 minutes (5 mL) after the injection point (*appendix figure 6.18*) and following use of the 50K MWCO spin column analysed with FACS. Injection of non-conjugated (naked) mal-liposomes on the AKTA, that eluted mainly 9 minutes after injection (7 mL) as seen on *figure 18*, shows a significant decrease in absorbance from 148 mAU (peak of mal-liposomal formulation conjugated to GFP -*figure 18*) to 44 mAU. Both conjugated and non-conjugated liposomes elute at about the same time and volume as the protein attached in conjugation is only a few nm in size and it wouldn't greatly affect elution down a column. Elution is also affected by the shape, however the main property utilised for

separation in this study is size due to the ease of comparison between different protein bands present in samples and also liposomes which are a lot larger.

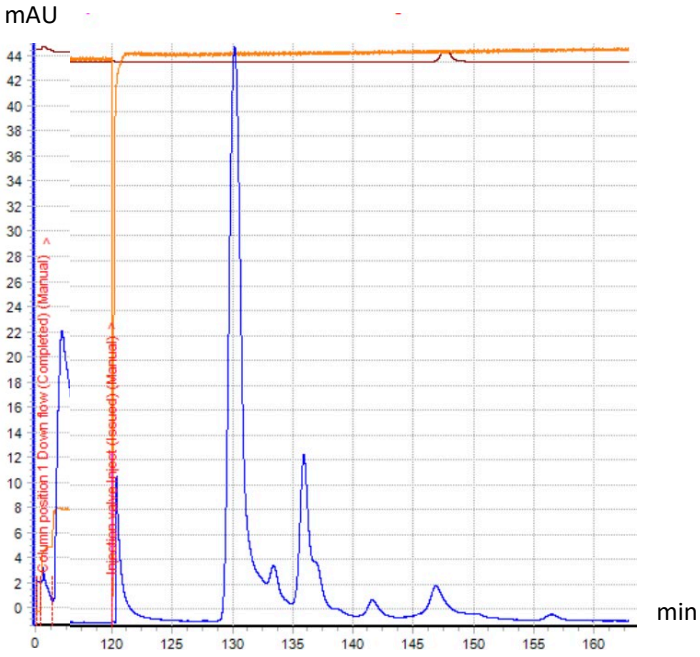

Figure 18. Showing AKTA purification of a naked (non-conjugated) mal-liposome. Key: brown line: conductivity pink line: injection point blue line: UV absorption at 280 nm. Figure has been edited to remove the column equilibration section for better visualisation of the results.

FACS analysis

Due to its conformation and its fluorescent properties, GFP was used to analyse conjugate samples with varying amounts of protein using FACS, which served as means to optimise the conjugation of antigens to liposomes and therefore preparation of *in vivo* samples. Following SEC purification of conjugates, liposomal peaks were analysed using methods states in sections **2.1.** Control measurement samples as also shown in *figure 19* were run together with the liposomal conjugates in order to validate conclusions drawn. PBS only was used as all samples are formulated in PBS and ensured there was no background fluorescence or interference being recorded. Naked liposomal formulations both containing the Maleimide linker and not, were also used to set the background

fluorescence i.e. act as negative controls. Gating was set to about 10^3 log units determined by the size of the liposomal formulations and used to assume that everything to the right of that gate was highly fluorescent. GFP alone was used to ensure that even though samples were thoroughly purified before being tested and no unbound GFP should be present in the conjugated sample since it has been removed with spin columns (centrifuged following separation from any unbound protein using SEC), all the fluorescent signals observed are being obtained because of GFP conjugated to the liposomal formulation. Theoretically, FACS only record events which are populations so if there happened to be some unbound or free GFP in the field of view when a snapshot of the liposomal population was taken then it could have been recorded and a fluorescent signal could appear, however, this is very rare. Since free GFP did not give a fluorescent signal based on the gated population used, then all signals observed were taken to have resulted from bound protein. Some electrostatic binding of GFP could also be possible due to surface charges of the liposomes, especially in cases where an excess amount of protein was used in conjugation reactions (e.g. 10.0 mg).

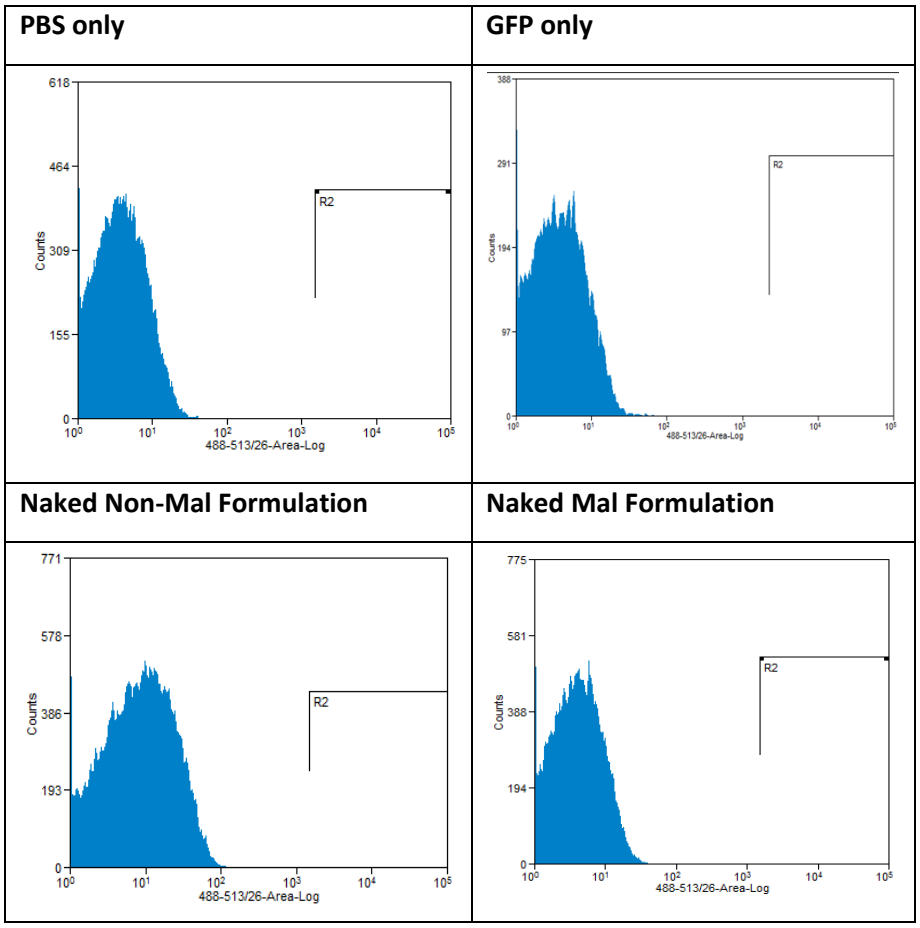

Figure 19. Showing the results for negative controls (PBS, unbound GFP, Naked mal- and non-mal-liposomes) recorded with FACS, analysis of which used to determine the protein equivalent to be conjugated to the liposomes, with no fluorescent populations present passed the 10^3 gating.

Mal-liposomes and non-mal liposomes were, as already stated, conjugated to different equivalents of GFP in order to optimise conjugation reaction of antigens through determination of loading of protein via fluorescent signals.

Firstly, efficiency of conjugations was tested with different ratios of GFP to mal-lipid; 2 (amounts as stated in subsection **2.5**) and 5 (150 μL of a 1 mM liposome formulation, to 75 mmol of GFP, with 129.25 μg of TCEP) mol equivalents of GFP conjugated to liposomes was repeated twice. Conjugations proceeded as described in section **2.6.** and then purified samples analysed with FACS. As seen in *figure 20* non-mal

liposomal conjugated samples gave a slightly fluorescent peak $< 10^3$ units. Comparing this histogram to the naked liposome shown in *figure 19* we can see there is a slight shift from non-conjugated to conjugated formulations, possibly owing to some GFP being electrostatically bound to the Non-Mal liposomes. Comparing the mal-liposomes with 2 and 5 equivalents of protein conjugated samples, we can see that increasing the amount of protein increased the fluorescence giving the observable shift from $< 10^4$ for 2 equivalents of GFP to $> 10^4$ for 5. This indicated that the liposomes and therefore lipid is in excess (3.72 x 10^{-5} mmol of GFP to 3.72 x 10^{-5} mmol of mal-lipid) and the potential for complete coverage of liposomal surface to occur. Higher fluorescent signal with a higher amount of GFP showed that more of the protein could be conjugated as mal-linkers in the formulation were still available for conjugation.

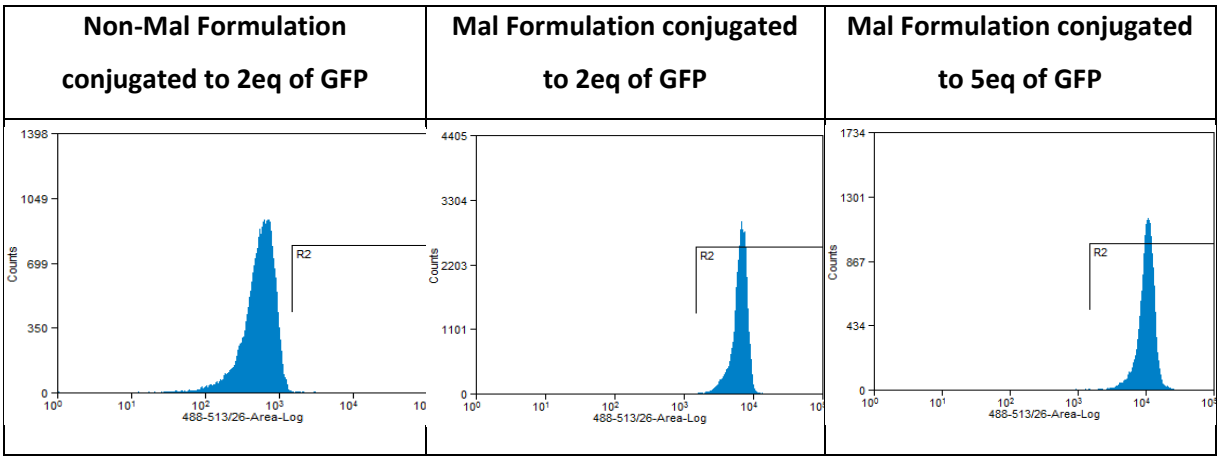

Figure 20. Showing FACS plots of counts over area/population obtained by analysis of non-mal liposomes conjugated to 2 mol equivalents of GFP and mal-liposomes conjugated to 2 and 5 equivalents. Gated population is set to 10^3.

Conjugations of GFP to liposomes were repeated with 1.00 mg of protein conjugated (to 3.71 mL of a 1.9 mM liposome solution) in order to determine effectiveness of loading of protein as this was the amount of protein required to be present in each sample for the *in vivo* study (1.00 mg of antigen per capsule). The conjugates were purified with SEC and the final solution concentrated to 0.80 mL. Concentration of protein in each sample was

determined with nanodrop. As derived from *table 11*, loading of protein onto the maleimide containing liposomes was a approximately a quarter of the amount conjugated.

Sample	Recorded concentration (mg/mL)	Amount of GFP present (mg)
Mal-liposomes	0.318	0.254
Non-mal liposomes	0.042	0.017

Table 11. Showing nanodrop results from 1.00 mg of GFP conjugated to mal- and non-mal-liposomes where around a quarter of the amount of GFP conjugated is actually loaded on the final sample.

This experiment was repeated in order to determine effects of lyophilisation onto the conjugated protein. The 0.80 mL solution was split into 2, 400 μL samples, one of which was lyophilised and reconstituted to make 1X PBS. *Table 12* shows nanodrop absorptions for fresh and lyophilised samples. Although the lyophilised sample gave slightly lower loading, the combined samples again add up to 0.253 mg of protein present on the liposomes. The samples obtained, along with non-mal liposome conjugated to 1.00 mg of GFP were analysed using FACS.

Sample	Recorded concentration (mg/mL)	Amount of GFP present (mg)
Fresh	0.352	0.141
Lyophilised	0.282	0.112

Table 12. Showing concentrations of GFP on mal-liposomes comparing loading of protein on fresh and lyophilised samples from 1.00 mg GFP conjugations to mal-liposomes.

As expected, the Non-Mal formulation histogram in *figure 21* shows very little fluorescence (peak at 10^2 log units) that could have resulted due to some residual GFP electrostatically binding to the surface of the liposomes. The SEC elution peak collected during purification after the elution point of the liposomal 'conjugated' peak shows more of the naked Non-Mal liposome present and some GFP that may be electrostatically bound. Two populations are present denoted by the two separate peaks also observed in the SEC traces as there were likely different amounts of GFP on different populations of liposomes. As seen for the maleimide containing formulation, most of the population was highly fluorescent with a fraction of the liposomal population potentially having some GFP electrostatically bound on their surface, or possibly less amount of protein conjugated and therefore samples were less fluorescent (peak $< 10^3$). As the lipid linker was used in excess in these conjugations over GFP, the liposomes would only sparsely covered by protein. Some of the liposomes would appear less fluorescent than others. Most of the liposomal population, however, was present in the high fluorescence region. The peak collected after the liposomal conjugated fraction gave a non-fluorescent peak ($\leq 10^2$) and therefore a conclusion that all the GFP present in the formulations was bound to the liposomes. The non-fluorescent peak ($\leq 10^2$) of the elution after the conjugated sample could also indicate that even if there was any GFP in that elution sample it was most likely not bound as no fluorescence was recorded, therefore most of the desired product (protein conjugated to liposome formulation) was successfully collected in the first peak eluded by the SEC. Plots are shown in *figure 21*.

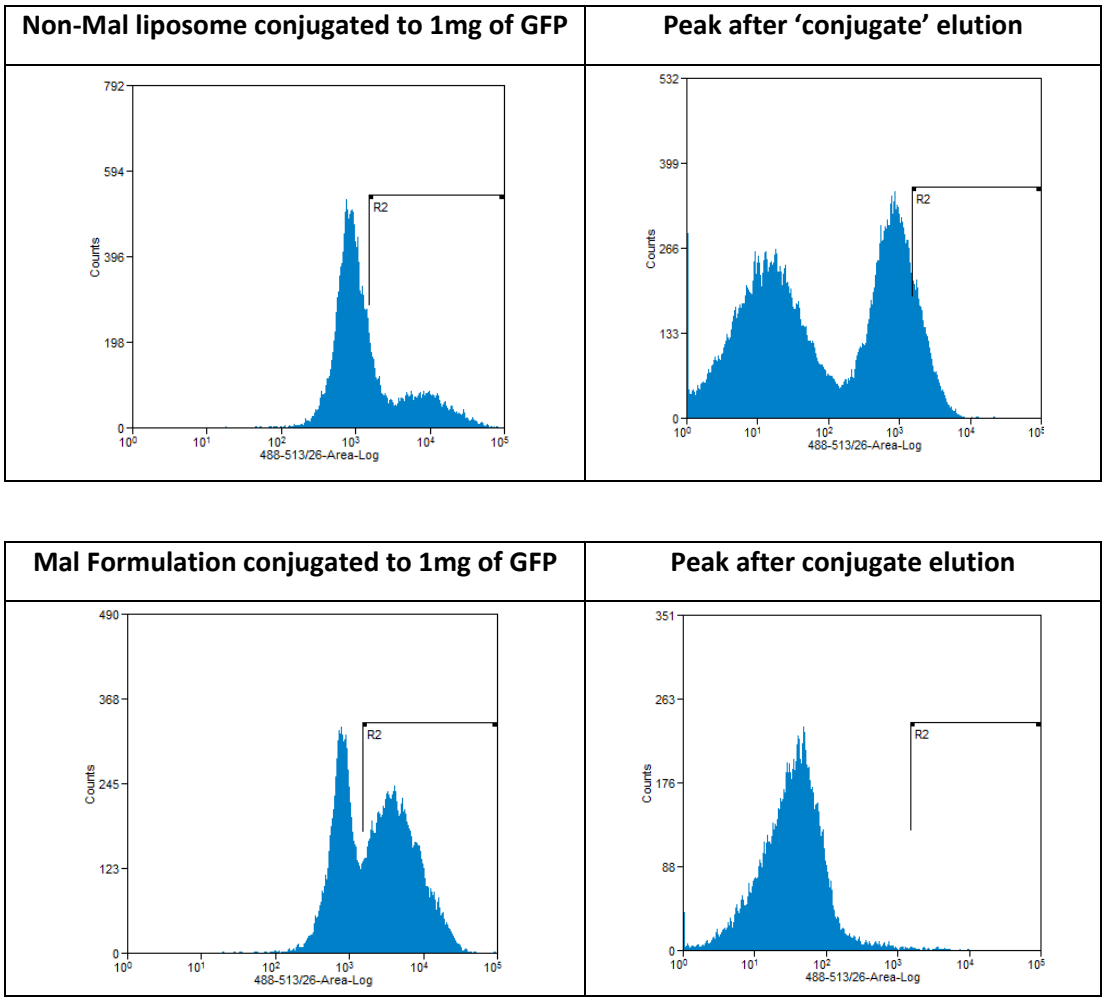

Figure 21. FACS analysis of a conjugate sample of 1.00 mg of GFP to liposomes both with and without the mal-linker. Graphs on the left show analysis of the first peak eluting from the SEC, what is thought to be the liposomal-protein conjugated peak and the fraction that elutes after that, is shown on the right. Gated population is set to 10^3.

Conjugations to mal and non-mal liposomes were then performed with 10.0 mg of GFP to ensure scaling up of the reaction was possible as *in vivo* samples with antigens conjugated had to be prepared as large batches in order to ensure high degrees of similarity between them and prevent high percentage loss of material. Preparation of samples occurred in the same way, however, using a more concentrated liposomal formulation to aid the conjugation reaction owing to the larger number of moles present. Following purification of the liposomal conjugated fraction, nanodrop analysis was carried out to determine

protein concentration in the sample, that gave a concentration of 3.556 mg/mL of a 2.73 mL solution and therefore 9.71 mg of GFP. These samples there then analysed by FACS.

Increasing the amount of GFP conjugated, as seen in *figure 22* (results obtained when 10.0 mg of the protein were used in the conjugation reactions), shifted the fluorescence peak to the right indicating an increase in fluorescence of the whole of the liposomal population in the given formulation. This also indicated that more of the maleimide linker groups were available for conjugation and an excess of protein increases possibility for full coverage of the liposomal surface. Similar results were observed for the 2 and 5 equivalents of GFP used as discussed previously (*figure 20*). The figure below also shows the histogram of the lyophilised GFP conjugated sample with 1.00 mg of protein, where a large distribution of the degree of fluorescence of the population is being indicated. Comparing this histogram to the one for 1.00 mg with mal-liposome fresh sample from *figure 21* we can claim an indication of change of the conformation of the protein as the sample is being freeze dried, that might however dispute the slight decrease in fluorescence for some of the population, create a more even distribution of the of the protein on the liposomal formulation. A single population with slightly lower fluorescence is being observed. Fluorescent signal was still high and the fraction of the population that wasn't fluorescence as much was also present in the fresh sample and was probably a result of liposomes being in excess and therefore, we could argue there was not enough GFP to conjugate onto the linker.

Mal Formulation conjugated to 1mg of GFP lyophilised and reconstituted	Mal Formulation conjugated to 10mg of GFP
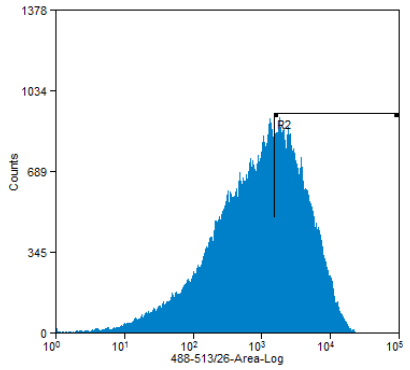	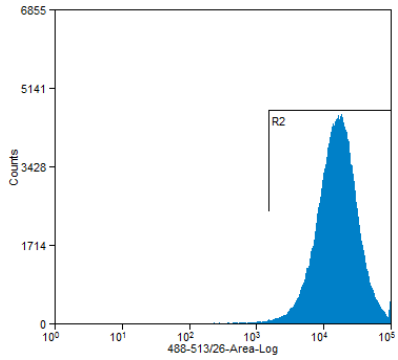

Figure 22. Showing FACS histograms of lyophilised sample of experiment with 1.00 mg of GFP conjugated to Mal-liposome and of fresh (not freeze dried) conjugated sample of the same liposome with 10.0 mg of protein originally conjugated. Gated population is set to 10^3.

3.6 Lyophilisation with trehalose

In preparation for *in vivo* samples, the ideal ratio of trehalose sugar with respect to the total amount of lipid present was determined. This was based on retention of shape and structure of the liposomes, protection of antigen integrity and appearance aiming for a fine powder that made the formulation easy to pack. Adding trehalose would also act as a packing agent to fill the space in the capsules. Trehalose was used to pack control capsules with no formulations and therefore adding it to all capsules would be essential to make sure only one variable was changed in the animal tests and ensured the formulation accounted for any effects. A fraction of the mal-liposome conjugated sample to 10.0 mg of GFP was divided into six portions of 1.50 mL of solution. Based on the amount of lipid present in each of the samples (1.045 mg), the samples were freeze dried with different percentages of trehalose sugar with respect to the amount of lipid. Stock solutions of trehalose in PBS were prepared to make for 15%, 30%, 50%, 100% and 1000% by mass of sugar. Once lyophilised the samples were stored at -20℃, reconstituted and analysed with FACS. All histograms in *figure 23* indicated there was no negative effect on the GFP around the liposome after the conjugate samples were freeze dried with

trehalose, owing to the fact that all samples maintained high levels of fluorescence, which presumably represented what would happen with the antigenic lipoproteins. Slight shift of the peak to the far right of the graph and an increase in counts to 8000 when 1000% by mass of trehalose was used could indicate better conformation of GFP around the liposomes after lyophilisation as fluorescence increases. This confirmed the theory that due to potential leakage of liposomes during lyophilisation (which however improves storage stability and is optimal for formulations containing proteins which are sensitive to heat), addition of cryoprotective agents (hydrophilic compounds such as carbohydrates) like trehalose have been established to preserve stability and quality of liposomes.[74] These results however, were not conclusive and therefore DLS analysis was carried out on all samples to provide more evidence for analysis.

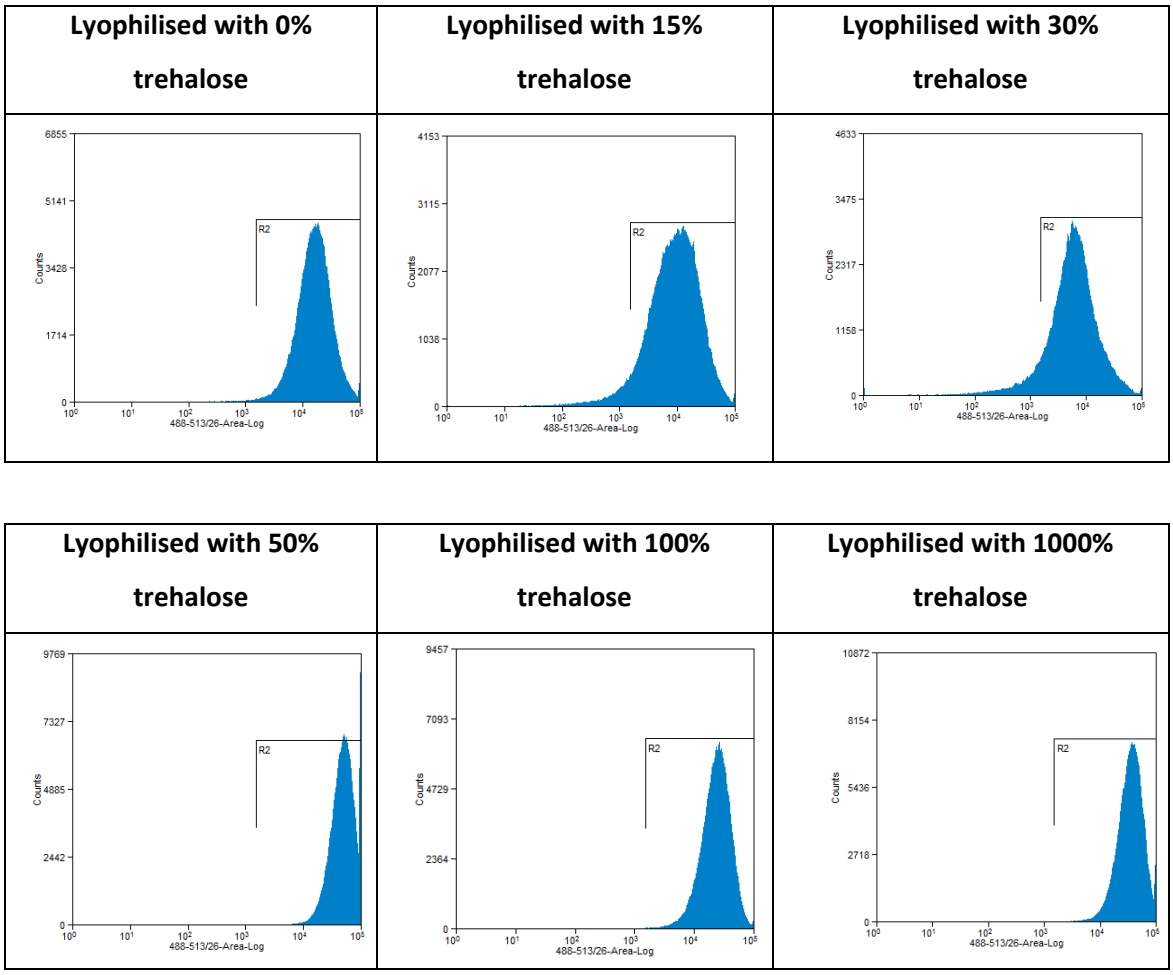

Figure 23. Histograms from FACS analysis of the GFP conjugated formulations (mal-linker present), lyophilised with different percentages (by mass) of trehalose sugar as shown to determine effect of the sugar on conformation of protein and preservation of liposomal formulations. Gated population is set to 10^3.

Evidently from *table 13,* showing the Z-average size and size distribution of formulations freeze dried with different percentages of trehalose, increasing the percentage of trehalose in the formulation improves the quality of the sample. 1000% by mass of trehalose sugar gave the most uniform population with the most concise shape, reinforcing the the theory that trehalose would be ideal to preserve liposome stability during and after freeze-drying treatments[74] This analysis of sample formulations with liposomes, GFP and trehalose gave results with high PDI values. Lyophilisation of samples

and rehydration are likely to change polydispersity, however this shouldn't affect the ability of these samples to act as vaccines. Conjugation to GFP caused the curve of measurements to shift to the right, i.e. average size to increase. This would most likely indicate the presence of newly formed particles, confirming conjugations once again, and not liposomes aggregating as those would be far larger than 400 nm. We can argue that as DLS provides information on the hydrodynamic diameter due to particle solvation, the liposome formulations are re-hydrated to a slightly larger size, than the one before the conjugations to GFP and lyophilisation with trehalose. Nonetheless, along with the FACS data where the same samples analysed are fluorescent, it can be concluded that the population analysed is GFP conjugated liposomes.

Percentage by mass of trehalose used in lyophilisation (%)	**Z-average (d.nm)**	**PDI**
0	312.0	0.588
15	656.8	0.729
30	497.8	0.572
50	438.8	0.552
100	404.5	0.667
1000	377.8	0.576

Table 13. Showing the z-average (mean hydrodynamic size) and polydispersity index of liposomal formulations conjugated with GFP and freeze-dried with different % by mass of sugar as stated.

DLS measurements in this case were carried out using both lipid and protein protocols created as stated in section **2.1** to get the most reliable results. DLS plot obtained for the lyophilisation with 1000% by mass trehalose (*figure 24)* as the ones obtained for the rest of the percentages of trehalose used (*appendix figure 6.19 - figure 6.21*) showed two size populations produced by the sonication method (adjusting time and power), smaller particles (50-100 nm) present as a small minority with intensity always less than 5%.

Further optimisation could be run to enable a more uniform particle distribution, via extrusion (the process of pushing the particles through a membrane with specific pore sizes), however this equipment wasn't available.

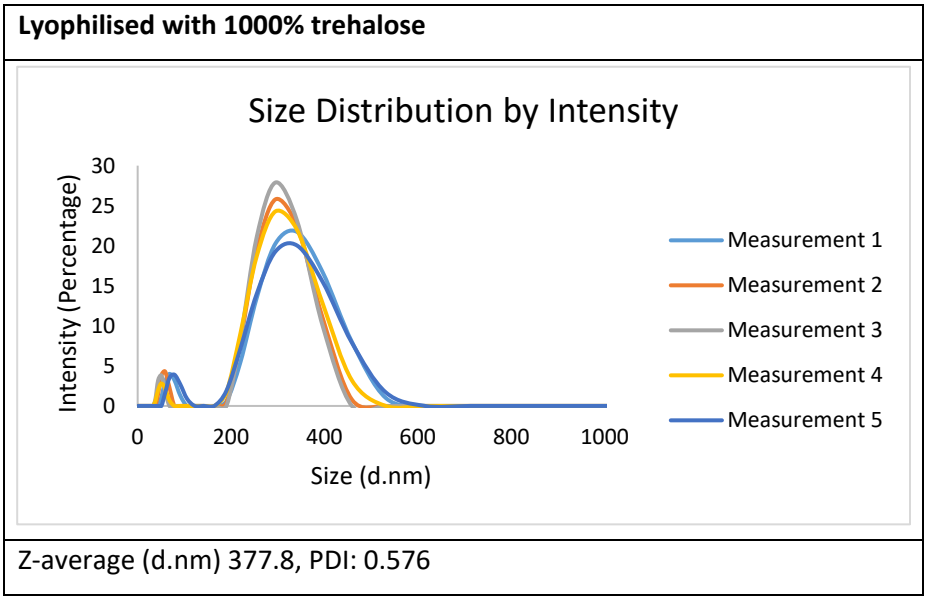

Figure 24. DLS plot from data obtain through analysis of lyophilised sample of mal-liposome conjugated to GFP with 1000% by mass of trehalose with respect to the mal-lipid present.

3.7 Antigen conjugations

Formulation analysis

Following attainment of the optimal formulation, conjugation and freeze drying conditions, antigen conjugations were performed for the *in vivo* experiments. Liposomal formulations were prepared with 10% mal-lipid, 25% DPPC, 25% DPPS and 40% cholesterol (v/v/v/v) for all antigenic conjugations and with 30% DPPC, 30% DPPS and 40% cholesterol (v/v/v) for the naked non-conjugated negative control groups of the *in vivo* study with specific volumes and concentrations as stated in section **2.8**. DLS analysis was carried out on all formulations to ensure quality requirements (of size and population uniformity) were being met. As seen from the plots in *figure 25* showing conjugated

samples and *figure 26* control group formulations, all formulations were of a similar size, < 120 nm.

Liposomes for conjugation to 08730

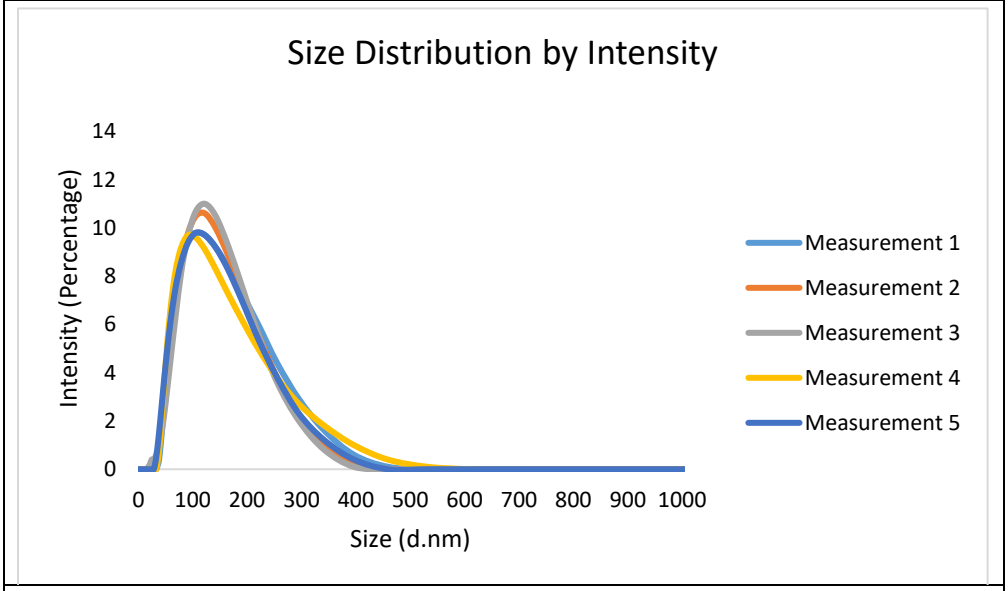

Z-average (d.nm) 113.3, PDI: 0.259

Liposomes for conjugation to TcdB

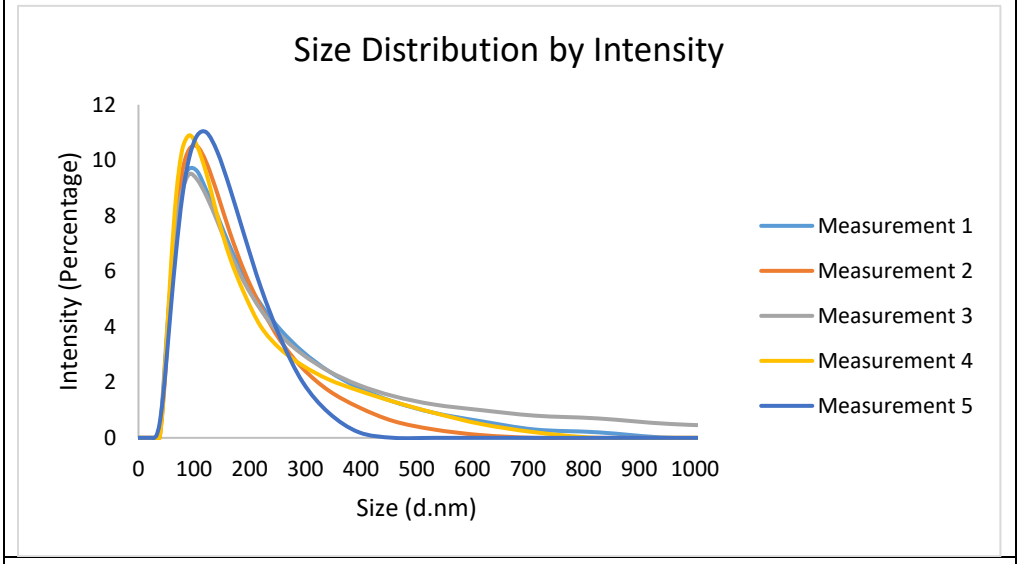

Z-average (d.nm) 115.1, PDI: 0.259

Figure 25. Showing DLS plots from analysis of liposomal formulations prepared to be conjugated to the two antigens for the in vivo study of immunisation in hamsters.

Degree of polydispersity was low with similar values between the formulation indicating good replication abilities of the formulation produced. Results produced were good to justify use of the formulations in the animal study and expect reliable results *in vivo* due to the high degrees of similarity of the samples with the only variable being the antigen conjugated.

Liposomes for control groups

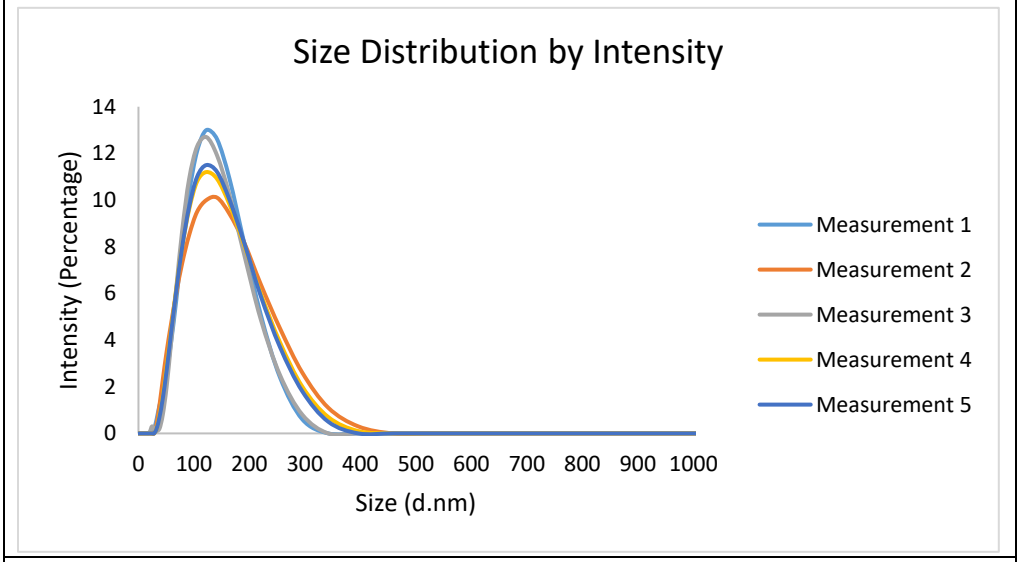

Z-average (d.nm) 118.2, PDI: 0.347

Figure 26. Showing DLS plots from analysis of liposomes formulated as controls (non-mal formulations) for the in vivo study.

Following analysis of the liposomal formulations, conjugation reactions were allowed to proceed overnight and included TCEP in order to keep all antigenic lipoproteins reduced by breaking any disulfide bonds that might form. 20.0 mg 08730 and 20.0 mg TcdB proteins was conjugated to each batch of liposomal formulations in an attempt to load at least 12.0 mg so that each antigen formulation was conjugated with enough protein for the whole of the immunisation study. Purification of each of the conjugated formulations was carried out using SEC.

Purification of TcdB loaded liposomes

As seen in *figure 27*, TcdB loaded liposomes eluted at 4 mL (5.5 minutes) after the injection point. High concentration of antigen loaded onto the formulation was indicated by the very high UV absorbance of the first liposomal peak. As seen in *figure 9* showing purification of TcdB antigen alone, eluted 11 minutes (about 8 mL) passed the injection point thus any free unbound protein would probably appear after 123 mL in this trace (beginning of elution point 3). To be sure however that all peaks collected and used were liposomal, only the first peak from each injection was used further for the in the *in vivo* sample preparation in order to prevent any of the higher molecular weight protein (79 kDa) that was present in the TcdB crude sample to be picked up. Even though the crude TcdB sample was thoroughly purified, care was taken not to collect any sample eluting after 8.5 minutes to be present in an *in vivo* sample decreasing purity. Even if lower molecular weight proteins were still present in the protein sample conjugated then they would have eluted way passed any peak collected for the immunisation samples. All of the first peak elutions from each injection were then concentrated using 50k MWCO spincolumns (that would in theory again get rid of any other higher molecular weight proteins present) before the Bradford assay.

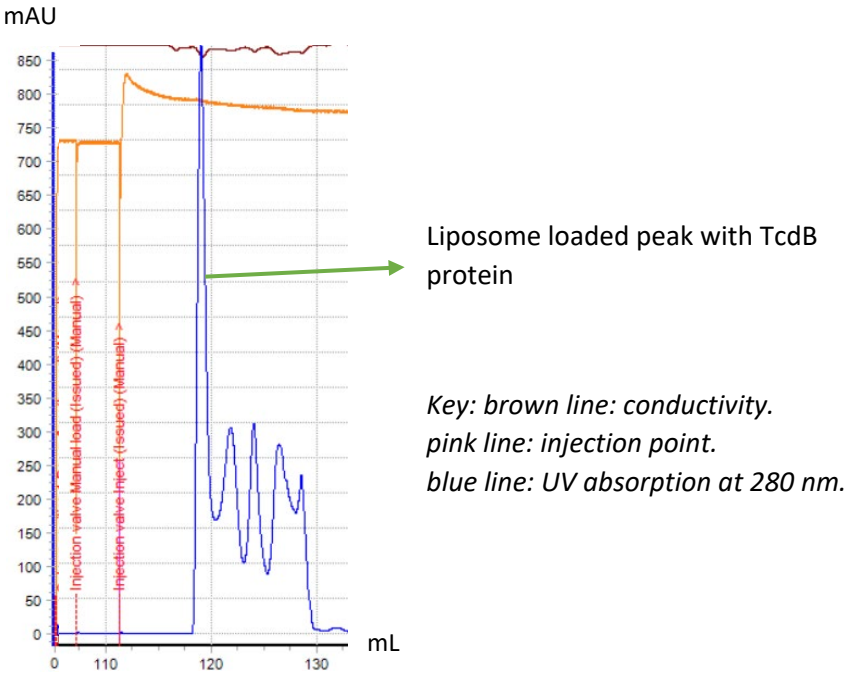

Figure 27. Showing SEC purification of TcdB loaded liposomes from any unbound protein to be used in the in vivo immunisation. Figure has been edited to remove the column equilibration section for better visualisation of the results. (Recorded as elution volumes)

Purification of 08730 loaded liposomes

Figure 28 shows that the loaded liposomes eluted 6.5 mL (elution point 1) after the injection. As for TcdB, high concentration of antigen loaded onto the liposomes was indicated by the very high UV absorbance of that first peak. As seen in *figure 8* showing purification of 08730 crude, the target protein eluted 19 minutes (15 mL) after the injection point and therefore any unbound protein would only elute at about 60 mL in this trace. Again, to be sure all peaks collected were liposomal, only the first peak from each injection was used further for the in the *in vivo* sample preparation preventing any higher molecular weight proteins (50-59 kDa) that were present in an 08730 crude sample and would have eluted 11 minutes (8 mL) from injection (possible position 56 mL on the trace – peak 3) to be present in an *in vivo* sample altering purity. Lower molecular weight proteins, as for TcdB, would have eluted a lot slower than any peak collected for the *in*

vivo samples and therefore good isolation was assumed. Conjugates were then concentrated using 50k MWCO spin columns before protein concentration was recorded.

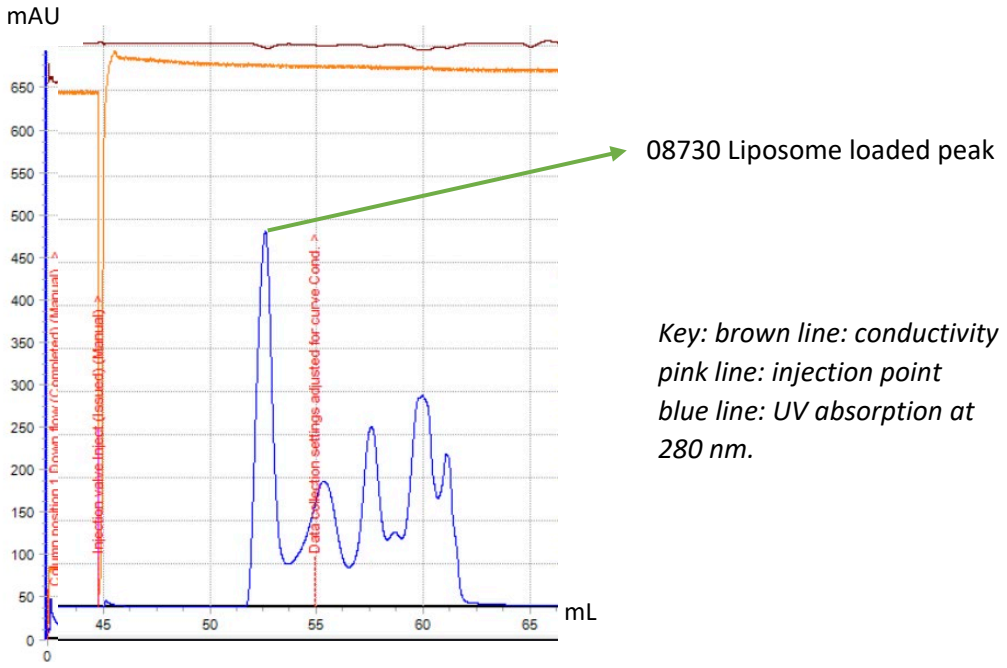

Figure 28. Showing SEC purification of 08730 loaded liposomes. Figure has been edited to remove the column equilibration section for better visualisation of the results.

3.8 *In vivo* samples

Bradford assay performed as described in section **2.6** indicated that both PBS and naked liposomal formulations gave an absorbance of 0.43 units, ensuring that the liposomes did not conjugate onto the dye and therefore the results observed were due to the conjugated antigens. Absorbance was recorded as follows and gave the protein concentrations shown in *table 14* by comparison to a standard linear trend concluding that enough protein was loaded for completion of the immunisation study.

TcdB	08730
Absorbance	
1.270432	0.60
1.30417	0.59
1.287301	0.60
0.867446	0.18
Concentration	
1077.5 µg/mL	751.22 µg/mL
Amount of protein loaded	
12.98 mg	15.22 mg

Table 14. Showing Bradford assay results used to determine protein concertation in the conjugate samples for each formulation prepared for the in vivo study.Absorbance readings are from different samples of that batch formulation tat were then combined.

Once the amount of protein in each conjugated formulation was confirmed by Bradford assay, a specific volume of each conjugated sample was used to prepare the capsule contents; so that it contained 1.00 mg of the desired protein. After lyophilisation with 1000% trehalose sugar (% by mass with respect to mal-lipid), the capsules were packed for the immunisation study using the kit shown in *figure 29*.

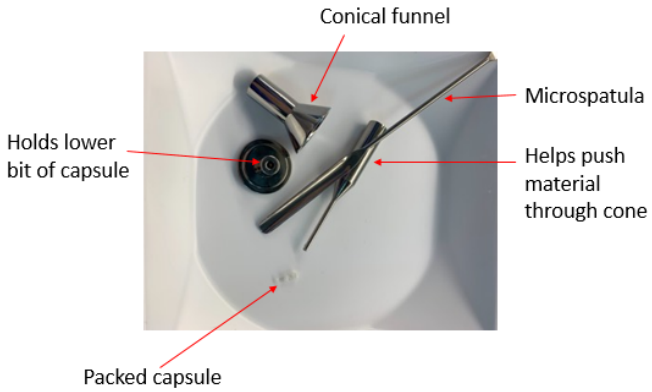

Figure 29. Showing kit used to manually pack each capsule used for in vivo immunisation of hamsters.

The *in vivo* study involved: 12 capsules packed with TcdB loaded liposomes freeze dried with trehalose (1000% by mass), 12 capsules with 08730 loaded liposomes freeze dried with trehalose (1000% by mass), 12 capsules of *each* of the antigen, TcdB and 08730, alone, freeze dried with trehalose (1000% by mass), 12 capsules packed with naked liposomes freeze dried with trehalose (1000% by mass), 6 capsules with trehalose sugar only (1000% by mass). This would enable direct comparison of the immunogenicity of the liposomal formulations with respect to antigen alone formulation and clear control groups (trehalose sugar only and naked formulations – as well as hamsters receiving no capsule at all) to set the background levels of binding to antibodies tested.

Porcine hard gelatin capsules were packed with bromophenol blue and coated with various coats of enteric coating prior to *in vivo* tests. *In vitro* testing was performed using gastric fluid and intestinal fluid to assess stability and effective release of contents. Following assessment within the Dr Griffin group, Eudragit L100 was determined the best coating to be tested *in vivo*. 4 capsules were packed with bromophenol blue, coated with Eudragit L100 and administered to 4 female Syrian strain hamsters. CT scans were performed on 4 hamsters by Michelle Kelly. Once the efficiency of the capsules was tested *in vivo* and following confirmation that the coating helped capsules by-pass the low pH (2-3) of the hamsters' stomach and allowed them to successfully release contents in the small intestine where the pH is more alkaline (pH 6.5-7), all capsules prepared as stated above were coated with Eudragit L100.

4. CONCLUSION

From a panel of antigens chosen as potential candidates for the development of a vaccine against *Clostridium difficile,* CD630_08730 and CD630_TcdB-RBD were successfully expressed by the Griffin group and purified extensively with SEC. A small scale expression and purification of antigen 08730 was also conducted during this project. Following an immunogenicity study with *C. difficile* patient serum, CD630_08730 and CD630_TcdB-RBD were concluded to be immunogenic and ability to retain immunogenicity following lyophilisation, allowed for the use of this antigens for conjugations to liposomes.

Maleimide linker lipid was successfully synthesised, however, neither the maleimide diether nor the maleimide diester were successfully isolated during this project. A previously conducted study of the group of the maleimide diether, allowed for the preparation of linker-containing liposomal formulations to be used as vehicles and adjuvants.

Optimisation of the vaccine formulation involved optimisation of the delivery vehicle i.e. formulation of the liposomes, and antigenic protein loading. Formulations containing 10% Mal-lipid, 25% DPPC, 25% DPPS and 40% cholesterol (v/v/v/v) and formulations with 30% DPPC, 30% DPPS and 40% cholesterol (v/v/v) were selected for this project based on analysis by DLS and TEM. Different sonication methods involving a variation of sonicators, amplitude and time of sonication were tested in order to achieve ideal size (100-150 nm) and shape with minimum degree of polydispersity. Using Qsonica sonicator at an amplitude of 90% for 10 minutes created < 120 nm spherical nanoparticles with low polydispersity values, confirmed via TEM, DLS and FACS. Optimisation of the protein concentration in the formulation employed the use of GFP as a surrogate and FACS analysis of samples. Conjugation conditions were kept constant while the amount of protein involved was altered. Conjugation of 2 and 5 equivalents of GFP with respect to the mal-linker was thoroughly investigated resulting in the conclusion that conjugations in low and high concentrations were feasible and increasing protein conjugated increased coverage of liposomal surface. Lyophilisation with trehalose sugar

as a packing agent was also optimised to enable protection of antigen integrity and liposomal structure.

For the *in vivo* studies to prove protective efficacy of the formulations, 20.0 mg of each lipoprotein was conjugated on the liposomes using the optimised methodology and the final sample aliquoted into samples containing 1.00 mg of antigen per capsule. Capsule efficiency was tested *in vitro* and *in vivo* before formulations were packed. Administration to Syrian hamsters was employed to test protective immunity of the vaccine formulation.

5. REFERENCES

1 Orthobullets, URL: https://www.orthobullets.com/basic-science/9059/antibiotic-classification-and-mechanism Accessed: 29/08/19.

2 Centers for Disease Control and Prevention (CDC), URL: https://www.cdc.gov/drugresistance/about/how-resistance-happens.html Accessed 29/08/19.

3 National Institute for Health Research (NIHR), URL: https://www.nihr.ac.uk/explore-nihr/campaigns/tackling-antimicrobial-resistance.htm Accessed 01/09/19.

4 World Health Organisation (WHO), URL: https://www.who.int/antimicrobial-resistance/en/ Accessed: 27/07/19.

5 Medical Research Council (MRC), URL: https://mrc.ukri.org/research/spotlights/antimicrobial-resistance/what-is-amr/ Accessed: 01/09/19.

6 P. Spigaglia, *Ther. Adv. Infect. Dis.* **2016**, 3, 23–42.

7 S. R. Curry, *Clin. Lab. Med.* **2017**, 37, 341–369

8 R. Leuzzi, R. Adamo and M. Scarselli, *Hum. Vaccines Immunother.* **2014**, 10, 1466–1477.

9 Pubic Health of England, URL: https://assets.publishing.service.gov.uk/government/uploads/system/uploads/attachment_data/file/765014/HCAI_fatality_report_201718_v2.pdf Accessed: 10/09/19.

10 National Institute of Allergy and Infectious Diseases, URL: http://www.imgt.org/IMGTeducation/Tutorials/ImmuneSystem/UK/the_immune_system.pdf Accessed: 01/08/19.

11 L. Oliveira-Nascimento, P. Massari and L. M. Wetzler, *Front. Immunol.* **2012**, 3, 79.

12 O. Takeuchi, K. Hoshino, T. Kawai, H. Sanjo, H. Takada, T. Ogawa, K. Takeda and S. Akira, *Immunity* **1999**, 11, 443–451.

13 J. H. Kauppila, A. E. Mattila, T. J. Karttunen and T. Salo, *Oncoimmunology* **2013**, 2, 638-643.

14 M. F. Cesta, *Toxicol. Pathol.* **2006**, 34, 599–608.

15 British society of Immunology, URL: https://www.immunology.org/public-information/bitesized-immunology/pat%C3%B3genos-y-enfermedades/immune-responses-bacteria Accessed: 01/09/19.

16 M. Wieczorek, E. T. Abualrous, J. Sticht, M. Álvaro-Benito, S. Stolzenberg, F. Noé and C. Freund, *Front. Immunol.* **2017**, 8, 292.

17 R. M. Anderson, and R. M. May, *Nature* **1985**, 318, 323.

18 L. B. J. Heinlen, *Am. J. Med. Sci.* **2011**, 340, 247–252.

19 National Health Service (NHS), URL: https://www.nhs.uk/conditions/c-difficile/ Accessed: 01/09/19.

20 S. S. Banawas, *Biomed Res. Int.* **2018**, 2018, 8414257.

21 D. Zhu, J. A. Sorg and X. Sun, *Front. Cell. Infect. Microbiol.* **2018**, 8, 29.

22 S. Bibbò, L. R. Lopetuso, G. Ianiro, T. Di Rienzo, A. Gasbarrini and G. Cammarota, *J. Immunol. Res.* **2014**,2014, 462740.

23 S. M. Twine, C. W. Reid, A. Aubry, D. R. McMullin, K. M. Fulton, J. Austin and S. M. Logan, *J. Bacteriol.* **2009**, 191, 7050–7062.

24 C. Janoir, J. Grénery, M. P. Savariau-Lacomme and A. Collignon, *Pathol. Biol.* **2004**, 52, 444–449.

25 R. Madan and W. A. Petri, *Trends Mol. Med.* **2012**, 18, 658–666.

26 S. Di Bella, P. Ascenzi, S. Siarakas, N. Petrosillo and A. di Masi, *Toxins (Basel).* **2016**, 8, 134.

27 L. Quemeneur, N. Petiot, N. Arnaud-Barbe, C. Hessler, P. J. Pietrobon and P. Londoño-Hayes, *Infect. Immun.* **2018**, 86, 6.

28 D. P. Humphreys and M. H. Wilcox, *Clin. Vaccine Immunol.* **2014**, 21, 913–923.

29 Medscape URL: https://emedicine.medscape.com/article/193031-overview Accessed 28/08/19.

30 K. Solomon, *Ther. Adv. Infect. Dis.* **2013**, 1, 19–35.

31 Z. Peng, D. Jin, H. B. Kim, C. W. Stratton, B. Wu, Y. W. Tang and X. Suna, *J. Clin. Microbiol.* **2017**, 55, 1998–2008.

32 T. Dapa, R. Leuzzi, Y. K. Ng, S. T. Baban, R. Adamo, S. A. Kuehne, M. Scarselli, N. P. Minton, D. Serruto and M. Unnikrishnan, *J. Bacteriol.* **2013**, 195, 545–555.

33 C. A.C., M. R.J.S., T. A.J., P. D.L. and R. T.V., *Lancet Infect. Dis.* **2010**, 10, 395–404.

34 S. Zhao, C. Ghose-Paul, K. Zhang, S. Tzipori and X. Sun, *Hum. Vaccines Immunother.* **2014**, 10, 3522–3530.

35 D. G. Binion, Gastroenterol. *Hepatol.* **2011**, 7, 750–752.

36 S. Péchiné, C. Janoir and A. Collignon, *Expert Opin. Biol. Ther.* **2017**, 17, 415–427.

37 B. D. Navalkele and T. Chopra, *Biol. Targets Ther.* **2018**, 12, 11–21.

38 L. Kyne, M. Warny, A. Qamar and C. P. Kelly, *Lancet.* **2001**, 357, 189–193.

39 Vaccines.gov URL: https://www.vaccines.gov/basics/types Accessed: 28/08/19.

40 E. R. Dubberke and M. A. Olsen, *Clin. Infect. Dis.* **2017**.

41 S. Péchiné, J. F. Bruxelle, C. Janoir and A. Collignon, *Front. Microbiol.* **2018**, 9, 1009.

42 N. Wang, T. Wu and T. Wang, *Liposomes*, **2017**, 2015, 318-323.

43 J. F. Bruxelle, S. Péchiné and A. Collignon, *Adv. Exp.Med. Bio.* **2018**, 1050, 197–225.

44 M. Alavi, N. Karimi and M. Safaei, *Adv. Pharm. Bull.* **2017**, 7, 3–9.

45 N. Monteiro, A. Martins, R. L. Reis and N. M. Neves, *J. R. Soc. Inter.* **2014**, 11.

46 L. O. De Serrano and D. J. Burkhart, *J. Nanobiotech.* **2017**, 15, 83.

47 G. Bozzuto and A. Molinari, *Int. J. Nanomed.* **2015**, 10, 975–999.

48 T. Ogiso, T. Yamaguchi, M. Iwaki, T. Tanino and Y. Miyake, *J. Drug Target.* **2001**, 9, 49–59.

49 S. Menina, J. Eisenbeis, M. A. M. Kamal, M. Koch, M. Bischoff, S. Gordon, B. Loretz and C. Lehr, *Adv. Healthc. Mater.* **2019**, 8, 1900564.

50 Avanti Polar Lipids Inc., URL: https://avantilipids.com/tech-support/liposome-preparation/lmv Accessed 05/06/19.

51 R. Griffin and N. P. Minton, *ClostPath 10th Int. Conf.* **2017**.

52 M. Goudarzi, H. Goudarzi, M. Alebouyeh, R. M. Azimi, M. FS. Shayegan, M. Zeli and M. Aslani, *Iran Red Crescent Med J.* **2013**, 15(8), 704-711.

53 R. Kaur, M. Henriksen-Lacey, J. Wilkhu, A. Devitt, D. Christensen, and Y. Perrie, *Mol. Pharm.* **2014** 11 (1), 197-207

54 D. Chapetón Montes, T. Candela, A. Collignon and C. Janoir, *J. Bacteriol*. **2011**, 193, 5314–5321.

55 M. Han, S. Watarai, K. Kobayashi and T. Yasuda, *J. Vet. Med. Sci.* **1997**, 59, 1109–1114.

56 R. Nisini, N. Poerio, S. Mariotti, F. De Santis and M. Fraziano, *Front. Immunol.* **2018**, 9, 155.

57 Y. Luo, O. V. Friese, H. A. Runnels, L. Khandke, G. Zlotnick, A. Aulabaugh, T. Gore, E. Vidunas, S. W. Raso, E. Novikova, E. Byrne, M. Schlittler, D. Stano, R. L. Dufield, S.

Kumar, A. S. Anderson, K. U. Jansen and J. C. Rouse, *AAPS J.*, **2016**, 18, 1562–1575.

58 Zaman, M.; Toth, I. *Front. Immunol.* **2013**, 318, 1-12.

59 D. P. Nair, M. Podgórski, S. Chatani, T. Gong, W. Xi, C. R. Fenoli and C. N. Bowman, *Chem. Mater.* **2014**, 26, 724–744.

60 R. A. G. da Silva, C. P. Churchward, A. V. Karlyshev, O. Eleftheriadou, A. K. Snabaitis, M. R. Longman, A. Ryan and R. Griffin, *Br. J. Pharmacol.*, **2017**, 174, 2247–2260.

61 C. H. Leng, S. J. Liu, H. W. Chen and P. Chong, *Expert Rev. Vaccines* **2015**, 14, 1623.

62 M. T. Nguyen and F. Götz, *Microbiol. Mol. Biol. Rev.* **2016**, 80, 891–903.

63 ScienceDirect, URL: https://www.sciencedirect.com/topics/neuroscience/tlr6 Accessed 01/09/19.

64 S. S. Ho, S. M. Michalek and M. H. Nahm, *Infect. Immun.* **2008**, 76, 206–213.

65 D. H. Hwang, J. A. Kim and J. Y. Lee, *Eur. J. Pharmacol.* **2016**, 785, 24–35.

66 A. Askarizadeh, M. R. Jaafari, A. Khamesipour and A. Badiee, *Ther. Adv. Vaccines* **2017**, 5, 85–101.

67 P. R. Hoffmann, A. M. DeCathelineau, C. A. Ogden, Y. Leverrier, D. L. Bratton, D. L. Daleke, A. J. Ridley, V. A. Fadok and P. M. Henson, *J. Cell Biol.* **2001**, 155, 649–659.

68 Avanti Polar Lipids, URL: https://avantilipids.com/tech-support/physical-properties/phase-transition-temps/ Accessed 01/01/19.

69 N. Mitchell, T. L. Kalber, M. S. Cooper, K. Sunassee, S. L. Chalker, K. P. Shaw, K. L. Ordidge, A. Badar, S. M. Janes, P. J. Blower, M. F. Lythgoe, H. C. Hailes and A. B. Tabor, *Biomaterials* **2013**, 34, 1179–1192.

70 B. Corthésy, *Front. Immunol.* **2013**, 4, 185.

71 H. He, Y. Lu, J. Qi, Q. Zhu, Z. Chen and W. Wu, *Acta Pharm. Sin. B.* **2019**, 9, 36–48.

72 S. Franzé, F. Selmin, E. Samaritani, P. Minghetti and F. Cilurzo, *Pharmaceutics* **2018**,

10, 139.

73 O. Stepanenko, V. Verkhusha, I. Kuznetsova, V. Uversky and K. Turoverov, *Curr. Protein Pept. Sci.* **2008**, 9, 338–369.

74 C. I. Nkanga, A. M. Bapolisi, N. I. Okafor and R. W. M. Krause (**2019**), URL: https://www.intechopen.com/books/liposomes-advances-and-perspectives/general-perception-of-liposomes-formation-manufacturing-and-applications Accessed: 01/09/20

75 M. Han, S. Watarai, K. Kobayashi, T. Yasuda, *Cell Chemistry*, **1997**, 1109-1114

76 M. J. Coolbaugh and D. W. Wood, *Methods Mol. Biol.*, **2014**, 1177, 47–58.

77 M. Alavi, N. Karimi and M. Safaei, *Adv. Pharm. Bull.* **2017**, 7(1), 3-9.

78 N. Pippa, N. Naziris and C. Demetzos, *J Liposome Res*. **2019**, 29(4), 313-321.

6. APPENDIX

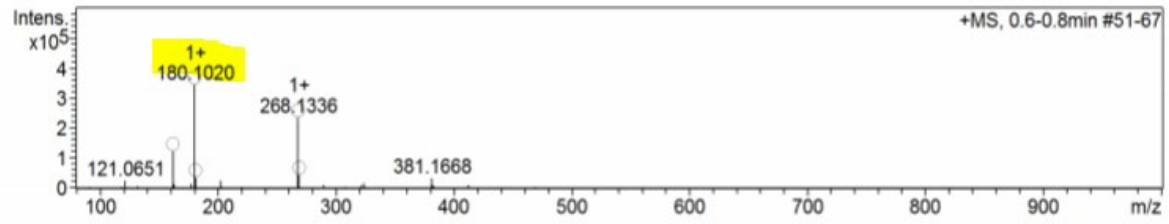

*Figure 6.1. HRMS of product **1a** in section **2.3**.*

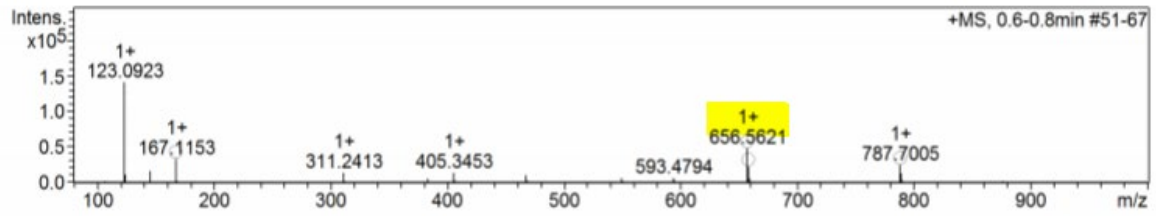

*Figure 6.2. HRMS of product **1b** in section **2.3.***

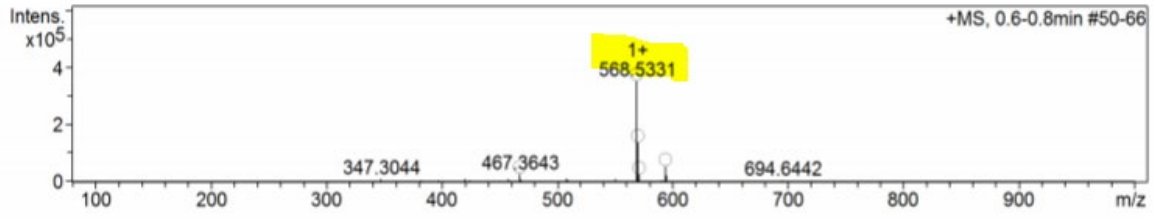

*Figure 6.3. HRMS of product **1c** in section **2.3**.*

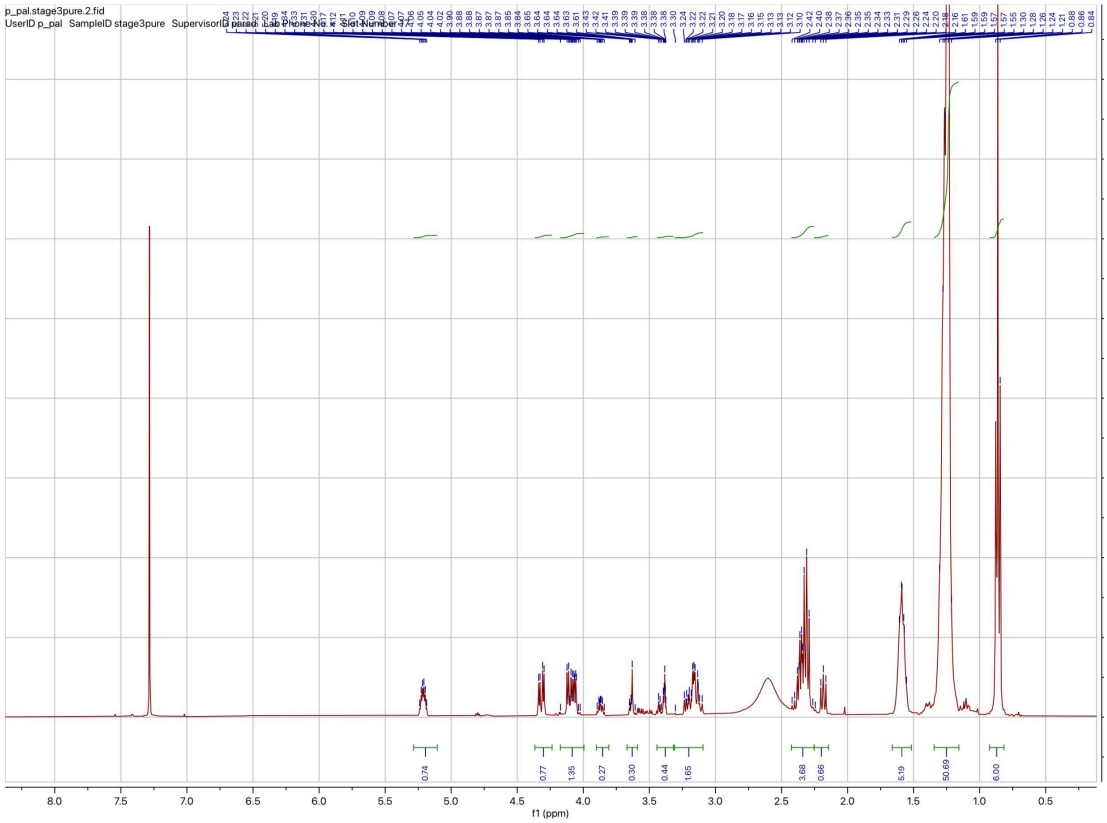

*Figure 6.4 . [1]HNMR of product **1c** in section **2.3***

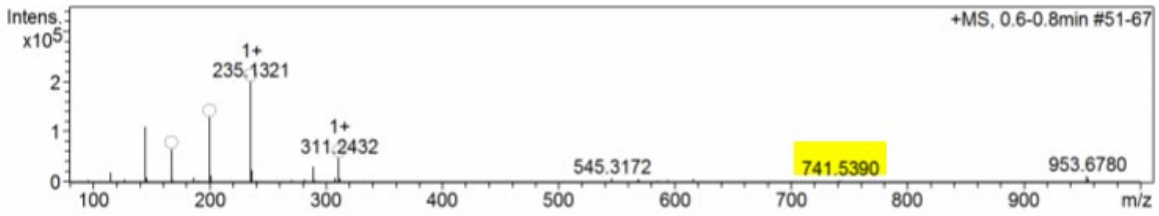

*Figure 6.5. HRMS of product **1d** in section **2.3**.*

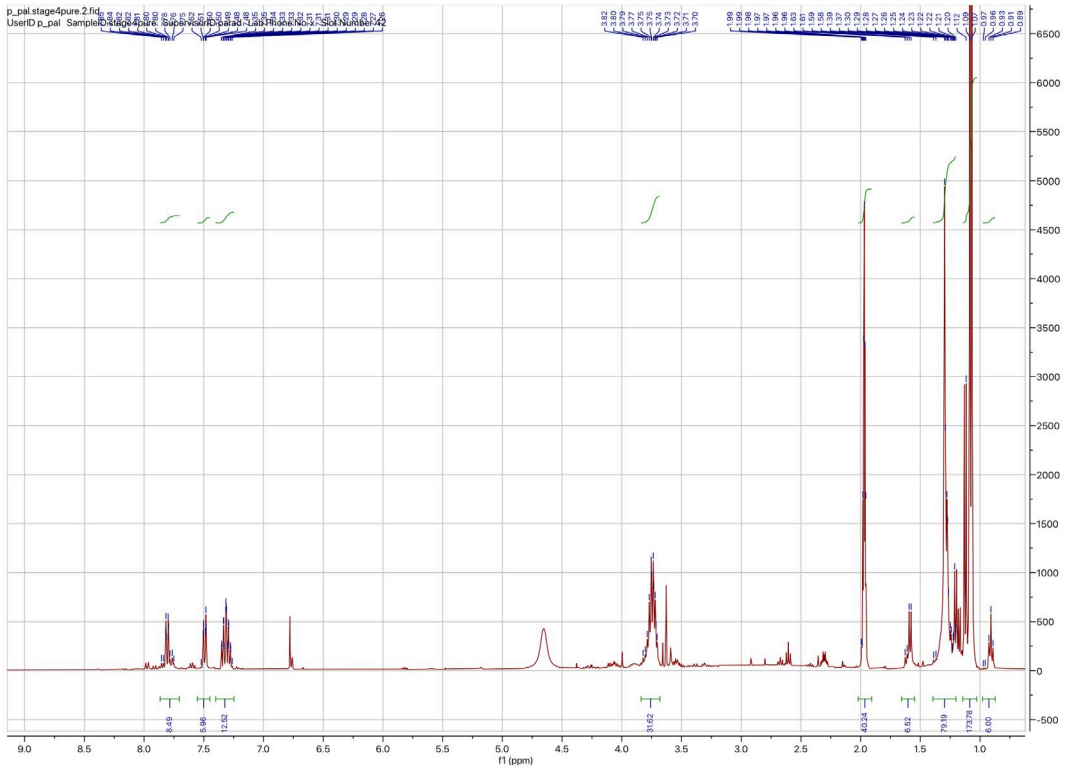

*Figure 6.6. [1]HNMR of product **1d** in section **2.3**.*

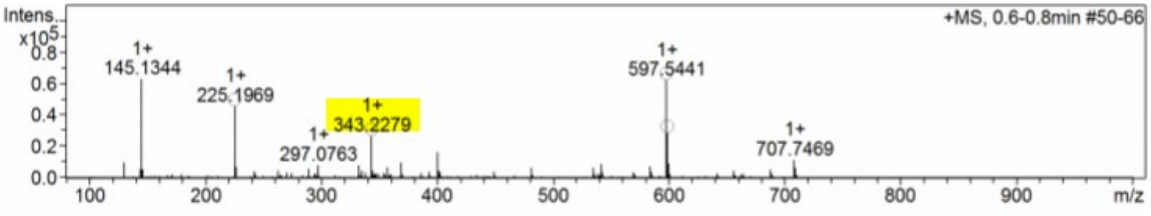

*Figure 6.7 HRMS of product **2a** in section **2.3.***

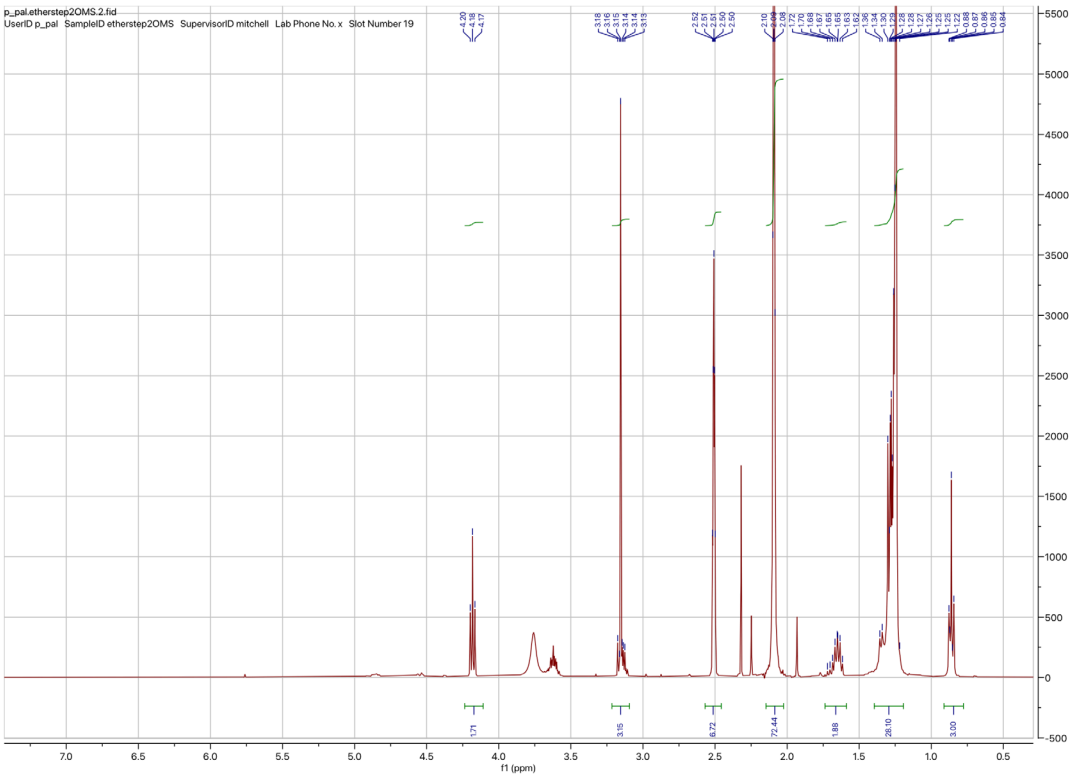

*Figure 6.8 . [1]HNMR of product **2a** in section **2.3.***

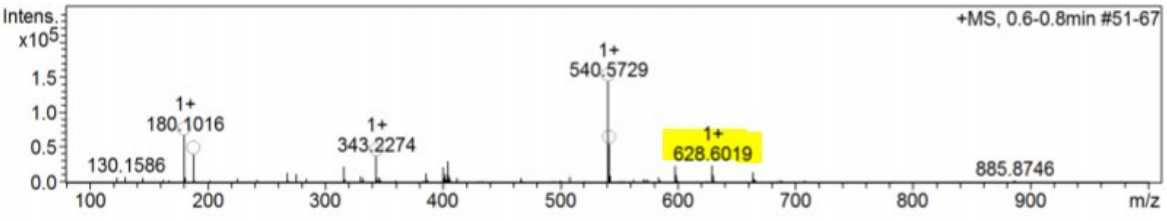

*Figure 6.9 . HRMS of product **3a** in section **2.3.***

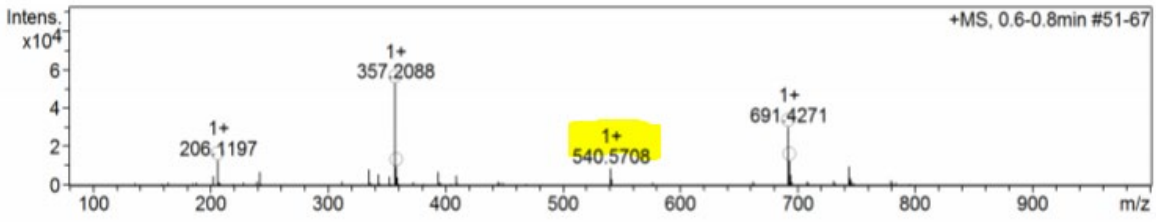

*Figure 6.10 HRMS of product **3b** in section **2.3.***

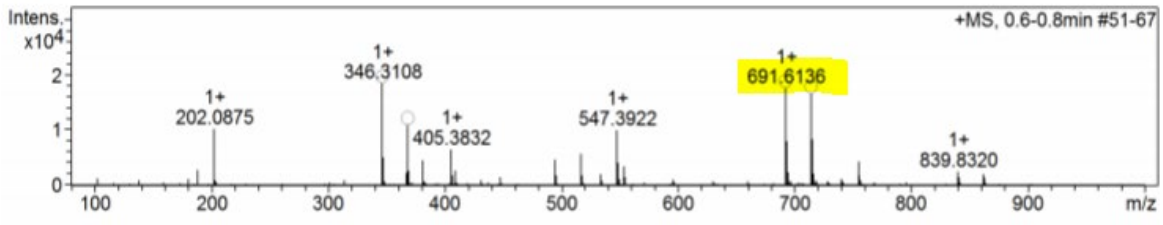

*Figure 6.11. HRMS of product **3c** in section **2.3.***

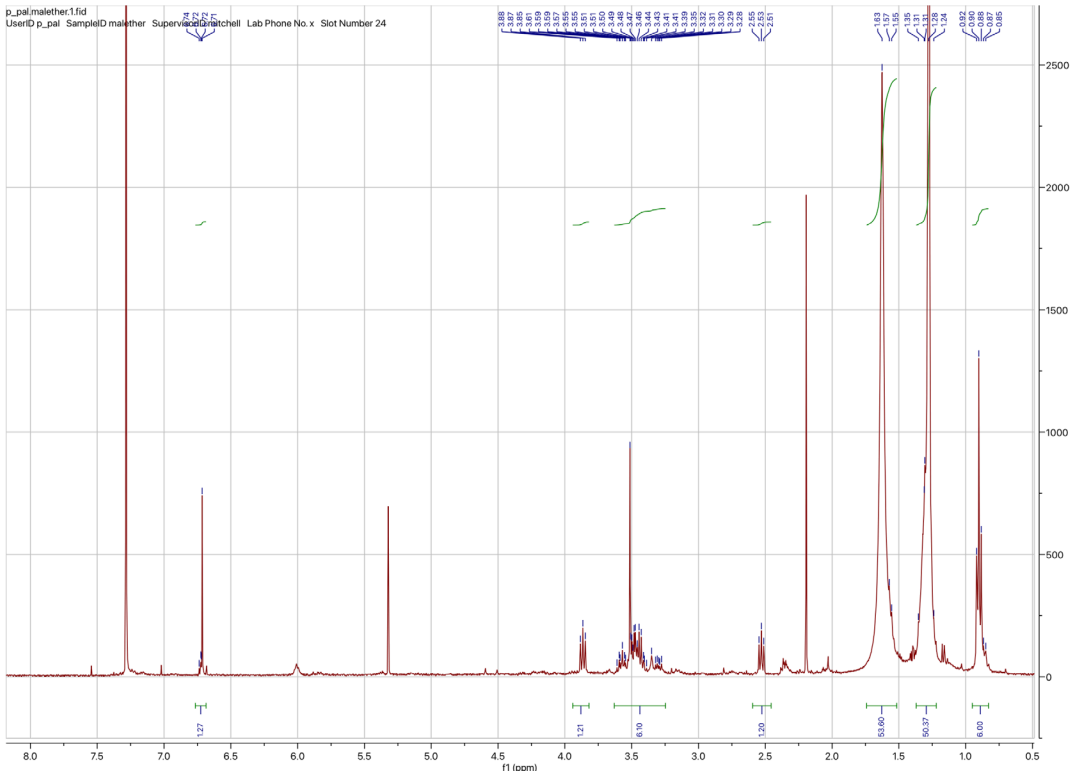

*Figure 6.12. [1]HNMR of product **3c** in section **2.3**.*

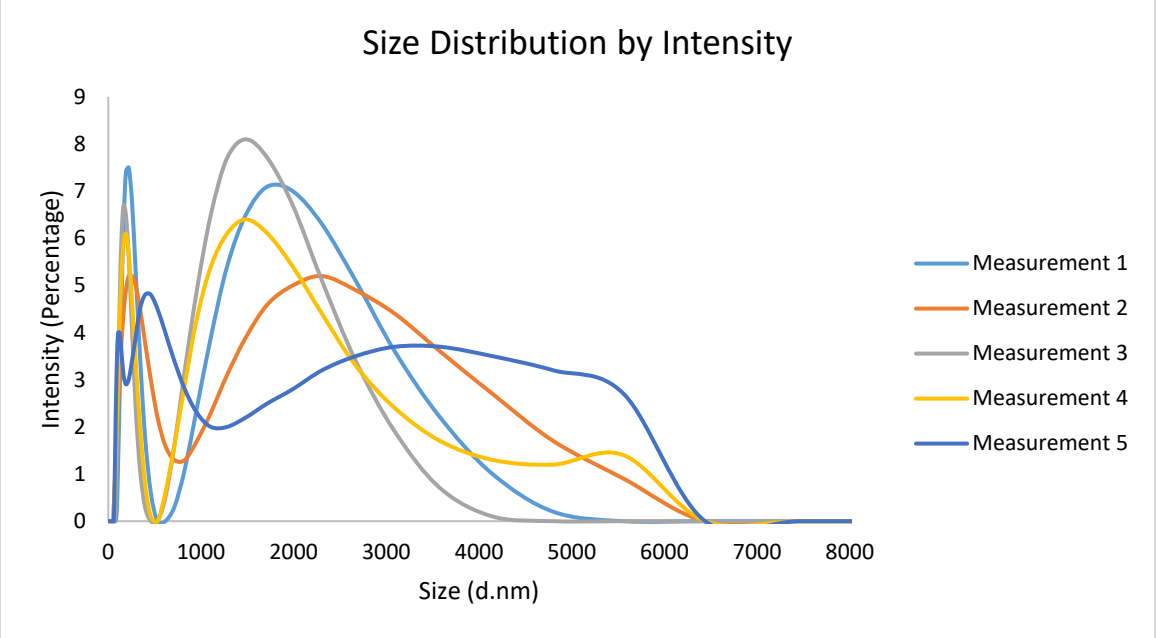

B: 70% cholesterol, 15% DPPS and 15% DPPC liposome with average size 370.5 nm and PDI 0.574.

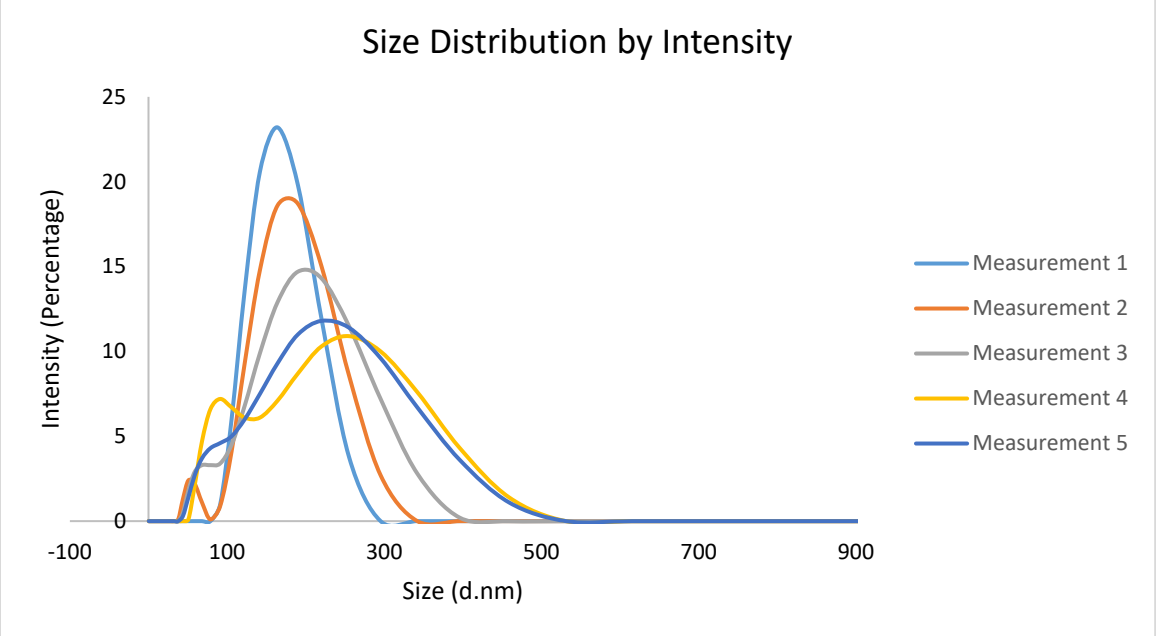

C: 10% cholesterol, 45% DPPS and 45% DPPC liposome with average size 245.0 nm and PDI 0.381.

Figure 6.13. DLS plots from analysis of liposomes with different percentages of lipids, section ***3.4-lipid ratio optimisation.***

Bath Sonicator (10 min continuous pulsing)

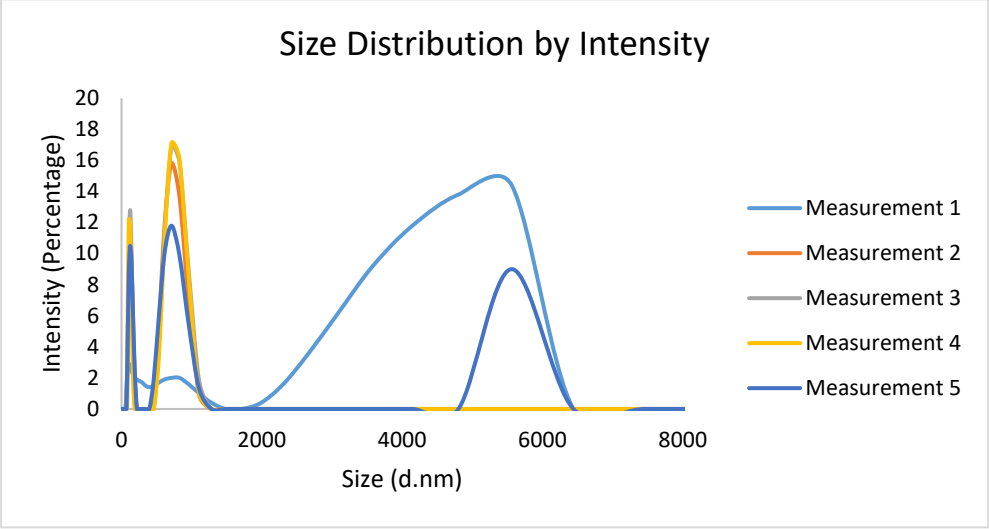

Z-average (d.nm) 564.0, PDI: 1.00

Q sonicator (100% amplitude, 10 min continuous pulsing)

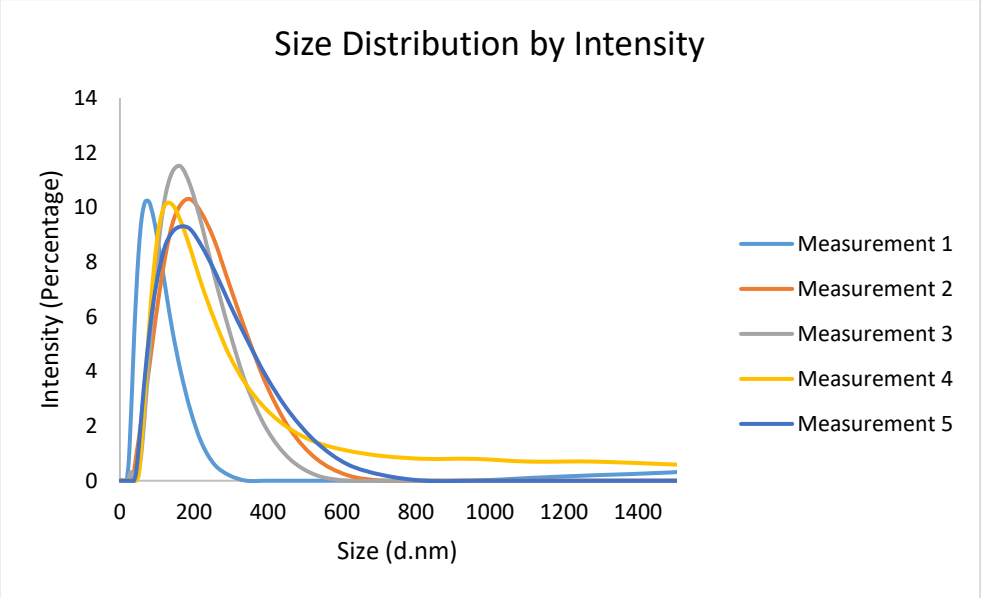

Z-average (d.nm) 124.4, PDI: 0.204

Figure 6.14. DLS plots from analysis of non-mal liposomes (containing 30% DPPC, 30% DPPS and 40% cholesterol) sonication using a bath (for 10 minutes) and QSonica sonicator (for 10 minutes, at 100% amplitude), to compare average size and polydispersity - section ***3.4-sonication method optimisation.***

S sonicator (50% amplitude, 10 min continuous pulsing)

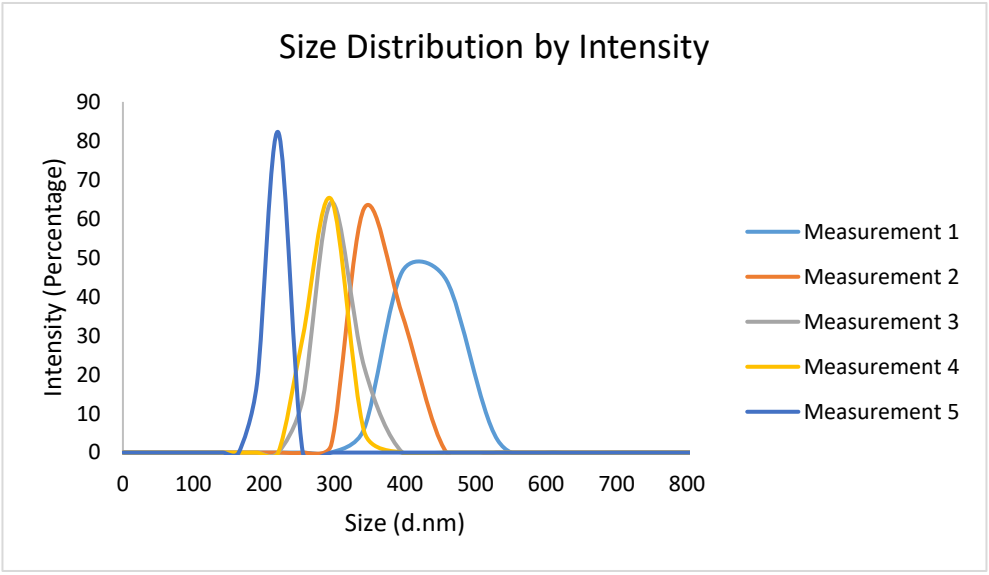

Z-average (d.nm) 201.8, PDI: 1.00

S sonicator (50% amplitude, 3x 2min pulsing on, 30 sec pulsing off)

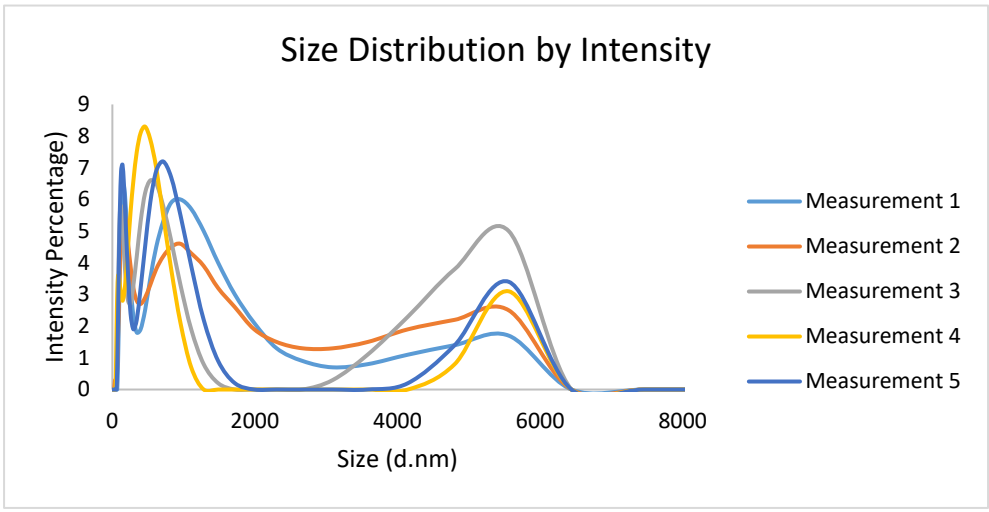

Z-average (d.nm) 301.7, PDI: 0.732

Figure 6.15. DLS plots from analysis of non-mal liposomes (containing 30% DPPC, 30% DPPS and 40% cholesterol) sonication using the Sonic Dismembrator-Ultra Liquid Processor (S sonicator) at 50% amplitude for 10 minutes and for 2 minutes (x3) with 30 pulsing off, to compare average size and polydispersity - section ***3.4-sonication method optimisation.***

Q sonicator (50% amplitude, 10 min continuous pulsing)

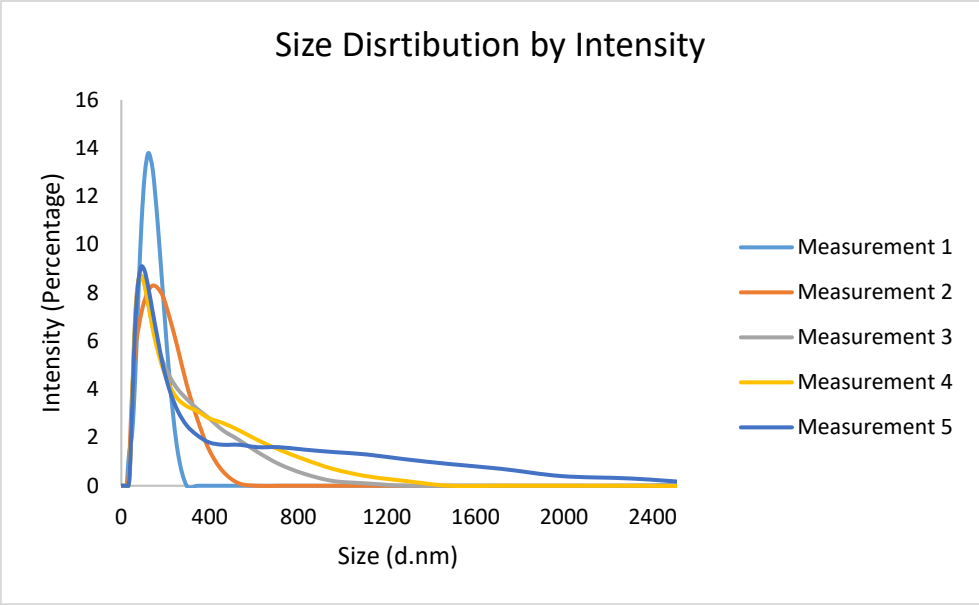

Z-average (d.nm) 132.8, PDI: 0.412

Q sonicator (50% amplitude, 3x 2min pulsing on, 30 sec pulsing off)

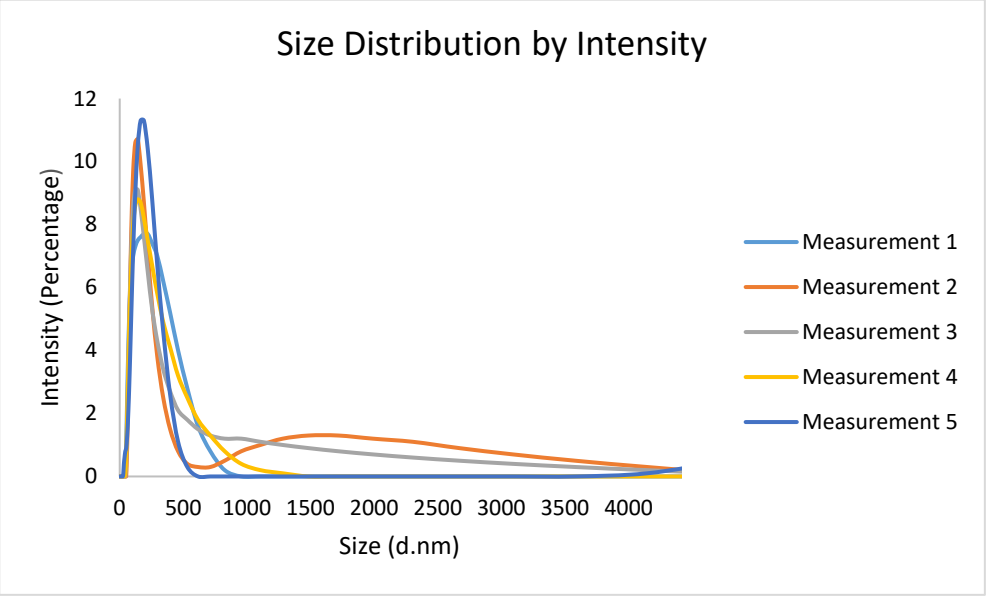

Z-average (d.nm) 156.5, PDI:0.668

Figure 6.16. DLS plots from analysis of non-mal liposomes (containing 30% DPPC, 30% DPPS and 40% cholesterol) sonication using the QSonica sonicator (Q sonicator) at 50% amplitude for 10 minutes and for 2 minutes (x3) with 30 pulsing off, to compare average size and polydispersity - section ***3.4-sonication method optimisation.***

S sonicator (90% amplitude, 10 min continuous pulsing)

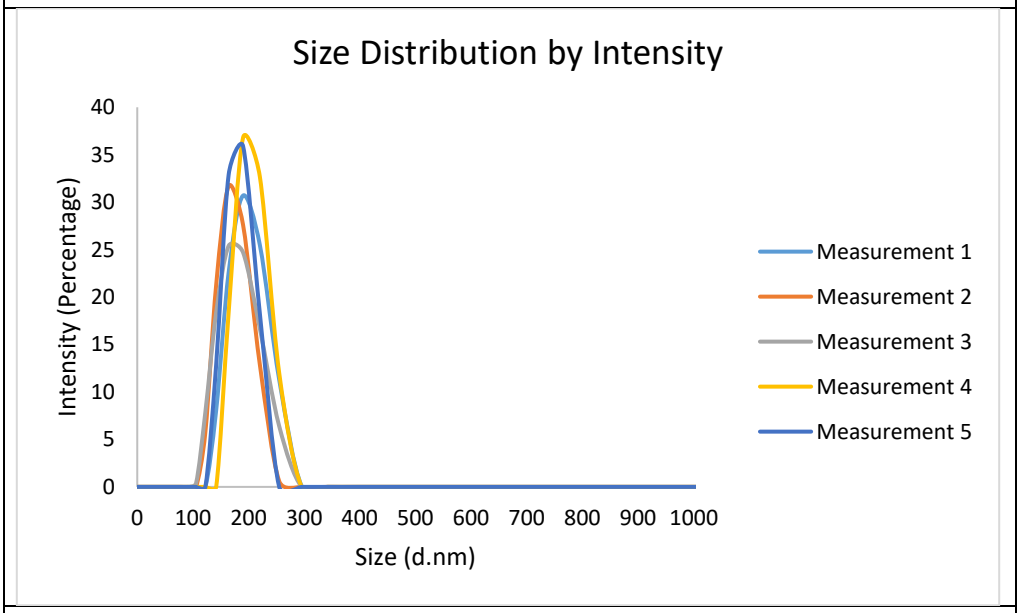

Z-average (d.nm) 276.0, PDI: 0.527

Q sonicator (90% amplitude, 10 min continuous pulsing)

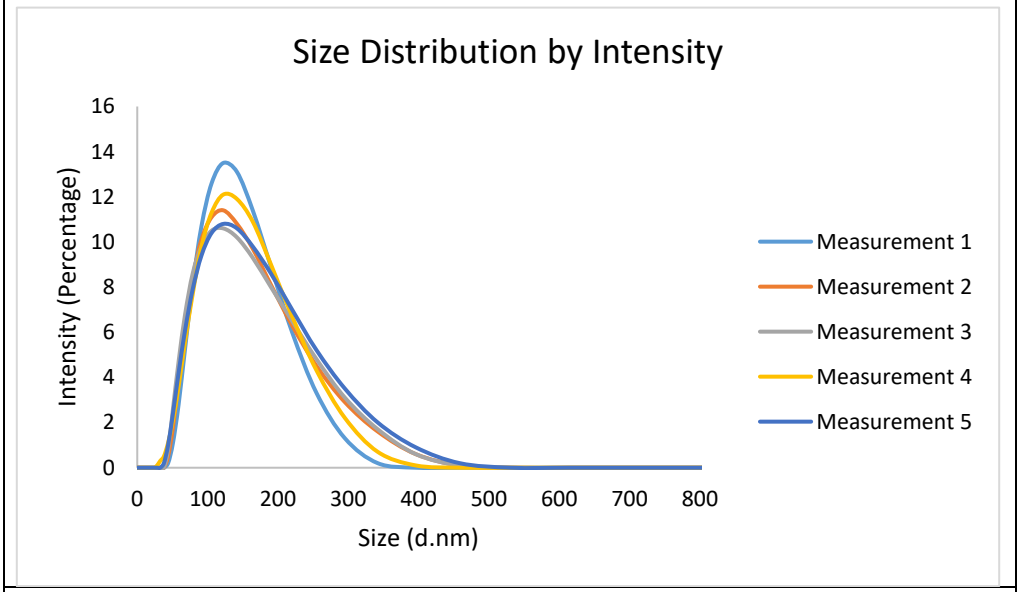

Z-average (d.nm) 119.1, PDI: 0.210

Figure 6.17. DLS plots from analysis of non-mal liposomes (containing 30% DPPC, 30% DPPS and 40% cholesterol) sonication using the Sonic Dismembrator-Ultra Liquid Processor (S sonicator) and QSonica Sonicator (Q sonicator) at 90% amplitude for 10 minutes, to compare average size and polydispersity - section ***3.4-sonication method optimisation.***

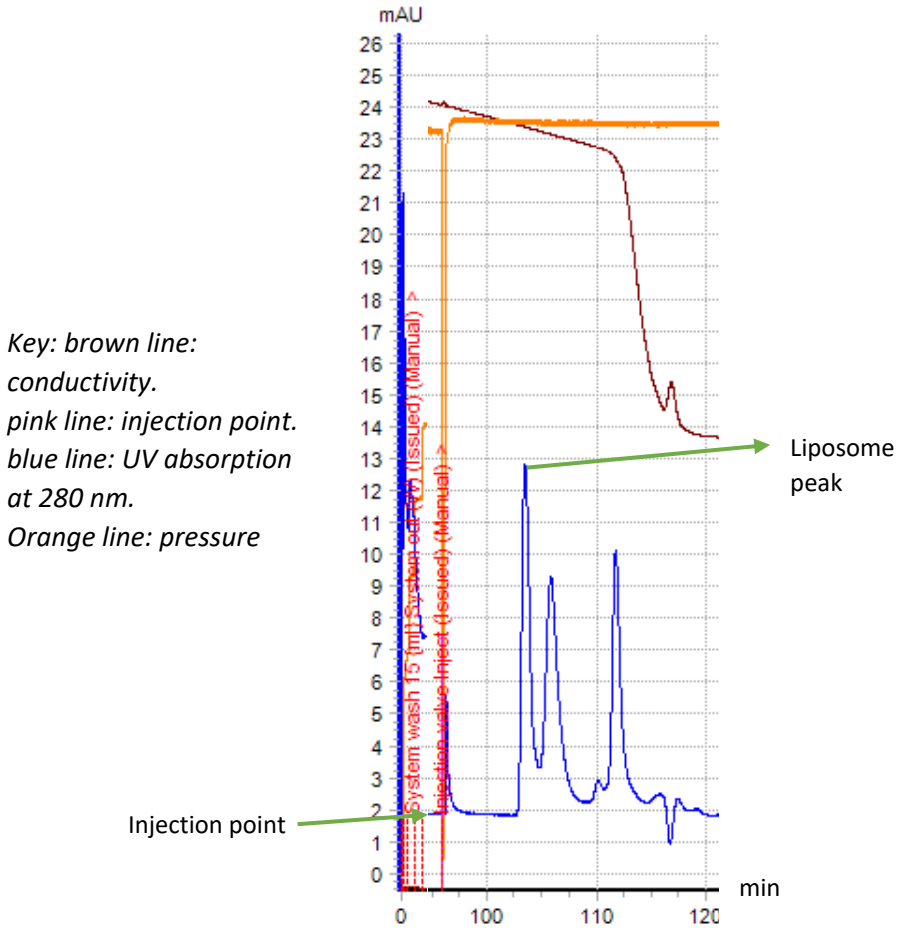

Figure 6.18. SEC trace of a single injection of non-mal liposome (30% DPPC, 30%DPPS, 40% cholesterol) conjugated to 2 equivalents (30 mmol) of GFP showing liposomes eluting about 6 minutes passed the injection point – (figure edited to omit equilibration of column) section ***3.5***

Lyophilised with 0% trehalose

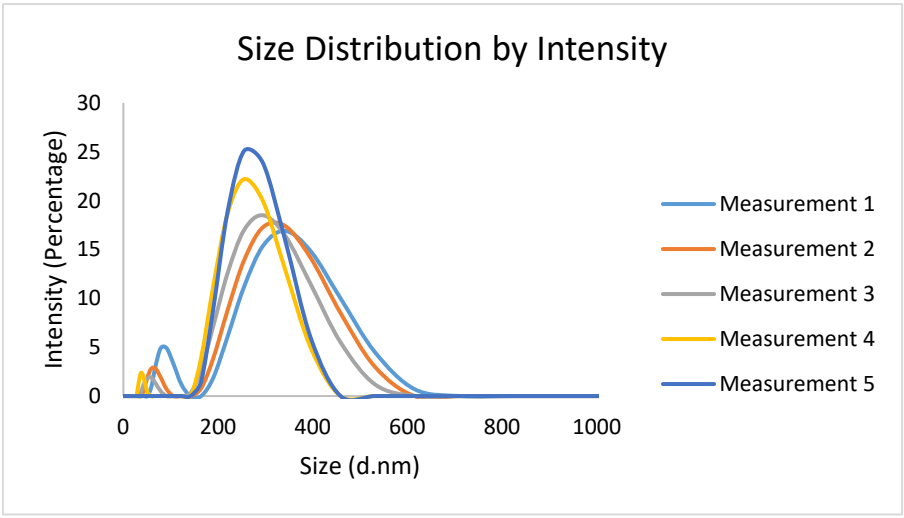

Z-average (d.nm) 312.0, PDI: 0.588

Lyophilised with 15% trehalose

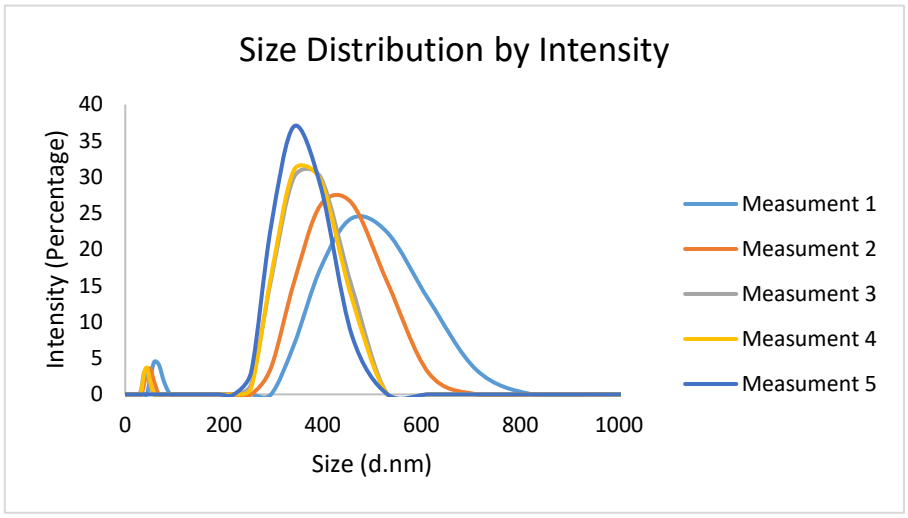

Z-average (d.nm) 656.8, PDI: 0.729

*Figure 6.19. DLS plots showing results of analysis of mal-liposomes conjugated to GFP lyophilised with no and with 15% by mass of trehalose sugar, respectively, to compare z-average size and polydispersity index of resulting samples – section **3.6**.*

Lyophilised with 30% trehalose

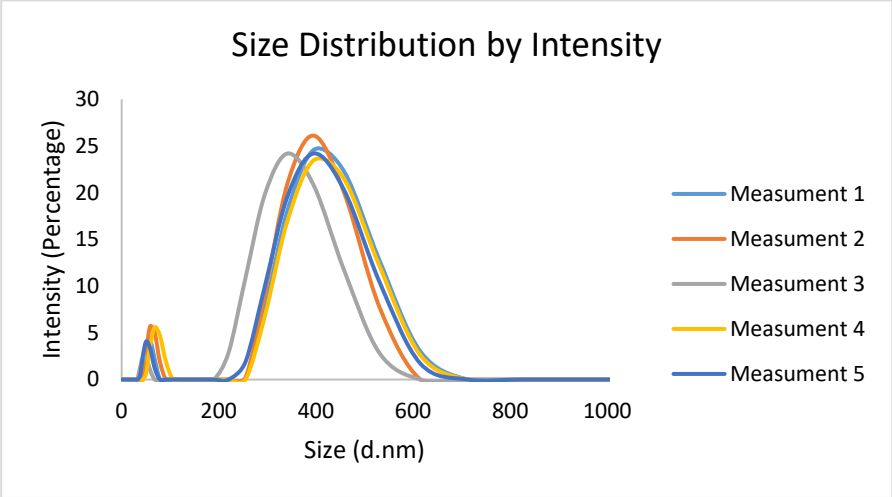

Z-average (d.nm) 497.8, PDI: 0.572

Lyophilised with 50% trehalose

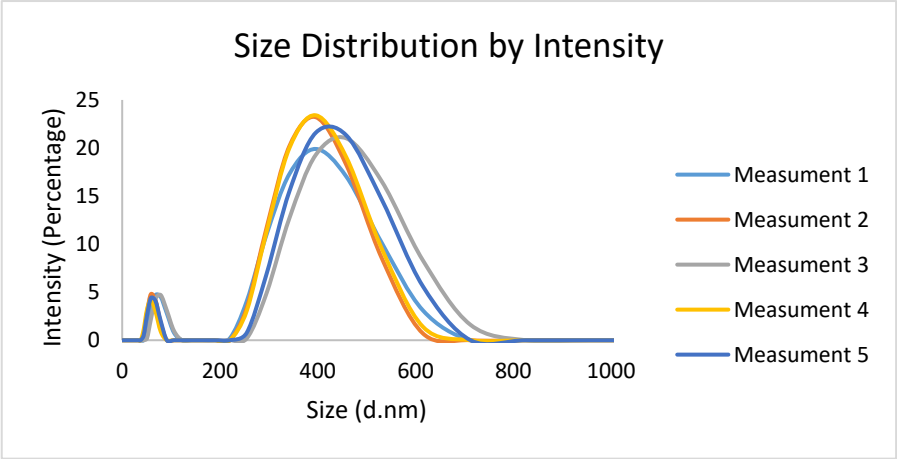

Z-average (d.nm) 438.8, PDI: 0.552

*Figure 6.20. DLS plots showing results of analysis of mal-liposomes conjugated to GFP lyophilised with 30% and with 50% by mass of trehalose sugar, respectively, to compare z-average size and polydispersity index of resulting samples – section **3.6**.*

Lyophilised with 100% trehalose

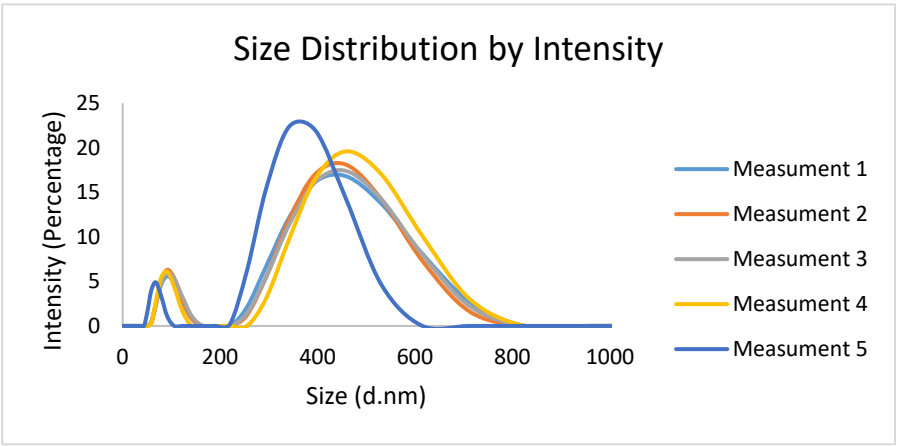

Z-average (d.nm) 404.5, PDI: 0.667

*Figure 6.21. DLS plots showing results of analysis of mal-liposomes conjugated to GFP lyophilised with 100% by mass of trehalose sugar, respectively, to compare z-average size and polydispersity index of resulting samples – section **3.6**.*